Mechanistic *in vitro* tests for genotoxicity and carcinogenicity of heavy metals and their nanoparticles

Dissertation

zur Erlangung des akademischen Grades
des Doktors der Naturwissenschaften

Eingereicht im Fachbereich Biologie
an der Universität Konstanz

vorgelegt von

Barbara Munaro

June 2009

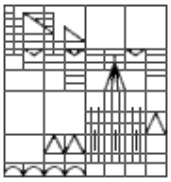

Universität Konstanz

ACKNOWLEDGEMENTS

I would like to express my gratitude to Prof. Dr. Thomas Hartung for his supervision and support for the preparation of this PhD work.

I am very grateful to all my colleagues who have helped me with the experimental work and for their friendship and support: Francesca Broggi, Patrick Marmorato, Renato Colognato and Antonella Bottini. Special thanks to Jessica Ponti and for her important help and contributions. Thanks to Marina Hasiwa and Gregor Pinski for their help and advices.

On the private side I wish to dedicate this thesis to my daughter Aurora. I would like to express a warm thank to my husband Nicola for his support and love. Special thanks to my mother, my father and my brother Marco who have always encouraged me throughout life.

Abbreviations

3Rs= Reduction, Refinement, Replacement
ADME= adsorption, distribution, metabolism and excretion
ANOVA= Analysis of variances
AS3MT= arsenic III methyl transferase
BN= binucleated cells
BNMN= binucleated micronucleated cells
BAS= bovine serum albumin
CA= chromosomal aberration
CBPI= cytokinesis block proliferation index
CFE= Colony Forming Efficiency
Co-nano= cobalt nanoparticle
CTA= Cell Transformation Assay
DEG= diethyl glycol
DLS= Dynamic Light Scattering
DMA= dimethylated arsenic
DMEM= Dulbecco's Modified Eagle medium
DMSO= Dimethyl sulfoxide
DNA= Deoxyribosenucleic Acid
ECVAM= European Centre of Validation of Alternative Methods
EDTA= ethylenediaminetetraacetic acid
EPA= Environmental protection Agency
FBS= Fetal Bovine Serum
FC III= Fetal Clone III
GFAAS= Graphite Furnace Atomic Absorption Spectrometry
GST= glutathione S-transferase
hGSTO1= human glutathione S-transferase omega 1 gene
IARC= International Agency for Research on Cancer
IC= inhibitory concentrations
ICPMS= Inductively Coupled Plasma Mass Spectrometry
MMA= monomethyl arsenic
MMC= Mitomicin C
MN= Micronucleus test
MNi= micronuclei
mNPs= manufactured nanoparticles

MTHFR= Methylenetetrahydrofolate reductase

MTT= 3-(4, 5-dimethylthiazol-2-yl)-2,5-diphenyltetrazolium bromide

NBUDs= nuclear buds

NC=negative control

NPBs= nucleoplasmic bridges

NS= No Statistically Significance

PBS= Phosphate Buffer Solution

PC=positive control

PEG-8= polyethylene glycol-8

REACH= Registration, Evaluation and Authorisation of Chemicals

RSD= Relative Standard Deviation

S= Statistically Significance

SD= standard deviations

SDS= Sodium Dodecil Sulphate

SEM= Scanning Electron Microscope

SHE= Syrian Hamster Embryo cells

SOP= Standard Operating Procedure

TEER= Trans-Epithelial Electrical Resistance

LIST OF FIGURES

Fig 1 Schematic insert system used for the study of the effect of Cr (VI) on the epithelial intestinal barrier, its transfer among the insert compartments and the uptake by Caco-2 cells

Fig 2 Web site page of Fisher analysis

Fig 3 DNA damage expressed as tail DNA percentage (median of 4 runs) in Balb/3T3 exposed for 2h to subtoxic concentrations of As compounds (statistical significance, $p<0.05$, is reported in Table 16). PC=positive control (H_2O_2, 300 µM), NC=negative control (culture medium)

Fig 4 DNA damage expressed as tail DNA percentage (median of 4 runs) in Balb/3T3 exposed for 2h to subtoxic concentrations of Pt compounds (statistical significance, $p<0.05$, is reported in Table 16). PC=positive control (H_2O_2, 300 µM), NC=negative control (culture medium)

Fig 5 DNA damage expressed as tail DNA percentage (median of 4 runs) in Balb/3T3 exposed for 2h to subtoxic concentrations of Hg compounds (statistical significance, $p<0.05$, is reported in Table 16). PC=positive control (H_2O_2, 300 µM), NC=negative control (culture medium)

Fig 6 DNA damage expressed as tail DNA percentage (median of 4 runs) in Balb/3T3 exposed for 2h to subtoxic concentrations of Be, Ni, Cr, Ag, Cd, V compounds (statistical significance, $p<0.05$, is reported in Table 16). PC=positive control (H_2O_2, 300 µM), NC=negative control (culture medium)

Fig 7 Cytotoxicity induced in Caco-2 cells by Na_2CrO_4 and $NaAsO_2$, Gentamicin Sulfate, Ochratoxin A after 24 h and 72 h respectively

Fig 8 Kinetic of Cr transfer between the two insert compartments (apical; basolateral) in presence of Caco-2 cells exposed to (a) 1, (b) 30 and (c) 50 µM of $Na_2{}^{51}CrO_4$ for 24 h and (d) 1 µM of $Na_2{}^{51}CrO_4$ continuous and discontinuous exposure for 33 days

Fig 9 Kinetic transfer of As between the two insert compartments in presence of Caco-2 cells exposed 0.1 µM of $Na^{73}AsO_2$ for 17 days (discontinuous exposure)

Fig 10 Kinetic transfer of gentamicin between the two insert compartments in presence of Caco-2 cells exposed 7 µM of gentamicin for 17 days (discontinuous exposure)

Fig 11 Kinetic transfer of Ochratoxin between the two insert compartments in presence of Caco-2 cells exposed 1 µM of gentamicin for 17 days (discontinuous exposure)

Fig 12 Co-nano aggregates in H_2O (A) and in culture medium (B) by SEM. Size distribution by DLS (C)

Fig 13 Cytotoxicity, expressed as CFE (% of the control), induced in Balb/3T3 cell lines by Co^{2+}, and Co-nano, after 2, 24,72 h of exposure (A, B and C, respectively). Curves are obtained as average of 3 experiments, 6 replicates each treatment, RSD< 20%.

Fig 14 DNA damage expressed as percentage tail DNA (median of 4 experiments) in Balb/3T3 exposed for 2 h to subtoxic concentrations (1-3-5 µM) of Co-nano and $CoCl_2$ (statistical significance, $p<0.01$ for each treatment). PC=positive control (H_2O_2, 300 µM), NC=negative control (culture medium)

LIST OF TABLES

Table 1 IARC classification of some metal compounds

Table 2 Common *in vitro* genetic toxicology tests

Table 3 Common *in vivo* genetic toxicology tests

Table 4 Chemicals tested

Table 5 Preparation of CH_3HgCl (10^{-3} M), $PtCl_2$ (10^{-3} M), cisPt (10^{-3} M) and ochratoxin (10^{-3} M) solutions

Table 6 Suspension of 10^{-2} M Co nano in culture medium

Table 7 Radio-chemical characteristics of radioisotopes

Table 8 Balb/3T3 cell line: cell culture procedures

Table 9 CaCo-2 cell line: cell culture procedures

Table 10 MTT assay

Table 11 CFE and morphological transformation assay

Table 12 Comet assay

Table 13 Micronucleus test (MN)

Table 14 Kinetics of transfers, uptake and intracellular distribution

Table 15 Elemental impurities in Na_2CrO_4 and $NaAsO_2$ salts used for carcinogenicity/genotoxicity studies

Table 16 Cell Transformation Assay in Balb/3T3 cell line: screening of 39 chemicals

Table 17 Comet assay in Balb/3T3 cells exposed to different compounds for 2h at concentrations ranging from 0.05 to 200 µM

Table 18 Micro Nucleus tests in Balb/3T3 cells exposed to different compounds for 24h at concentrations ranging from 0.01 to 100 µM

Table 19 Concentration of Co in diluted suspensions in Balb/3T3 culture medium

Table 20 Co^{2+} leaked from 100 µM Co-nano in complete culture medium expressed as percentage Co^{2+} (%)

Table 21 Concurrent cytotoxicity and morphological transformation induced by Co^{2+}, Co-nano in Balb/3T3 after 72 h of exposure

Table 22 Chromosomal aberration by MN assay induced by Co-nano and $CoCl_2$ in Balb/3T3 after 24 h of exposure

Table 23 Uptake of ^{60}Co-nano and $^{57}Co^{2+}$ in Balb/3T3 after 2-24 and 72h of exposure to the corresponding IC_{50}

Table 24 Carcinogenic potential and genotoxicity of 18 metal compounds

LIST OF PHOTOS

Photo 1 Balb/3T3 clone A31-1-1 (A) and Caco-2 clone TC7 cell lines in culture (inverted optic microscope Olympus, Italy)

Photo 2 Balb/3T3 cells in monolayer after 5 weeks of culture (control)

Photo 3 Type III foci induced in Balb/3T3 by exposure to $(C_6H_5)_4AsCl$ 3 µM (A) and $NaAsO_2$ 10 µM(B) for 72h

Photo 4 Type III foci induced in Balb/3T3 by exposure to cisPt 1 µM (A) and carboPt 1 µM (B) for 72h

Photo 5 Type III foci induced in Balb/3T3 by exposure to CarboPt 3 µM (A) and CarboPt 1 µM (B) for 72h

Photo 6 Type III foci induced in Balb/3T3 by exposure to $PtCl_2$ 7 µM (A) and $PtCl_4$ 10 µM (B) for 72h

Photo 7 Balb/3T3 cells in monolayer after 5 weeks of culture (control) (A) and type III focus induced in Balb/3T3 by exposure to Co-nano 7 µM for 72 h (B)

Photo 8 Balb/3T3 morphology after exposure to Co-nano (1-7-100 µM) and $CoCl_2$ (1-30-100 µM) for 24 h, corresponding to the same cytotoxicity, by confocal imaging. Staining: Alexa Fluor 488 (green)-conjugated phalloidin and propidium iodide

Photo 9 Balb/3T3 morphology after exposure to Co-nano (100 µM) by SEM imaging. White circle indicates a Co-nano aggregate

LIST OF PUBLICATIONS

Chromium (VI)-induced immunotoxicity and intracellular accumulation in human primary dendritic

Burastero SE, Paolucci C, Breda D, Ponti J, **Munaro B**, Sabbioni E.

Int J Immunopathol Pharmacol. 2006 Jul-Sep; 19(3):581-91.

Comparison of impedance-based sensors for cell adhesion monitoring and in vitro methods for detecting cytotoxicity induced by chemicals.

Ponti J, Ceriotti L, **Munaro B**, Farina M, Munari A, Whelan M, Colpo P, Sabbioni E, Rossi F.

Altern Lab Anim. 2006 Oct; 34(5):515-25.

An optimised data analysis for the Balb/c 3T3 cell transformation assay and its application to metal compounds.

Ponti J, **Munaro B**, Fischbach M, Hoffmann S, Sabbioni E.

Int J Immunopathol Pharmacol. 2007 Oct-Dec; 20(4):673-84.

Genotoxicity and morphological transformation induced by cobalt nanoparticles and cobalt chloride: an in vitro study on Balb/3T3 mouse fibroblasts

Ponti J, Sabbioni E, **Munaro B**, Broggi F, Marmorato P, Franchini F, Colognato R and Rossi F

Mutagenesis 2008 (Accepted with minor revision).

TABLE OF CONTENTS

1. INTRODUCTION 1

1.1. Metals as cause of cancer 1

1.2. Metal nanoparticles and the challenge to toxicology 8

1.3. Genotoxic and epigenetic mechanisms of cancer 9

1.4. Tests for genotoxic hazards and carcinogenic potential *in vitro* 11

1.5. *In vitro* biokinetics 17

2. AIM 21

3. MATERIALS & METHODS 23

3.1. Source, solubility and purity of chemicals tested 23

3.2. Source of nano- and microparticles tested 26

3.2.1. Physicochemical characterisation of Co-nano 26

3.2.2. Determination of Co concentration in Co-nano suspension 27

3.2.3. Radiotracers and radioactivity counting 27

3.3. Cell lines and cell culture procedures 30

3.4. Basal Cytotoxicity 33

3.4.1. MTT assays 33

3.4.2. Colony Forming Efficiency (CFE) 33

3.4.3. Colony Forming Efficiency (CFE) and Morphological Transformation assay (CTA) 35

3.5. Genotoxicity studies 37

3.5.1. Comet assay 37

3.5.2. Micronucleus test 39

3.6. Biokinetics studies by Caco-2 cells: short- and long-term toxicity 42

3.7. Cell morphology 45

3.7.1. Confocal microscopy 45

3.7.2. Scanning electron microscopy 45

3.8. Statistical treatment of the data 46

3.8.1. CFE and MTT 46

3.8.2. Cell Transformation Assay and Micronucleus 46

3.8.3. Comet assay 46
4. RESULTS 48
4.1. Screening 48
4.1.1. Solubility of $CdMoO_4$, CH_3HgCl, $PtCl_2$ and cisPt 48
4.1.2. Elemental analysis of metal compounds 48
4.1.3. Cell Transformation Assay in Balb/3T3 cells 50
4.2. Genotoxicity studies 54
4.2.1. Comet assay 54
4.2.2. Micronucleus test 54
4.3. Biokinetic studies 63
4.3.1. Cytotoxicity and epithelial integrity 63
4.3.2. Kinetics of transfer 64
4.3.3. Cr biokinetics 65
4.3.4. As biokinetics 67
4.3.5. Gentamicin biokinetics 69
4.3.6. Ochratoxin biokinetics 70
4.4. Nanotoxicology studies 72
4.4.1. Physicochemical characterization 72
4.4.2. Carcinogenicity and genotoxicity induced by Co-nano and $CoCl_2$ 75
4.4.3. Morphological studies on Balb/3T3 exposed to Co-nano and $CoCl_2$ 79
4.4.4. Metabolic studies on Balb/3T3 exposed to Co-nano and $CoCl_2$ 80
5. DISCUSSION 82
5.1. Carcinogenicity/ genotoxicity studies 82
5.1.1. Importance of purity of metal compounds tested 82
5.1.2. Cell transformation assay by Balb/3T3 82
5.1.3. Metal speciation 89
5.2. Biokinetic studies 91
5.3. Nanotoxicology studies 94
6. SUMMARY 97

7. ZUSAMMENFASSUNG 99

ANNEX 1 101

ANNEX 2 103

ANNEX 3 106

8. REFERENCES 109

1. INTRODUCTION

1.1. Metals as cause of cancer

Different regulatory agencies, utilising both epidemiological and experimental animal data, classify a compound as carcinogenic if there is an evidence of its carcinogenic potential in humans, as reported by the International Agency for Research on Cancer (IARC) or place different emphases on the results of animal and genotoxicity studies as reported by the Environmental Protection Agency (EPA), by the Chemical Manufactures Association and by the European Community. In order to estimate the carcinogenic and genotoxic potential of chemicals, several factors, based on the pharmacokinetic and pathological response between humans and the surrogate test species, are considered.

In spite of the limitations of these classifications, an agent cannot be proven to be carcinogenic for humans unless substantial epidemiological evidence supporting that claim is available. Despite this restriction, a number of chemical agents, processes, and lifestyles have been shown to be carcinogenic in humans according to the IARC classification (Pitot & Dragan, 1996).

In particular, the IARC classification divides the carcinogens in four groups:

Group 1: the agent (mixture) is definitely carcinogenic to humans. The exposure circumstance entails exposures that are carcinogenic to humans.

Group 2A: the agent (mixture) is probably carcinogenic to humans. The exposure circumstance entails exposures that are probably carcinogenic to humans.

Group 2B: the agent (mixture) is possibly carcinogenic to humans. The exposure circumstance entails exposures that are possibly carcinogenic to humans.

Group 3: the agent (mixture or exposure circumstance) is not classifiable as to its carcinogenicity to humans.

Group 4: the agent (mixture) is probably not carcinogenic to humans.

Table 1 summarises some metal compounds classified by IARC (IARC, 1990a).

Hereafter, literature survey information related to some of the metal compounds analysed in this study for their *in vitro* carcinogenic potential and genotoxicity is summarised.

Table 1: IARC classification of some metal compounds

Compound	IARC classification	
	Group	Evidence
Aluminium[a]	Group 1: Carcinogenic to humans	Sufficient[b] in human
Arsenic[a]		
Beryllium[a]		
Cadmium[a]		
Chromium[a]		
Iron[a]		
Nickel[a]		
Cisplatinum	Group 2A: Probably carcinogenic to humans	Limited[c] in human, sufficient in animal
Antymony trioxide	2B. Possible carcinogenic	Limited in human
Cobalt[a]		
Vanadium pentoxide		
Lead[a]	2B. Possible carcinogenic	Inadequate[d] in human
Methylmercury		
Metallic nickel	Group 2B: Possibly carcinogenic to humans	Sufficient in human
Manganese[a]	Group 3: Not classifiable as to carcinogenicity to humans	-
Antimony trisulfoxide		
Organolead[a]		
Metallic mercury		
Inorganic mercury[a]		
Selenium[a]		
Silver		
Titanium dioxide		
-	Group 4: Probably not carcinogenic to humans	Inadequate in human and in animal

a: element and its compounds

b: there is a causal relationship between the agent or agents and human cancer

c: there is a credible causal interpretation, but alternative explanations such as chance, bias and confounding variables could not completely be excluded

d: one or three conditions prevailed: (i) there are few pertinent data; (ii) the available studies, while showing evidence of association, don't exclude change, bias or confounding variables; (iii) studies are available, but they do not show evidence of carcinogenicity.

Arsenic. The predominant species of arsenic in water and wine are the inorganic As (III) and As (V), however, small concentrations of mono- and dimethylated forms were also found in waters (Bertolero et al., 1987). Arsenobetaine and arsenocholine are the main organo-arsenic compounds identified in many edible marine organisms. Different As metabolites (tetrametilarsonium and arsenate) were found in tissues of cooked shellfish (Honaoka et al., 2001). The use of arsenic-based pesticides, of coal for electrical energy production, of fertilisers for agriculture and releases from non ferrous smelters as well as geothermal power plants contribute to environmental arsenic pollution so that human exposure to arsenic can occur via inhalation of industrial dust and via ingestion of contaminated water and food (Sabbioni et al., 1985).

Chronic As (III) exposure is known to be related to skin, lung, and bladder cancers (IARC, 1980; NRC, 1999) as well as neurotoxicity and hepatic injuries (Simeonova & Luster, 2000). Cases of environmental exposure to high level of As are related to ingestion of the metal, naturally present in soil, from drinking water in the region of Cordoba (Argentina), in Taiwan and Antofagasta (Chile). Dramatic health effects were observed including high mortality from skin cancer.

The toxicological effects of inorganic arsenic are generally related to its oxidation state, trivalent arsenite being more toxic than pentavalent arsenate. Studies on laboratory animals showed dose-dependent retention of arsenite, implying that the higher toxicity of trivalent arsenic may be related to its higher affinity for cellular constituents (Csanaky et al., 2003). *In vivo* and *ex vivo* genotoxicity studies on As (III) in the form of As trioxide has shown that it induces high DNA damage in comet tail length (Banu Saleha et al., 2001). Inorganic trivalent and pentavalent species induce morphological transformation *in vitro* both in immortalized mouse fibroblast cell line (Balb/3T3) and in primary Syrian Hamster Embryo cells (SHE) (Bertolero et al., 1987; Lee et al., 1985). Such effect was not induced in Balb/3T3 cells by arsenobetaine (Sabbioni et al., 1985).

The toxicity of arsenobetaine is generally considered low compared to inorganic arsenic, the knowledge of their metabolism in laboratory animals is of particular interest to the toxicological assessment of the total impact of environmental arsenic on health. No biotransformation of arsenobetaine occurred in rats and rabbits. This conclusion is supported by results of determination of arsenobetaine in the urine and soluble extracts of the tissue. In all tissues analysed, no As-compounds other than arsenobetaine were identified (Sabbioni et al., 1985).

Concerning the metabolism of As, there are several *in vivo* studies suggesting that As (V) is reduced to As (III). This reaction is fundamental for the consequent detoxification process by addition of CH_3 groups. The four principal metabolites are methylated (MMA (III) and MMA (V)) and dimethylated arsenic (DMA (III) and DMA (V)) species (Styblo et al., 2000). *In vitro* studies demonstrated that As (V) is less methyladed than As (III). In humans, methylated and dimethylated arsenic are mainly found as metabolites in urine (Crecelius, 1977; Smith et al., 1977). Methylated arsenic is less toxic than inorganic arsenic, and methylation has been

considered to be a detoxification reaction. On the other hand, a recent study has shown that methylated As (III) (MMA III) is more cytotoxic (Styblo et al., 2000) and genotoxic (Mass et al., 2001) than arsenate and arsenite. It has also been suggested that there is large inter-individual variation in the arsenic metabolism (Vahter, 2000), which may be related to the genetic polymorphism of the enzyme participating in arsenic methylation (Fujihara et al., 2007). As (III) methyltransferase (AS3MT; previously designated as CYT19) is an S-adenosyl-L-methionine-dependent enzyme which catalyzes the methylation of arsenite in the rat (Lin et al., 2002). In several studies, researchers have investigated the relationship between genetic polymorphisms in enzymes other than AS3MT and the arsenic metabolism. Chiou et al. (1997) showed that subjects with the null genotype of glutathione S-transferase (GST) M1 had an elevated percentage of inorganic arsenic in urine and those with the null genotype of GST T1 had an increased percentage of dimethylarsinic acid (DMA). Marnell et al. (2003) investigated the relationship between polymorphisms in the human GST omega 1 (hGSTO1) gene and urinary arsenic profiles, suggesting that the deletion of E155 and E208K is related to abnormal urinary arsenic profiles. In addition, a subject with the TT/AA variant at methylenetetrahydroforate reductase (MTHFR) 677 and 1298 was shown to excrete a significantly higher proportion of inorganic arsenic and a lower proportion of DMA (Steinmaus et al., 2007). Lindberg et al. (2007) showed that the A222V (677 C to T) polymorphism in MTHFR is related to an increased percentage of methylated arsenic in urine. Further studies investigating the genetic polymorphism of the above-mentioned enzymes will be required, especially in individuals living in areas with high levels of arsenic.

Cadmium. A large number of workers are potentially exposed to cadmium compounds in a variety of occupational sectors such as smelting, refining of zinc, electroplating, manufacturing of cadmium alloys, nickel-cadmium batteries and welding. Cigarette smoke also contains cadmium (Thun et al., 1991). Laboratory studies have demonstrated that cadmium is mutagenic and carcinogenic in experimental animals.

Chromosomal aberrations (CA) were seen in mouse bone marrow cells exposed to $CdCl_2$. Frequency of CA increased in peripheral blood lymphocytes of workers exposed to cadmium in the metal industry. Results of epidemiological studies seem to indicate that there is a correlation between occupational exposure to this metal and lung cancer in workers. However, the possible mechanism of cadmium-induced carcinogenesis has not been adequately studied (Keshava et al., 2000).

DNA strand breaks, gene mutations, chromosomal aberrations, micronuclei, and cell transformation have been observed *in vitro* as a result of $CdCl_2$ exposure. Cadmium compounds inhibit the repair of DNA damaged by others agents, thereby enhancing their genotoxicity

(Keshava et al., 2000). $CdCl_2$ induces morphological transformation *in vitro* both in Balb/3T3 and in SHE cells (Saffiotti & Bertolero, 1989; Gibson et al., 1995).

Chromium. Chromium is a widely used industrial chemical, extensively used in paints, metal finishes, steel including stainless manufacturing, alloy cast irons, chromium and wood treatment. On the contrary Cr (III) salts such as chromium polynicotinate, chromium chloride and chromium piconilate, are used as micronutrients and nutritional supplements and have been demonstrated to exhibit a significant number of health benefits in rodents and humans (Bagchi et al., 2001).
Chromate compounds are well established as human carcinogens and are potently genotoxic at a number of *in vitro* and *in vivo* end points. The most toxicological active form of chromium is the hexavalent oxidation state that reacts with a number of reducing agents in cells, including glutathione and ribonucleotides. Cr (VI) is eventually reduced to the kinetically inert and stable trivalent form. During its reduction, intermediate oxidation states of Cr are thought to be important in Cr genotoxicity (Costa, 1991).
Cr (VI) induces morphological transformation *in vitro* in SHE cells (Elias et al., 1991). It has been shown to produce a variety of lesions in the DNA of mammalian cells, including single-strand breaks, alkaline-labile sites, DNA-DNA, and DNA-protein crosslinks. In addition, Cr (VI) is a very broad-acting genotoxic agent, as evidenced by its ability to directly induce lesions as well as to indirectly generate oxygen radicals and reactive intermediates. Cr (VI) is positive in almost every genotoxicity assay in which it has been tested (Costa, 1991).
DNA-protein complexes are considered lesions that, unlike the strand breaks and other DNA lesions, are readily repaired and relative persistent in cells. Thus these complexes are likely to be present during DNA replication machinery and could be important explaining Cr carcinogenic potential if the deleted DNA sequences code for tumour-suppressor gene or are involved in the regulation of these genes (Costa, 1991).

Platinum. The most common oxidation states are (II) and (IV) with a prevalence of planar tetra coordinate compounds, such as cisPt and $(NH_4)_2PtCl_4$, as well as hexacoordinate (IV) compounds with tetrahedral form. Platinum is present in the biosphere only as few parts per billion. The major amounts are principally in Siberia, South Africa and Canada (Wodd, 1974). A source of Pt pollution as new potential environmental pollutant is its use in catalytic converters containing Pt, Pd and Rh as active components (Petralia, 1994). This item can oxide CO, unburned hydrocarbons and nitrogen oxides. This property together with the use of poor mixture and the optimisation of their combustion cycle greatly reduced the automotive emission of pollutants. However, it was already observed that these metals are still released into the environment as traces (from 0.02µg to 1-2µg Pt/kg at a speed of 100 km/h). Their impact on different ecosystems is still unknown (Koning et al., 1989).

Concerning the health impact, it was shown that workers exposed to Pt compounds develop within few years respiratory diseases (asthma, rhinitis together with conjunctivitis and chronic bronchitis characteristic of “platinosis”) as well as skin diseases (e.g. contact dermatitis). The reason is assumed to be the sensitisation to soluble Pt compounds used as intermediate products of refining processes (i.e. $(NH_4)_2PtCl_6$, $(NH_4)_2PtCl_4$, H_2PtCl_6) and catalytic converters production (Petralia, 1994). Platinum compounds are in themselves not allergens because they have a low molecular weight. However, they can act as haptenes by binding high molecular weight carriers such as blood proteins. In some people this Pt-protein complex stimulates lymphocytes to produce specific antibodies against the allergen. Some studies demonstrated that Pt (II) reacts with human transferrin and with sulphur atoms of albumin, the most abundant plasma protein (Tryinda & Kuduk-Jaworska, 1994).

Epidemiological studies confirmed an increase of health risk particularly with chronic exposure (asthmatic and allergic symptoms, different forms of leukaemia, lung carcinoma, interactions with the lymphatic system and with DNA, chromosome abnormalities) (Petralia, 1994). *In vitro* studies have shown that $(NH_4)_2PtCl_4$, $PtCl_2$ and $PtCl_4$ are able to induce significant cytogenetic damage allowing the micronuclei formation either centromere-positive or centromere-negative (Migliore et. al, 2002a).

In the last decades, two Pt-based compounds, cis-$(NH_3)_2PtCl_2$ (cis-diamminedichloro(II)platin or cisPt) and 1,1-ciclobutane-dicarboxilate-diammine platin (carboPt), were among the widely used and effective anticancer drugs (against testicular, ovarian and genital-urinary cancer). However, many tumours develop resistance during therapy, while others have intrinsic resistance to cisPt and carboPt. Moreover, cisPt induces severe neuro- and nephrotoxicity. The lesser nephrotoxicity, nausea and ototoxicity of carboPt are probably due to its stability and lower proportion of reactive Pt-species available to react with renal tubules (Harrap et al., 1980; Laszlo 1983). Cytotoxicity and carcinogenicity of these Pt-compounds is believed to result from the formation of Pt-DNA adducts. In particular, the major adducts formed *in vitro* are the Pt-GG (guanine, guanine) and Pt-AG (adenine, guanine) intrastrand crosslinks (Terheggen et al., 1991). Some studies led to discovery of some interesting representatives of a new generation of Pt-based cytostatic drugs that are currently in clinical trials, such as lobaplatin (1,2-diamminethylcyclobutane platin(II) lactate) and oxaliPt (1,2-diamminecyclohexane platinum(II) oxalate). It was shown that there is a substantially higher rate of *in vitro* adducts formation by cisPt, compared with lobaPt and oxaliPt (Saris et al., 1996).

Vanadium. Vanadium has different oxidation states, from II to V, the tetravalent and the pentavalent being most common and stable in the environment. Vanadium represents 100-200 ppm of the earth’s crust and is widely distributed. For industrial purposes, vanadium salts are used as catalyst for the production of sulphuric acid, for colouring glass and ceramic glazes, for

accelerating the drying of paints and inks and for the oxidation of organic molecules such as benzene, aniline, toluene. Very high concentrations of vanadium are found in tobacco. Vanadium is an essential element in plants involved among others in the fixation of nitrogen. At the same time, its role in mammalian nutrition has been doubted. However, some studies seem to confirm that lack of vanadium induces retards in general and in skeletal growth and affects thyroid functions (Leonard & Gerber, 1994).

Vanadate compounds are cytotoxic and mitogenic, and modify several cell functions involved in mitosis. They are not clastogenic and only mildly, if at all, mutagenic at high exposure concentrations in bacteria. *In vitro*, V (IV) has been shown to modify DNA synthesis and repair (Sabbioni et al., 1991), Vanadyl sulfate and sodium orthovanadate stimulate the incorporation of thymidine into DNA of cultured quiescent Swiss mouse 3T3 and 3T6 cells in a manner similar to colchicine (Smith, 1983). Previous *in vitro* studies showed a dose-dependent carcinogenic potential of V (V) (but not V (IV)) in Balb/3T3 (Sabbioni et al., 1993b) and dose-time dependent in SHE (Kerckaert et al., 1996).

Vanadium acts on DNA in similar as but lesser way than chromium, particularly by forming of DNA-protein crosslinks (Nechay et al, 1986). Sodium vanadate produces *in vitro* structural aberrations, micronuclei, sister-chromatid exchange or satellite chromosome associations in human lymphocytes (Migliore et al., 1993).

No studies are known relating human cancer to vanadium exposure except for V_2O_5 classified as possible carcinogen by IARC (1990a). Also, there exists no evidence that vanadium and vanadium salts are carcinogenic to whole animals. However, vanadate may promote cell transformation and stimulation of phosphorylation of tyrosine kinases that might be considered in light of the relation of this enzymes to oncogenes. Moreover, the mitogenic action and the possible mutagenic effects make this element a candidate for carcinogenic risks (Leonard & Gerber, 1994).

1.2. Metal nanoparticles and the challenge to toxicology

Nanotechnology is a new fast emerging field that involves the development, manufacturing and measurement of materials and systems from the sub-micrometer down to a few nanometers (nm) range. This pervasive technology is expected to have a large economic and social impact in almost all sectors of industrial and scientific activity. Furthermore, the unique and diverse physicochemical properties of nanoscale materials suggest that toxicological properties may differ from the corresponding bulk materials (Bergamaschi et al., 2006).

Potential occupational and public exposure, through inhalation, oral ingestion, dermal absorption or by injection, of manufactured nanoparticles (mNPs), with particles size ≤ 100 nm probably will increase in the near future due to the ability of nanomaterials to improve the quality and performance of many consumer products as well as the development of therapeutic strategies and tests. However, there is still a lack of information about the impact on environment and on human health of mNPs as well as reliable data on risk assessment (Colvin, 2003).

In this context, the European Commission, through the Communication "Towards a European Strategy for Nanotechnology" (COM (2004) 338) in combination with the "European Action Plan for Nanosciences and Nanotechnologies" (COM (2005) 243) suggests a safe and responsible strategy to reinforce the EU's leading position in this Research and Development area, calling for increasing research using appropriate methods to assess the toxicological profile of mNPs. In particular, *in vitro* systems that could reduce, refine and replace animal methods (Hartung et al., 2004) are recommended to understand the mechanisms of action of mNPs (e.g., intracellular trafficking, metabolism, toxicological profile, carcinogenic potential).

To support this strategy, the Joint Research Centre of the European Commission (DG-JRC), has developed in the last years a research plan on nanoparticle toxicology based on an integrated approach combining cell-based *in vitro* assays with specific radiochemical and physicochemical facilities (Sabbioni et al., 2005). The experimental approach consists in the selection of mNPs to be studied, based on industrial interest, the assessment of their physicochemical characterisation and their testing to assess toxicological profile by *in vitro* systems relevant for human exposure.

In this work, we studied cobalt nanoparticles due to their industrial interest: metallic cobalt, as nanoparticle, is used in biology and medicine in different forms from the simplest, such as cobalt oxide, to complex organic compounds or biopolymers (Wang et al., 2005, Yang et al., 2006). Cobalt was used in this work as a "model" to study nanoparticles toxicology. In particular, we studied the cytotoxicity, carcinogenic potential and genotoxicity of cobalt nanoparticles (Co-nano) and cobalt chloride (Co^{2+}) in Balb/3T3 cell line. Thanks to the possibility to use radiolabelled compounds (^{60}Co-nano and $^{57}Co^{2+}$), we also studied Co-nano behaviour in cell culture medium and Co-nano and Co^{2+} uptake in the cellular system.

1.3. Genotoxic and epigenetic mechanisms of cancer

A crucial characteristic of preneoplastic and neoplastic cell populations is an excess of cell multiplication over cell death. The multistage concept of carcinogenesis implies that the rates of both cell birth and cell death are increased over those in the tissue of origin and the malignant tumours develop via a sequence of intermediary cell populations with increasing growth advantage over normal cells (IARC, 1987).

The epigenetic mechanism of the cancer refers to changes in gene expression caused by mechanism other than changes in the underlying DNA sequence. It involves modifications of the activation of certain genes, but not the basic structure of DNA. Additionally, the chromatin proteins associated with DNA may be activated or silenced. Epigenetic changes are preserved when cells divide. Most epigenetic changes only occur within the course of one individual organism's lifetime, but some epigenetic changes are inherited from one generation to the next.

In this context, the Morphological Transformation Assay with the Balb/3T3 cell line is a promising *in vitro* test to give general information about the potential of a compound to be carcinogenic, although it does not allow to discriminate if a carcinogen is genotoxic or not (Hayashi Y., 1992).

To better understand the mechanism of action of tested compounds we plan to apply a battery of tests using the same cell line, in particular the Balb3T3 cells. Regarding this battery of tests we took into account the Comet Assay and the Micronucleus Test. In particular the Comet and Micronucleus Assay give us the information about the genotoxicity or not of metals: the Comet allows detecting a general DNA damage, instead the Micronucleus will allow detecting both loss of chromosomes and events of break (Rojas E. et all. 1999).

Although our understanding of chromosome structure is incomplete, evidence suggests that chromosome abnormalities are a direct consequence and manifestation of damage at the DNA level; for example, chromosome breaks may result from unrepaired double strand breaks in DNA and chromosome rearrangements may result from misrepair of strand breaks in DNA. It is also recognised that chromosome loss and malsegregation of chromosomes (non-disjunction) are an important event in cancer and ageing and that they are probably caused by defects in the spindle, centromere or as a consequence of undercondensation of chromosome structure before metaphase. In the classical cytogenetic techniques, chromosomes are studied directly by observing and counting aberrations in metaphases. This approach provides the most detailed analysis, but the complexity and labour of enumerating aberrations in metaphase and the confounding effect of artefactual loss of chromosomes from metaphase preparations has stimulated the development of a simpler system of measuring chromosome damage (Fenech M., 2000), that is the development of the Micronucleus test.

Moreover, genotoxicity testing is an important part of the hazard assessment of chemicals for regulatory purposes (DHO, 2000). It is undertaken for two main reasons:

- to detect chemicals that might cause genetic damage, including point mutation, in germ cells, and thus increase the burden of genetic disease in human population
- to detect chemicals that might be carcinogenic (based on the assumption that mutagenesis is a key event in the process of carcinogenesis).

At this moment, the standard regulatory approach to genotoxicity testing is to use a tiered-testing scheme comprising at least two *in vitro* tests in the first level of the tier: a bacterial mutagenicity assay (OECD TG 471, Ames test using Salmonella or E. Coli) and a cytogenetics assay (OECD TG 473, usually a metaphase analysis either with human lymphocytes or with rodent cell lines) (Zeiger, 2001).

1.4. Tests for genotoxic hazards and carcinogenic potential *in vitro*

Until now the only regulatory accepted test to estimate the carcinogenic potential of chemicals still remains the *in vivo* life-time bioassay in rats and mice of both sexes, with full pathological analysis of all tissues (Van der Laan, 2000). This test is time-consuming, labour-intensive and costly, both financially and in terms of animal numbers and animal welfare. The rodent bioassay is used to detect complete carcinogens, as well as tumour promoters and co-carcinogens. Moreover, rat and mouse data do not correlate well, and extrapolating the information to humans is problematic (Gottman et al., 2001).

Carcinogenicity is a multistage process, which involves sequential genetic alterations in a single target cell (expression of oncogenes and/or tumour suppressor genes) (Lewin, 1997) and which cause subtle alterations in growth control and culminate in cells that are able to form malignant tumours (Maronpot, 1991).

In particular, in cell culture the phenomenon of morphological transformation involves changes in the behaviour and growth control of cultured cells characterised by one or more of the following in relation to the cell system considered (Yuspa, 1988): (i) alteration in cellular morphology; (ii) disorganised patterns of colony growth; (iii) acquisition of anchorage independent growth. Research to elucidate the mechanisms of carcinogenicity involves experimental animals, human clinical material, and *in vitro* cellular and molecular biological methods that are very useful for research.

During the workshop number 39 at ECVAM a review on the available cell transformation assay was done (Combes et al., 1999) and three different *in vitro* models were specifically mentioned:

- primary culture assay: Syrian Hamster Embryo cells (SHE). The end-point of the assay is the formation of transformed colonies. Cells are diploid and are used a few passages after the isolation of mixed population of embryonic cells which are at various stages of differentiation. SHE cells have a limited life-span in culture and rarely become tumourogenic, unless exposed to a carcinogen (Di Paolo, 1980)
- transformation assay with immortalised mouse fibroblast cell line: Balb/3T3 clone A31-1-1 and C3H/10T½. These cell transformation systems are based one the use of established spontaneously immortalised cell lines, which have an aneuploid karyotype. They grow in a monolayer on which transformed colony (foci) are scored (Reznikoff et al., 1973)
- human cell-based transformation system: the HaCaT cell line is derived by spontaneous immortalisation of normal human keratinocytes, most probably due to mutations in the p53 gene and the consequent loss of senescence genes. Until now no particular end-point to evaluate carcinogenicity in HaCaT has been found. Nevertheless, this cell line is a convenient model for studying tumour progression by various carcinogenic agents (Fusening & Boukamp, 1998).

Genetic toxicology tests are designed to detect mutations. The diversity and specifity of these tests, with respect to test species and genetic endpoints, may seem bewildering. The reasons for this diversity are that most test methods were adopted directly from existing genetic research systems by researchers for mutagen screening. The valididy of these tests is based on the assumption that DNAs in different organism are similarly susceptible to chemical or physical damages.

Since each genetic toxicology test measures only mutations in a single species with a specific genetic marker, a battery of several genetic toxicology tests is necessary to assess the mutagenicity of a chemical. Indeed, all regulatory agencies require a battery of genetic toxicology tests for mutagen identification, but the tests that are required for each battery are different.

The common tests conducted in recent years are listed in tables 2 and 3. In each test battery there are four basic types of tests: the bacterial mutagenicity assay, the mammalian cell mutagenicity assay, the *in vitro* chromosomal aberration assay, and the *in vivo* cytogenetic assay. The DNA repair assay is sometimes required to clarify questionable findings (Harvey al., 1997).

Table 2. Common *in vitro* genetic toxicology tests

Bacteria	*Salmonella typhimurium* (Ames Test)
	Escherichia coli or Salmonella
Mammalian Cells	
Gene mutations	Chinese Hamster ovary cells (CHO/HGPRT)
	Chinese Hamster ovary AS 52 cells (CHOAS52/XPRT)
	Mouse lymphoma cells (L5178/TK)
Chromosomal aberrations	Human peripheral blood lymphocytes (HPBL)
	Chinese Hamster lung fibroblasts (CHL)
	Chinese Hamster ovary cells (CHO)
DNA repair	Primary rat hepatocytes (unscheduled DNA synthesis; UDS)
	Primary human hepatocytes (unscheduled DNA synthesis; UDS)
Neoplastic transformation	Syrian hamster embryo fibroblast (SHE)
	BALB/3T3 mouse fibroblasts

Table 3. Common *in vivo* genetic toxicology tests

Cytogenetics		
	Chromosomal aberrations	
	Micronucleus	Mouse bone marrow erythrocytes
		Mouse peripheral blood erythrocytes
		Rat bone marrow erythrocytes
Gene mutations		
	Somatic Cells	Transgenic mice (Muta^{TM} Mouse and Big Blue^{TM})
		Human lymphocytes
	Germ Cells	Mouse dominant lethal test
		Mouse specific locus test
DNA Repair		Rat hepatocytes (unscheduled DNA synthesis; UDS)

We selected the Balb/3T3 model because it is one of the *in vitro* systems recently considered by the European Centre of Validation of Alternative Methods (ECVAM) for prevalidation exercises evaluating the cytotoxicity and the morphological transformation of chemicals (Hartung et al., 2003). This model has been applied at ECVAM as a screening test for several metal compounds (Mazzotti et all., 2001) and this is the first attempt to apply this methodology for nanoparticle studies.

The Balb/3T3 assay detects chemical carcinogens, but it is not able to discriminate between genotoxic-carcinogens and non-genotoxic-carcinogens. So it was proposed to set up a testing strategy including a battery of tests in which experiments of Cell Transformation Assay (CTA) are carried out in parallel to other *in vitro* genotoxicity tests (e.g. Comet assays and Micronucleus test) (Hartung et al., 2003).

Balb/3T3 Cell Transformation Assay. One of the most promising *in vitro* tests used to evaluate the carcinogenic potential of different organic and inorganic compounds is the Balb/3T3 clone A31-1-1 assay. Balb/3T3 cells are mouse fibroblast initially derived from mouse embryo by repeated cell passages (Aaroson & Todaro, 1968) and subsequently cloned to generate the line A31-1-1 that is typically used in the CTA (Kakunuga, 1973). These cells are contact-inhibited and grow at high dilution showing a low saturation density, 50-60% of plating efficiency, hypotetraploydia with telocentric and acrocentric chromosomes. They can be transformed in tissue culture by oncogene DNA, SV40 virus and murine sarcoma virus. They grow in monolayer showing a fibroblast-like morphology. The split period is about 16 hours and the cell division control is density-dependent. Even though this cell line has some specific characteristic of a transformed cell line (such as heteroploydia, infinite life span, high cloning efficiency, altered morphology in comparison with the primary culture, lack of anchorage-independent growth when treated with a carcinogenic compound and tumour formation when inoculated in nude mice after treatment) the spontaneous transformation frequency is low (about 10^{-5} foci/survived cells) (Little,1979), while the chemically induced transformation frequency is depending on concentrations of carcinogens, duration of the treatment and cell density (Aaroson & Todaro, 1968; Di Paolo et al., 1972).

The CTA assay using Balb/3T3 consists in the estimation of the concurrent cytotoxicity and morphological transformation. The duration of the test is 5 weeks in total (10 days for cytotoxicity and 5 weeks for morphological transformation) (Ponti et al., 2007). The end-point of the cytotoxicity is the formation of colonies (Colony Forming Efficiency, CFE) and of the neoplastic potential is the presence of type III foci (see below). Concentrations to be used for the CTA are previously determined by the study of cytotoxicity (80%-50%-20% of CFE). However, there is not a direct relationship between cytotoxicity and morphological transformation; in fact, some compounds show high cytotoxicity, but no morphological transformation (Kakunuga, 1973).

In the Balb/3T3 assay three kind of foci can be induced by chemical exposure:

- type I foci that show a very low overlapping and piling-up of cells
- type II foci are colonies that grow in a multilayer with ramification on the periphery
- type III foci are colonies with all the following characteristics: basophilic, dense multilayered, cells randomly orientated at focus edge, invasion into the monolayer, cells spindle-shaped

Only type III foci are considered tumourigenic because it was demonstrated that they induce neoplastic transformation in nude mice with a frequency of 85% (Saffiotti et al., 1984; IARC/INCI/EPA, 1985).

One of the major databases on Balb/3T3 was made by Matthews (Matthews et al., 1993) evaluating 168 chemicals, including 84 carcinogens and 77 non-carcinogens. The overall

concordance of the assay for 161 chemicals for which the results of carcinogenicity bioassays were available: 71% (104/147), with a sensitivity of 80% (64/80) and a specificity of 60% (40/67). Fourteen of the 161 chemicals gave an “intermediate” response in the Balb/3T3 assay and were not included in the correlation analysis. For chemicals active in the *Salmonella* assay, the Balb/3T3 assay had a sensitivity of 94% (43/46) and a specificity of 30% (7/23). For chemicals that were not active in the *Salmonella* assay, the Balb/3T3 assay had a sensitivity of 64% (21/33) and a specificity of 74% (31/42). This study showed that the Balb/3T3 assay can detect both carcinogenic chemicals and non-carcinogenic ones.

It is also worth noting that surveys of the published *in vitro* activities of 31 chemical entities, classified as Group I human carcinogens by the International Agency for Research on Cancer (IARC), showed that the use of several different cell transformation assays (in rodent and in human cells) exhibited a high level of predictivity (IARC, 1987). This is encouraging for a further development of cell transformation assays, particularly if they would be used for regulatory purposes.

Comet assay. The Comet assay is widely used in ecotoxicology (Cotelle & Ferard, 1999), in biomonitoring (Moller et al., 2000; Migliore et al., 2002b), and in clinical radiobiology (Olive, 1999). Its versatility allowes the investigation of DNA repair mechanisms, the detection of apoptosis and the study of alkylating, oxidizing and crosslinking agents such as metals, pesticides, opiates, nitrosamines and anticancer drugs (Rojas et al., 1999). This technique is a sensitive, easy to perform and rapid technique to evaluate the DNA damage in individual cells (Fairbairn et al, 1995). In particular, it permits the detection and quantification of DNA single strand and double strand breaks, crosslinks and alkaline-labile sites induced by a series of physical and/or chemical agents (Guillamet et al., 2004).

The principle of the test is remarkably simple: the cells are embedded in agarose and lysed, leaving unbroken DNA in a supercoiled state. Strand breaks relaxing the supercoiling are detected by electrophoresis, extending to the anode to form a comet-shaped structure, because in the cells with a damaged DNA, these fragments move to the anode and they produce the characteristic tail, or comet, typical of this assay. These comets can be either classified by visual examination or measured from morphological parameters obtained by image analysis and integration of intensity profile. Computed parameters include the comet tail length, the proportion of DNA in the tail (tail DNA) and derived parameters (e.g. olive tail moment) intended to combine information from both tail length and tail DNA (Tice et al., 1999).

Micronucleus test. The *in vitro* micronucleus assay is a mutagenicity test system for the detection of chemicals which induce formation of small membrane bound DNA fragments, i.e. micronuclei, in the cytoplasm of interphase cells. These micronuclei may originate from acentric

fragments (chromosome fragments lacking a centromere) or whole chromosomes which are unable to migrate with the rest of the chromosomes during the anaphase of cell division. The assay thus has the potential to detect the activity of both clastogenic (chromosome breakage) and aneugenic (loss of chromosomes) chemicals (Fenech & Morley , 1986).

Micronuclei originate mainly from chromosome breaks or whole chromosomes that fail to engage with the mitotic spindle when the cell divides. Micronuclei result from lesions/ adducts at the level of DNA or chromosomes, or at the level of proteins directly or indirectly involved in chromosome segregation (e.g. tubulin) (Kirsch-Volders et al., 2003). Formation of micronuclei originating from chromosome fragments or chromosome loss events requires a mitotic or meiotic division. The cytokinesis-block in the micronucleus cytome assay enables a comprehensive system for measuring DNA damage, cytostasis and cytotoxicity. DNA damage events are scored specifically in once-divided binucleated (BN) cells and include (a) micronuclei (MNi), a biomarker of chromosome breakage and/or whole chromosome loss, (b) nucleoplasmic bridges (NPBs), a biomarker of DNA misrepair and/or telomere end-fusions, and (c) nuclear buds (NBUDs), a biomarker of elimination of amplified DNA and/or DNA repair complexes. Cytostatic effects are measured via the proportion of mono-, bi- and multinucleated cells and cytotoxicity via necrotic and/or apoptotic cell ratios. Further information regarding mechanisms leading to MNi, NPBs and NBUDs formation is obtained using centromere and/or telomere probes. The assay is being applied successfully for biomonitoring of in vivo genotoxin exposure (Migliore et al., 2002b), *in vitro* genotoxicity testing and in diverse research fields such as nutrigenomics and pharmacogenomics (Fenech, 2007) as well as a predictor of normal tissue and tumor radiation sensitivity and cancer risk (Saran et al., 2008). The procedure can take up to 5 days to complete (Fenech, 2007).

The simplicity of scoring and the wide applicability of the *in vitro* micronucleus test in different cell types make it an attractive tool to assess cytogenetic abnormality. The addition of the actin inhibitor cytochalasin-B during the targeted *in vitro* mitosis allowed the identification of once-divided nuclei as binucleates and provided an efficient approach to study the mechanism leading to the induction of micronuclei. The cytochalasin B inhibits microfilament assembly and cytokinesis and thus prevents separation of daughter cells after mitosis and leads to binucleated cells. The evaluation can thus be limited to proliferating cells. Since the background frequency of micronuclei will influence the sensitivity of the assay, it is recommended that cell types with low and stable background frequency of micronuclei (lower than 30/1000 cells with cytochalasin B) are used in these study.

1.5. *In vitro* biokinetics

In vitro biokinetic studies on the absorption, distribution, metabolism and excretion (ADME) of chemicals are important for understanding their mechanisms of action. In this work, we studied the absorption, after long term exposure to low doses, of Cr (VI), As (III), Gentamicin and Ochratoxin A, in the intestinal barrier using the most promising *in vitro* Caco-2 cell model for intestinal absorption (Le Ferrec et al., 2001).

Long-term or repeated-doses toxicity tests are usually defined as studies of longer than three months duration *in vivo*. For rodents, this represents 10% or more of their life-span. The studies are conducted in all classes of laboratory animals (mammals, birds, fish etc.), including some economically important wild and domestic animals. Long-term toxicity encompasses the classic subchronic and chronic systemic toxicology studies, and carcinogenicity studies.

In vitro short-term testing refer to assays with exposure periods of up to 72h which reflect the maximum survival time of most conventional static culture systems without repeated renewal of culture the nutrient medium. Acute testing is usually related to administration of a single high dose of the test compound. Long-term testing is linked to exposure of appropriate *in vitro* systems over at least 5 days and is related to either continuous exposure of the system to low concentrations of a test compound, or to the repeated administration of a test compound in this study we considered *in vitro* long-term exposure more than 72 h and we exposed cells for 17-33 days.

Caco-2 cell line. Caco-2 cells derive from a human rectal colon cancer. In culture, they differentiate spontaneously into polarised intestinal cells showing an apical brush border and tight junctions between adjacent cells and they express hydrolases and typical microvillar transporters (Le Ferrec et al., 2001). The differentiation process starts after 7 days of confluence under standard culture condition and is completed after 14-21 days. They have high electrical resistance. They express typical membranous peptidases and disaccharides of the small intestine and also active transporters (e.g. amino acids, sugars, vitamins, hormones), membrane ionic transporters (Na^+/K^+ ATPases, H^+/K^+ ATPases, Na^+/H^+ exchange, $Na^+/K^+/Cl^-$ co-transport, apical Cl^- channels), membrane non-ionic transporters (permeability-glycoprotein, multidrug resistant associated protein) and receptors (vitamin B_{12}, vitamin D_3, epithermal growth factor, glucose transporters) (Chantret et al., 1994).

The human origin of this cell line avoids the animal inter-species differences concerning the morphological features of intestinal cells. It is a relatively fast, simple and flexible method. The Caco-2 model is well accepted for absorption studies. It is suitable for automation and high-throughput systems. Permeability data obtained with Caco-2 cell monolayers are used to predict quantitatively absorption in humans. It is a useful model to rank compounds according to their

permeability. The *in vitro* measurement of trans-epithelial permeability coefficient can be used to predict the oral absorption of compounds.

An interesting subclone of the parental Caco-2 cell line is Caco-2 TC7. It was isolated from a late passage of Caco-2 cells by the limited dilution technique. Characteristics of both cell lines are comparable, however, combing biochemical analysis and morphological characterisation it seems that the TC7 clone is closer to normal enterocytes as compared to parental CaCo-2 cells, with regard to structure of the glucose transporters associated with the brush-border. TC7 cells offer marked advantages because they express CYP 3A4, actively transport taurocolic acid, and have lower levels of P-glycoprotein. TC7 trans epithelial resistance values are lower than for Caco-2 and therefore closer to small intestine (Gres et al., 1998).

Chromium and gastrointestinal tract. It is well known that trivalent Cr as organic complex with nicotinic acid is the biologically active form being an essential element in human nutrition, while the hexavalent specie is toxic and carcinogenic to humans. For this, under nutritional situations Cr (VI) is rapidly reduced to Cr (III). The gastric juice has been shown to play a role in the detoxification of ingested hexavalent chromium by reducing it to trivalent form, which is poorly absorbed and eliminated with the faeces (De Flora & Boido, 1980).

The absorption of Cr is affected by the route of entry, its oxidation state, and the nature of its ligands. (Katz & Salem, 1994). Animal experiments indicate that Cr (III) is poorly absorbed from the gastrointestinal tract; values less than 1% of an oral dose have been reported (Mertz et al., 1969). Chromates are absorbed at 3-6% in rats (Mertz et al., 1965), and about 2% in man (Donaldson & Barreras, 1966). There is evidence that not only the valence state of chromium in the diet but also the functional state of intestines have a bearing on absorption, since the balance between Cr (III) and Cr (VI) may be altered (Donaldson & Barreras, 1966). Increased absorption of Cr (VI) has been observed in achylic patients, probably due to the absence of reduction of the hexavalent state by gastric juice. These absorption values, which are based on urinary excretion after oral administration, may be underestimated as the gastrointestinal tract also takes part in chromium excretion (Hopkins, 1965).

The toxicological effects of Cr compounds are mainly related to Cr (VI). The following symptoms and signs were reported in workers engaged in the production of chromium salts: hyperchlorhydria, elevated pepsin and pepsinogen level, oedema, hyperaemia and erosion of the mucosa, polyposis, dyskinesia and gastritis. However, other studies reported that the incidence of peptic ulcer in chromate workers was below the expected rate and that the mortality rate for diseases of the digestive system was lower in chromate workers than in the control population (Satoh et al., 1981).

Arsenic and gastrointestinal tract. It has been established that soluble inorganic arsenic is readily absorbed from the gastrointestinal tract of the human volunteers. For instance, between 80% and 90% of a single dose of arsenite, As(III), or arsenate, As(V), has been found to be absorbed from the gastrointestinal tracts of humans (Tam et al., 1979; Freeman et al., 1979; Pomroy et al., 1980). The most direct evidence is from measurement of fecal excretion in humans given oral doses of arsenite, wherein 5% was recovered in the feces (Bettley & O'Shea, 1975), indicating that absorption was at least 95%. This is supported by studies in which urinary excretion in humans was found to account for 55–80% of daily oral intakes of arsenate or arsenite (Buchet et al., 1981 a). In contrast (Mappes, 1977), ingestion of arsenic triselenide (As_2Se_3) did not lead to increase in urinary concentration, indicating that gastro intestinal absorption may be much lower when highly insoluble forms of arsenic are ingested.

Both short-term and chronic oral exposures to inorganic arsenicals have been reported to result in irritant effects on gastrointestinal tissues. Numerous studies of acute, high-dose exposure to inorganic arsenicals have reported nausea, vomiting, diarrhea, and abdominal pain, although specific dose levels associated with the onset of these symptoms have not been identified. Chronic oral exposure to 0.01 mg As/kg/day generally results in similar reported symptoms. For both acute and chronic exposures, the gastrointestinal effects generally diminish or resolve with cessation of exposure. Similar gastrointestinal effects have been reported after occupational exposures to inorganic arsenicals, although it is not known if these effects were due to absorption of arsenic from the respiratory tract or from mucociliary clearance resulting in eventual oral exposure.

Gentamicin and gastrointestinal tract. Gentamicin is an important antibacterial agent for the treatment of a wide variety of Gram-negative bacilli and Gram-positive cocci infections (Sande et al., 1990). However, its clinical use is limited to injection or topical dosage forms. In the case of intravenous (i.v.) therapy, many problems are associated with the use of gentamicin in injection form (i.e. low quality of life of the patients resulting from the inconvenience of injections for long-term administration). Parenteral administration of gentamicin has been associated with side effects that include mainly nephrotoxicity and ototoxicity (Kaloyandres & Munoz, 1980; Kitasato et al., 1990).

Many scientists have been challenged to develop new dosage forms of gentamicin to solve these problems. Alternative administration routes, such as the oral delivery was considered in order to improve the patients quality of life. However, it was observed that gentamicin has poor transmucosal permeability (Poretz, 1994; Recchia et al., 1995). Therefore, gentamicin is poorly absorbed from the gastrointestinal tract and it has a low oral bioavailability (Cox, 1970).

Ito et al. (Itoa et al., 2005) demonstrated that the bioavailability of gentamicin was greatly increased by formulating it in a self-microemulsifying drug delivery system using PEG-8

caprylic/capric glycerides (Labrasol). Labrasol is a safe pharmaceutical additive that shows high tolerance and low toxicity for animals permitting the absorbance of the drug by the rat's small intestines after oral administration (Hu et al., 2001).

Ochratoxin A and gastrointestinal tract. Ochratoxin A was discovered (Van der Merve et al., 1965) as one of the first group of fungal metabolites that are toxic to animals, which, with the aflatoxins, launched the distinctive and diverse science of mycotoxicology in the 1960s.

The compound is bioproduced only by some representatives of very few species of Aspergillus and Penicillium fungi, which are natural opportunistic biodeterioration agents of carbohydrate-rich agricultural commodities worldwide from latitudes ranging from cool temperate to tropical. The major cereal and legume seed commodities are particularly at risk, but the wide range of agricultural substrates includes coffee. It is important not to exaggerate the degree of natural contamination. Generally, the concentration of ochratoxin A does not exceed a few ppb. In very exceptional cases values of the order of 1 ppm have been detected, and at the low end of the scale increasingly sophisticated analytical methodology, involving the use of immuno-affinity columns, has revealed trace amounts of ochratoxin A quite widely in foodstuffs. The same methodology can find traces of the toxin in human serum, that match the intake of trace amounts in food, and even in human milk. More recently traces have been detected in some wines.

In 1993, the International Agency for Research on Cancer (IARC) classified ochratoxin A as a possible human carcinogen based on sufficient evidence in experimental animals and inadequate human evidence. However, if ochratoxin A is in any way carcinogenic, presumably it or a metabolite generated in animals can bind to DNA and change its function. In seeking experimental evidence of genotoxicity there is evidence that ochratoxin A does not bind to DNA (Mantle, 2002).

In Europe, there are wide variations both in consumption of the more risky foods, and in the occurrence of ochratoxin A in human serum. Therefore, if intakes are not greatly above what seems tolerable, the average intake means that some individuals exceed this value and so some people may be at risk. Also, individuals may differ in their sensitivity to ochratoxin A.

Intestinal absorptions of mycotoxins such as ochratoxin A measured by Avantaggiato et al. for gastrointestinal digestion showed (Avantaggiato et al., 2007) that, when no sequestering material was added to the feed (control), the absorption of mycotoxins occurred mainly from the upper part of the small intestine (jejunum) and less from the ileum.

2. AIM

In this work we studied the toxicological profile starting from basal cytotoxicity and going through carcinogenic potential and genotoxicity till toxic kinetics of selected chemicals. Additionally, manufactured nanomaterials (mNPs) were tested for their toxicological profile due to the increasing interest of the European Commission in understanding their potential impact on human health.

Since, for toxicological studies, a high animal number per test is used, we decided to concentrate the work on the most promising *in vitro* testing in order to contribute to the 3Rs policy (Reduction, Refinement, Replacement) that provides a strategy for a rational and stepwise approach to minimizing animal use without compromising the quality of the scientific work (Fentem et al., 1997).

In particular, mainly two *in vitro* models were used: (i) Balb/3T3 immortalised mouse fibroblast cell line to detect cytotoxicity, carcinogenic potential and genotoxicity and (ii) Caco-2 cell line as a model of human intestinal epithelial barrier for intestinal adsorption.

Using the Balb/3T3 cell transformation assay (CTA), we are able to discriminate among carcinogenic and non-carcinogenic compounds due to the formation of morphologically transformed colonies after the treatment of Balb/3T3 cells. In addition, to better understand the mechanism of action of the selected compounds which resulted positive in the CTA or of interest for other studies, we applied two tests i. e. the Comet assay and the Micronucleus test able to verify pre-mutational and mutational lesions. We believe that this battery of tests could be useful to evaluate the mechanism of action of chemicals on carcinogenicity.

Moreover in this work we also considered studies on *in vitro* toxicokinetic concerning adsorption, distribution, metabolism and excretion (ADME) of chemicals and nanoparticles since we consider then fundamental to understand their mechanism of action and their toxicological profile. In particular, we decided to study, in this work, the biokinetics (adsorption) both in *in vitro* model of intestinal epithelial barrier for intestinal adsorption (Caco-2 cells) and in single cells (Caco-2 and Balb/3T3). We evaluated the effect of Cr (VI), As (III), Gentamicin and Ochratoxin A in our cell models and mainly the potential toxicity of manufactured nanoparticles (mNPs).

In details, the aims of this study were:

1. to evaluate the mechanism of action of selected metal compounds using Balb/3T3 model by:
    - identification of compounds inducing neoplastic morphological transformation
    - optimization of existing protocols for genotoxic tests on Balb/3T3 cell model
    - determination of genotoxic potential with the Comet assay and the Micronucleus test of compounds identified as potential carcinogens

2. to investigate the biokinetics process using

- the *in vitro* model of intestinal epithelial barrier for intestinal adsorption, in particular the Caco-2 cell model, to determine the effect of Cr (VI), As (III), Gentamicin and Ochratoxin A on the integrity of the intestinal barrier by the measure of the Trans-Epithelial Electrical Resistance (TEER)
- the single cells, Caco-2 and Balb/3T3, with the uptake and the intracellular distribution, to identify where these compounds are accumulated in the cells

3. to identify a mechanistic approach of manufactured nanoparticles (mNPs) focusing on

- the physicochemical characterization of the selected mNPs and their behaviour in culture medium
- the determination of the basal cytotoxicity of the selected mNPs in Balb/3T3 cell line at a fixed exposure dose and the setting dose-effect relationships in order to establish the IC_{50} values
- the study of cobalt nanoparticles aggregates with regard to their carcinogenic and genotoxic potentials by the interaction with cells and their uptake

3. MATERIALS & METHODS

3.1. Source, solubility and purity of chemicals tested

Table 4 reports source, name, formula and CAS number of chemicals used in this study. Most of the compounds tested were dissolved in ultrapure water at the concentration of 10^{-2}M or 10^{-3}M by weighing suitable amounts of solid salt on AG 245 Mettler Toledo analytical balance and using a spatula covered by Teflon film. Every solution was sterilized under a laminar flow hood using a 10 mL sterile syringe equipped with 0.2 µm filters (Millipore, Italy) and stored at 4 °C in a dark environment for not more than one month. Before addition to complete culture media to obtain the appropriate tested solutions, the concentrated solutions were wormed for 5 min at 37 °C.

Elemental impurities of metal compounds tested were analyzed using analytical techniques such as Inductively Coupled Plasma Mass Spectrometry (ICP-MS, Perkin Elmer SCIEX-ELAN DRC II) or Graphite Furnace Atomic Absorption Spectrometry (GFAAS, Perkin Elmer IHGA Graphite tubes).

Due to problems of solubility $CdMoO_4$, CH_3HgCl, $PtCl_2$, cisPt and Ochratoxin salts were dissolved following specific protocols (Table 5) and their solubility was determined preparing 10 mL solution of 100 µM of each compound in culture medium (DMEM low glucose) and after centrifugation at 100.000 x g, 90 min (OPTIMAMAX 130.000 rpm, Beckman, USA), the concentrations of Cd, Hg or Pt was determined in the apical, central and basal parts of the tube by ICP-MS. For Ochratoxin the Standard Operating Procedure (SOP) provided by the supplier (SIGMA) was followed.

Table 4. Chemicals tested

Formula	Name	CAS number
Sigma-Aldrich, Milan, Italy		
$(C_6H_5)_4AsCl \cdot H_2O$	Tetra phenyl arsenic chloride	507-28-8
$Na_2HAsO_4 \cdot 7H_2O$	Sodium arsenate	10048-95-0
$NaAsO_2$	Sodium meta arsenite	7784-46-5
CH_3HgCl	Methyl mercury chloride	115-09-3
$PtCl_2$	Platinum (II) chloride	10025-65-7
$PtCl_4$	Platinum (IV) chloride	13454-96-1
$(NH_3)_2PtCl_2$	cis-Diammineplatinum(II)dichloride	15663-27-1
$[C_2H_6(CO_2)_2]Pt(NH_3)_2$	Carbo-platinum	41575-94-4
$C_8H_{14}N_2O_4Pt$	Oxali-platin	63121-00-6
$(NH_4)_2PtCl_6$	Ammonium hexachloroplatinate(IV)	16919-58-7
C_{19}-$21H_{39}$-$43N_5O_7 \cdot 2.5H_2SO_4$	Gentamicin	1405-41-0
$C_{20}H_{18}ClNO_6$	Ochratoxin A	303-47-9
Alfa Aesar, Milan, Italy		
$AgNO_3$	Silver nitrate	7761-88-8
$KAsF_6$	Potassium hexafluoride arsenate	17029-22-0
$NaAsF_6$	Sodium hexafluoride arsenate	12005-86-6
$(CH_3)_3As+CH_2COO^-$	Arsenobetaine (Asβ)	64436-13-1
$BeCl_2$	Beryllium chloride	7787-47-5
$CdCl_2 \cdot H_2O$	Cadmium chloride	34330-64-8
$CoCl_2$	Cobalt chloride	75-44-5
$Na_2CrO_4 \cdot 4H_2O$	Sodium chromate	10034-82-9
$NaVO_3$	Sodium vanadate	13718-26-8
Johnson Matthey, London, UK		
$HgCl_2$	Mercury chloride	7487-94-7
$NiSO_4 \cdot 7H_2O$	Nickel sulphate	7786-81-4
Trichemical Laboratory, Osaka-fu, Japan		
$CH_3AsO(OH)_2$	Mono methyl arsine oxide (MMA V)	124-58-3
CH_3AsO[a]	Mono methyl arsine oxide (MMA III)	25400-23-1
$(CH_3)_2AsOH$[b]	Di methyl arsine acid (DMA III)	

a: kindly supplied by Prof. Miroslav Styblo, University of North Carolina, Chapel Hill USA, synthesised by Prof. W.R. Cullen, University of British, Columbia, Canada

b: synthesized by Dr. Massimo Farina at EC, JRC-Ispra, ECVAM laboratory

Table 5. Preparation of CH_3HgCl (10^{-3} M), $PtCl_2$ (10^{-3} M), cisPt (10^{-3} M) and ochratoxin (10^{-3} M) solutions

CH_3HgCl
▪ Weigh 3 mg ▪ Dissolve the salt in 1mL DMSO[a] ▪ Add 9 mL ultrapure H_2O
$PtCl_2$
▪ Weigh 2.6 mg ▪ Dissolve the salt in 1 mL HCl ▪ Add 1 mL ultrapure H_2O ▪ Add 1 mL NH_4OH ▪ Add 7 mL ultrapure H_2O
cisPt
▪ Weigh 3 mg ▪ Dissolve the salt in 100 µL DMSO[a] ▪ Add 9.9 mL ultrapure H_2O
Ochratoxin A
▪ Weigh 0.4 mg ▪ Dissolve the salt in 1000 µL DMSO[a]
a: Dimethyl sulfoxide

3.2. Source of nano- and microparticles tested

Particles, in particular cobalt nanoparticles (Co-nano), were supplied in powder or suspended in diethyl glycol (DEG) solvent from the University of Modena and Reggio Emilia, Italy. Their size is about 80 nm. They were synthesized using different industrial patents (e.g. 15B, 20, 25, not reported in this thesis) and with or without organic/inorganic coating (c.1- c.2).

Stock suspensions were prepared at concentration of 10^{-2} M in sterile ultrapure water by weighing suitable amounts of particles powder on AG 245 Mettler Toledo analytical balance.

Stock suspensions in DEG were diluted in complete culture media at concentration of 10^{-2} M and DEG in testing suspensions was not more than 0.1 % (w/v).

Stock suspensions of cobalt nanoparticles aggregates, freshly prepared from powder, were washed by centrifugation (6.000 x g. 30 min), suspended in water, immediately ultrasonicated in ultrasonic bath (Transonic T 420, Elma, HF-Freq. 35 KHz) for 15 min and diluted at concentrations ranging from 1 to 100 µM in complete culture medium (Table 5).

Stock and testing suspensions of particles were prepared under sterile conditions in a biological hood but they were not sterilized in order to avoid any interference of this procedure. Anyway, the antibiotics added to the culture media were sufficient to maintain sterile conditions.

3.2.1. Physicochemical characterisation of Co-nano

Co-nano particles were characterized as to their purity, size, morphology and behavior in culture media using advanced physicochemical techniques. In particular, element impurities and behavior in culture medium (ions released) were analysed by Inductively Coupled Plasma Mass Spectrometry (ICP-MS) and Graphite Furnace Atomic Absorption Spectrometry (GFAAS, Perkin Elmer-SIMAA 6000); size distribution was studied by Dynamic Light Scattering (DLS: Zetasizer Nano-ZS, Malvern Instruments Ltd, UK) and by nanoparticles tracking analysis with NanoSight (LM20 Nanoparticles Analysis System, Salisbury, UK) and morphology by Scanning Electron Microscope (LEO 435P SEM-EDX).

Size distribution. Samples for size distribution analysis were prepared in water and culture media adding 100 µM of Co-nano, they were ultrasonicated as previously described and aliquots of 500 µL were immediately analysed by DLS and NanoSight.

Morphology. Samples for morphological analysis were prepared by deposition a 20 µL of water or culture media containing 10^{-2} M of Co-nano on silicon (0.5 x 0.5 cm). Drops were dried for 2 h under infrared lamp and immediately analysed by SEM-EDX technique.

Behaviour in culture medium. Ions released into culture medium were studied after incubation of Co-nano in complete culture medium from 2 to 72h in standard cell culture conditions (37 °C, 5 % CO_2, 95 % humidity; Heraeus incubator, Germany). After incubation, aliquots of culture medium were ultra-centrifuged (105.000 x g, 90 min) to separate particles (pellet) from ions (supernatant). Ion concentration was analysed by ICP-MS.

3.2.2. Determination of Co concentration in Co-nano suspension

One stock suspensions of Co-nano was prepared as described in Table 6 and diluted in complete Balb/3T3 culture medium to reach theoretical concentrations ranging from 10 to 300 µM. The analysis of Co content was carried out by GFAAS according to the analytical procedures previously reported (Farina, 2003).

Table 6. Suspension of 10^{-2} M Co-nano in culture medium

- Weigh 59 mg of Co-nano powder
- Add 10mL of complete culture medium
- Disaggregate particles by ultrasonic bath (15 min.)

3.2.3. Radiotracers and radioactivity counting

Table 7 shows radio-chemical characteristics of radioisotopes used in this work.

$Na^{73}AsO_2$ in 0.1M HCl was purchased from Amersham, Perkin Elmer Life Sciences, Boston. It was added to stable solution of $NaAsO_2$ 0.1 µM. ^{73}As radioactivity was measured by an automatic γ-counting system (Wallac 1480 3", Sweden) equipped with NaI (Tl) and using the characteristic line of 359 and 366KeV photon emission.

$^{57}Co^{2+}$ with high specific radioactivity was purchased as cobalt chloride by Amersham Biosciences, Milan, Italy. To prepare radiolabelled solutions, aliquots of $CoCl_2$ stock solution in water were added to sterile ultrapure water to reach concentrations ranging from 10 to 100 µM and they were equilibrated for 10 min at room temperature with an appropriate amount of ^{57}Co. Radioactivity was measured by an automatic γ-counting system (Wallac 1480 3") equipped with NaI (Tl) detector.

^{60}Co-nano were prepared by neutron irradiation of solid Co-nano in the nuclear reactor (HFR, Petten, Netherland) at a thermal neutron flux $2x10^{14}$ neutrons cm^{-2} sec^{-1}. Before incubation with cells, ^{60}Co-nano were washed as described above and added to culture medium to get concentrations of 10 µM and 20 µM of cobalt. ^{60}Co and ^{57}Co radioactivity was measured by automatic γ-counting system (Wallac 1480 3") equipped with NaI (Tl) detector, using the windows of 800-2000 KeV (^{60}Co) and 50-800 KeV (^{57}Co).

^{51}Cr as Na_2 [^{51}Cr] CrO_4 in aqueous saline solution was purchased from Amersham. It was used to prepare ^{51}Cr-labelled chromate solutions by adding the ^{51}Cr radiotracer to aliquots of stable $Na_2CrO_4 \cdot 4H_2O$ solutions in ultrapure water at final Cr concentrations ranging from 1 to 50 µM. Before their use, the oxidation state of the resulting solutions was tested according to Minoia's protocol (Sabbioni et al., 1993a) the hexavalent state of Cr being more than 99 %. ^{51}Cr radioactivity was measured by an automatic γ-counting system (Wallac 1480 3") equipped with NaI (Tl) detector and using the characteristic line of 320 KeV photon emission. At any time ^{51}Cr radioactivity was interpreted in terms of Cr concentration by comparison with ^{51}Cr standard solution of known specific radioactivity.

Gentamicin sulfate [^{3}H] and Ochratoxin A [^{3}H(G)] were added to stable solutions of 7 μM and 1 μM, respectively. Their radioactivity was measured by automatic β-counter system (Perkin Elmer, Wallac 1414 Win Spectral Liquid Scintillation counter, Italy).

Table 7. Radio-chemical characteristics of radioisotopes

$^{73}NaAsO_2$
▪ Physical state: solution in 0.1 M HCl ▪ Radioactive concentration: 625 MBq ml^{-1} ▪ Radiochemical purity: > 99.9% ▪ Physical data and sensitivity: - Decay mode: Electron Capture - $T_{1/2}$: 80.3 days - Main photon emission: 359 and 366 KeV ▪ Experimental limit of detection: 5 fg absolute of Co in the sample
$^{57}CoCl_2$
▪ Physical state: solution in 0.1 M HCl ▪ Radioactive concentration: 185 MBq ml^{-1} ▪ Radiochemical purity: > 99.3% ▪ Physical data and sensitivity: - Decay mode: Electron Capture - $T_{1/2}$: 271.7 days - Main photon emission: 122 and 136 KeV ▪ Experimental limit of detection: 5 fg absolute of Co in the sample
^{60}Co-nano
▪ Physical state: Co metallic ▪ Specific radioactivity: 22.2 MBq mg^{-1} Co ▪ Radiochemical purity: > 99% ▪ Physical data and sensitivity: - Decay mode: β-decay - $T_{1/2}$: 5.2 years - Main photon emission: 1173 and 1332 KeV ▪ Experimental limit of detection: 10 pg absolute of Co in the sample
$^{51}Na_2CrO_4$
▪ Physical state: saline solution ▪ Radioactive concentration: 185 MBq mL^{-1} ▪ Radiochemical purity: 99% ▪ Radionuclidic purity: 99.9% ▪ Physical data and sensitivity: - Decay mode: Electron Capture - $T_{1/2}$: 27.7 days - Main photon emission: 320 KeV (9.8%) ▪ Experimental limit of detection: 5 cpm (0.2 pg absolute of Cr in the sample)

Gentamicin Sulfate [^{3}H]

- Physical state: ethanol solution
- Specific radioactivity: 7,4 GBq g^{-1}
- Radiochemical purity: 99%
- Radionuclidic purity: 99%
- Physical data and sensitivity:
  - Decay mode: β-decay
  - $T_{1/2}$: 12.3 years

Ochratoxin A [^{3}H(G)]

- Physical state: ethanol solution
- Radioactive concentration: 37 MBq mL^{-1}
- Radiochemical purity: 98.6%
- Physical data and sensitivity:
  - Decay mode: β-decay
  - $T_{1/2}$: 12.3 years

3.3. Cell lines and cell culture procedures

In vitro studies were carried out using immortalised mouse fibroblasts (Balb/3T3 clone A31-1-1) and immortalised human intestinal epithelial barrier cells (Caco-2 clone AQ and clone TC7) (Photo 1). Cell lines were purchased from Istituto Zooprofilattico, Brescia, Italy and from Istituto superiore di sanità, Roma, Italy respectively and certified as bacteria, fungi and mycoplasma free.

Cells were maintained in standard conditions (37 °C, 5 % CO_2, 95 % of humidity; HERAEUS incubator). Standard cell culture procedures (growth and maintenance) are summarised in Tables 8 and 9.

They were counted using a "Bürker" chamber 0.0025 mm^2 (Blau-Brand, Germany) and Trypan blue staining solution (Sigma, Milan, Italy). Number of cells/mL was calculated by the following formula:

$N = (a / b) \cdot 10^4 \cdot DF$

where: N = number of cells / mL
a = number of cells counted in minimum 3 squares
b = number of squares considered (minimum 3)
10^4 = conversion factor of chamber volume
DF= Dilution Factor (usually equal to 2 or 10)

Table 8. Balb/3T3 cell line: cell culture procedures[a]

Cell line	Source
BALB/c 3T3 clone A31-1-1 / Mouse fibroblasts	Istituto Zooprofilattico, Brescia, Italy
Culture medium (500 mL)	
Dulbecco's Modified Eagle Medium (1X), liquid (Low Glucose) 1000 mg/L D-glucose, with L-Glutamine and Sodium Piruvate	GIBCO, Invitrogen Corporation, Italy
10 % v/v of Fetal Clone III serum, bovine serum product	HYCLONE, CELBIO, Italy
4.8 mM of L-Glutamine 200 mM (100X)	GIBCO
1% v/v of Fungizone liquid (250 µg/mL)	GIBCO
0.6 % v/v of Penicillin / Streptomycin Solution, liquid, 5000 U/mL Penicillin and Streptomycin 5000 µg/mL	GIBCO
Cell culture maintenance	
Seed $4x10^5$ cells (passages 78-83) in $75cm^2$ flask with 15 mL complete medium in order to get an 80% confluent culture in 4 days as follow ❑ 1^{st} day ▪ Wash cells twice (10 mL of Phosphate Buffer Solution (PBS) (1X) without calcium, magnesium and with sodium bicarbonate GIBCO) ▪ Replace PBS solution with 0.5 mL of trypsin/EDTA (1X), liquid, 0.5 g/L trypsin (1:250) and 0.2 g/L EDTA·4Na in Hanks' B.S.S., GIBCO ▪ Harvest cells (10 mL of fresh medium) ▪ Count and seed (15 mL of fresh medium) ❑ 2^{nd} day ▪ Change culture medium	
Freezing	
Add DMSO (10% v/v) and FC III (10% v/v) to culture medium (80% v/v) Store at -80 ºC (24 h) and then in liquid nitrogen	
a: Mazzotti et al., 2001	

Table 9. CaCo-2 cell line: cell culture procedures[a]

Cell line	Source
CaCo-2 / Human, Rectal Colon Adenocarcinoma	Istituto superiore di sanità, Roma, Italy
Culture medium (500 mL)	
▪ Dulbecco's Modified Eagle Medium (1X), liquid (High Glucose) 4500 mg/L D- glucose, without Sodium Pyruvate	GIBCO
▪ 10% v/v of FBS North America origin	GIBCO
▪ 4 mM of L-Glutamine 200 mM (100X)	GIBCO
▪ 1% v/v of Non essential amino acid (100 U/mL)	GIBCO
▪ 1% v/v of HEPES Buffer solution 1 M	GIBCO
▪ 1% v/v of Penicillin / Streptomycin Solution, liquid, 10000 U/mL Penicillin and 10000 µg/mL Streptomycin	GIBCO
Cell culture maintenance	
Seed $1x10^6$ cells (passages 80-90) in 75 cm^2 flask with 15 mL complete medium in order to obtain an 80 % confluent culture in 4 days	
❑ 1^{st} day	
▪ Wash cells twice (10mL of PBS solution)	
▪ Replace PBS solution with 1 mL of trypsin/EDTA (1X), liquid, 0.5 g/L trypsin (1:250) and 0.2 g/L EDTA·4Na in Hanks' B.S.S., GIBCO	
▪ Harvest cells (10 mL of fresh medium)	
▪ Count and seed (15 mL of fresh medium)	
❑ 2^{nd} day	
▪ Change culture medium	
Freezing	
▪ Add DMSO (10% v/v) and FC III (10% v/v) to culture medium (80% v/v)	
▪ Store at -80 °C (24 h) and then in liquid nitrogen	
a: Ponti, 2004	

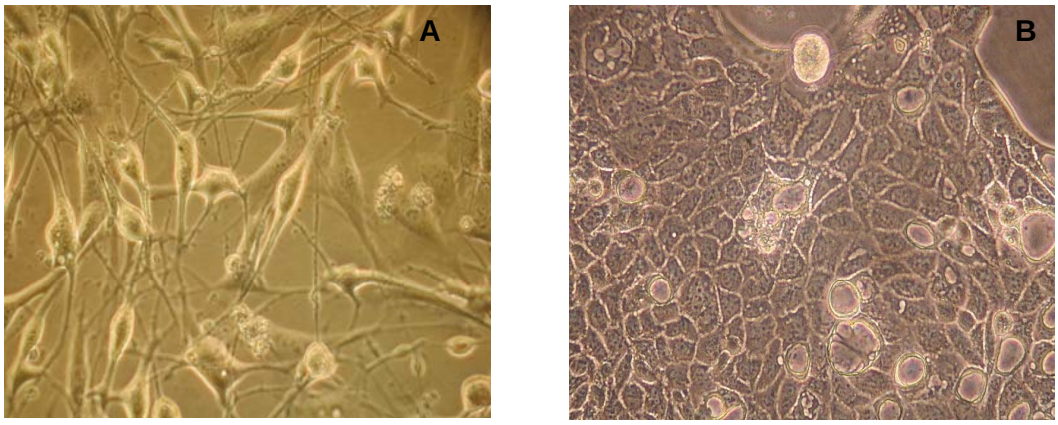

Photo 1. Balb/3T3 clone A31-1-1 (A) and Caco-2 clone TC7 cell lines in culture (inverted optic microscope Olympus, Italy)

3.4. Basal Cytotoxicity

Two different assays were used to evaluate the cytotoxicity of chemicals and nanomaterials (hereafter called testing material) in Balb/3T3 and Caco-2 cells: (i) 3-(4,5-dimethylthiazol-2-yl)-2,5-diphenyltetrazolium bromide (MTT) (Caco-2; Balb/3T3); (ii) Colony Forming Efficiency (CFE) (Balb/3T3).

3.4.1. MTT assays

MTT assays protocol is summarised in Table 10.

In order to choose the best number of cells/well (96well/plate, Falcon, Italy) to be seeded, a preliminary experiment was carried out seeding 10^3, $5x10^3$, 10^4, $5x10^4$ and 10^5 cells/well (6 replicates for every cell number). The viability after exposure to fresh complete medium was measured by a spectrophotometer (MTT: λ= 570 nm).

Results are expressed as relative viability of cells, assuming the absorbance of the control equal to 100 % of cell viability, and as mean of 3 experiments (6 replicates each treatment) with the corresponding Relative Standard Deviation (RSD % = (SD/average of the treatment) x 100)). The IC_{50} (concentration causing 50% reduction in growth compared to the control) value was interpolated from the graph of the dose-response curve (Ponti et al., 2006).

3.4.2. Colony Forming Efficiency (CFE)

The CFE test was used to evaluate the basal cytotoxicity of testing materials in Balb/3T3 cells. According to a previously reported protocol (Ponti et al., 2006), 200 cells were seeded in 4 mL of complete culture medium in 60 x 15 mm culture dish (Falcon, Italy) using 6 culture dishes for every treatment and control (complete medium) (Table 11).

After 24 h culture medium was replaced with fresh medium containing testing material at the appropriate concentrations. After exposure (2-72 h), the testing material containing medium was replaced with fresh complete medium that was changed twice/week.

Five days later the culture medium was removed, cells were washed with 4 mL PBS/dish for 10 min, fixed with 4 mL/dish of a 10% v/v in PBS formaldehyde 37% solution (Sigma) for 20 min and stained with 4 mL/dish of a 10 % v/v in Ultrapure water Giemsa stain stock solution (0.4 %) for 30 min. Dishes were rinsed with Ultrapure water and let to dry at room temperature.

Colonies with more than 50 cells were manually counted using a stereo Wild Heerbrugg microscope (Switzerland). CFE was expressed by number of colonies in the treated cultures as percent of those observed in untreated controls (CFE (%) = average of treatment colonies/average of control colonies) ×100) with the corresponding Relative Standard Deviation (RSD % = (SD x 100/average of the treatment). The IC_{50} value was calculated from the graph of the dose-response curve.

Table 10. MTT assay[a]

Reagents	Source
▪ Complete cell culture culture medium	(Table 9)
▪ MTT powder	SIGMA
▪ Phosphate Buffer Solution (1X) without calcium, magnesium and sodium bicarbonate (PBS)	GIBCO
▪ 96 well/plate	FALCON
▪ Lysing buffer (pH=4.7):	
20 g of Sodium Dodecil sulphate (SDS)	SIGMA
50 mL ultrapure water	
50 mL N,N-Dimethyl formammyde	SIGMA

Protocol

- ❑ 1st day
- ▪ Seed $3x10^4$ cells/well in 100 µL of fresh medium (6 wells per treatment)

- ❑ 2nd day
- ▪ Replace the fresh medium with 100 µL of testing solution/well

- ❑ 3rd day
- ▪ Add 20 µL/well of MTT solution (5 mg MTT/1 mL PBS)

- ❑ After 2h
- ▪ Add of 100 µL/well of lysing buffer solution

- ❑ 4th day
- ▪ Read absorbance at λ= 570 nm

a: Ponti et al., 2006

3.4.3. Colony Forming Efficiency (CFE) and Morphological Transformation assay (CTA)

Cytotoxicity and carcinogenic potential of testing materials were evaluated in the Balb/3T3 cell line using concurrent CFE and CTA (Bertolero et al., 1987; Mazzotti, 2001).
The protocol (Table 11) is divided into two parallel steps:

- evaluation of basal cytotoxicity by CFE
- evaluation of morphological transformation by Foci Type III formation.

We exposed cells to testing materials concentrations extrapolated from dose-effect relationship curves previously studied by CFE (data not shown) and corresponding to inhibitory concentrations of 20, 50 and 90% (IC_{20}, IC_{50} and IC_{90}).

Results concerning the morphological transformation were elaborated considering the following parameters:

- Plating Efficiency (mean of colonies in CFE dish x 100) / 200 cells seeded in every dishes)
- total number of seeded cells (number of dishes used for morphological transformation x 10.000 cells seeded in every dish)
- surviving cells ((total number of cells seeded x Platting Efficiency) / 100)
- Transformation Frequency (total number of foci type III per treatment / Surviving cells)

The significance of the Transformation Frequency was calculated using Fisher's exact test analysis selected as the best statistical analysis after comparison between Student's t-test (equal variances and unequal variances) and Fisher's exact test (Ponti et al., 2007) . The details of the statistical analysis are reported in the section "3.8. Statistical treatment of the data" that follows.

Table 11. CFE and morphological transformation assay[a]

Reagents	Source
▪ Balb/3T3 complete cell culture medium	(Table 7)
▪ Formaldehyde solution (37% formalin)	SIGMA
▪ Giemsa solution 0.4%	SIGMA
▪ Culture dish 60x15 mm	FALCON
▪ Phosphate Buffer Solution (1X) without calcium, magnesium and sodium bicarbonate (PBS)	GIBCO
▪ Ultrapure water	

Protocol

❑ 1st day

▪ Seed 200 cells/dish 60x15 mm in 4 mL of fresh medium (6 dishes per treatment) for CFE and 10^4cells dish 60x15 mm in 4 mL of fresh medium (20 dishes per treatment) for morphological transformation assay

❑ 2nd day

▪ Replace the medium with 4mL testing solution and treat for 72h

❑ 5th day

▪ Replace the tetsing solution with 4 mL of fresh complete culture medium

❑ 8th day

▪ Change the medium (4 mL)

❑ 11th day (end of CFE)

▪ Fix the colonies with 4mL/dish of formaldehyde solution 10 % v/v in PBS for 20 min.

▪ Stain colonies with 4 mL/ dish of Giemsa solution filtered solution 10 % v/v in ultrapure water for 30min.

❑ 11th day (morphological transformation)

▪ Change the medium (4 mL) and culture cells for 4 weeks changing medium every 3 days

❑ 40th day (end of morphological transformation)

▪ Fix the cells with 4 mL/petri dish 60x15 mm of formaldehyde solution 10 % v/v in PBS for 20 min.

▪ Stain the cells with 4mL/petri dish 60x15 mm of Giemsa solution filtered solution 10 % v/v in Ultrapure water

▪ Count the foci type III and estimate transforming frequency

a: Ponti, 2001

3.5. Genotoxicity studies

Study of the genotoxicity induced by testing materials was carried out using the Comet assay and the Micronucleus test (MN) in Balb/3T3 cell line (Table 12 and 13).

3.5.1. Comet assay

Four different runs were carried out for 3 different subtoxic concentrations of each testing materials, a control (only culture medium) and a positive control (H_2O_2, 300µM). In order to evaluate the cell viability (internal control of the experiment), cells were suspended in Fluorescein DiAcetate Ester (FDA) (Sigma) and Ethidium Bromide (EtBr) (Sigma) staining solution (30 µL of FDA stock solution: 5 mg/mL acetone + 200 µL of EtBr stock solution 0.2 mg/mL PBS 1X + 4.8 mL PBS). 400 cells/run were counted before the electrophoresis was run (Guillamet, 2001). The cell viability for each experiment was > 80%.

Data analysis was done using Komet Image Analysis system fitted with Olympus 3x50 fluorescein microscope equipped with a wide band excitation filter of 480-550 nm and a barrier filter of 590 nm. The DNA percentage in tail was measured for 25 cells per slide (total of 100 cells per treatment). The significance was evaluated by 1-way ANOVA statistical analysis.

Table 12. Comet assay

Reagents	Source
▪ Balb/3T3 complete cell culture medium	Table 8
▪ Phosphate Buffer Solution (1X) without calcium, magnesium and sodium bicarbonate (PBS)	GIBCO
▪ Ultrapure water	
▪ Trypsin / EDTA (1X)	GIBCO
▪ 6 well/plate	FALCON
▪ Glass slides and cover-slips	FORLAB, Carlo-Erba, Italy
▪ Normal melting point agarose	FLUKA, Italy
▪ Low melting point agarose	SIGMA
▪ FDA solution	SIGMA
▪ Ethidium Bromide	SIGMA
▪ Lysing solution (pH=10):	
NaCl (2.5 M)	SIGMA
Na_2EDTA (100 mM)	SIGMA
Tris (10 mM)	Carlo-Erba, Italy
DMSO (10%)	SIGMA
1% Triton X-100	SIGMA

- Electrophoresis buffer (pH=13.5):

Na_2EDTA (1mM)	SIGMA
NaOH (300 mM)	MERCK, Italy

- Neutralisation solution (pH=7.5):

0.4 M Tris	Carlo-Erba

- Absolute ethanol — Carlo-Erba

Protocol

Sample preparation

- ❑ 1st day
- Seed $6x10^5$ cells in every well of a 6-well tissue culture plate (Costar, Italy) with 4 mL cell culture medium
- ❑ 2nd day
- Remove the cell culture medium and treat the cells for 2 h with 4 mL of solution:

  Treatment: testing materials

  Negative control: culture medium

  Positive control: known genotoxic agent, H_2O_2 300 µM
- ❑ After 2 hours
- Remove testing material solution and collect in 50 mL tube (FALCON)
- Wash twice with 4 mL of PBS and collect in 50 mL tube
- Replace the PBS solution with 0.5 mL of trypsin/EDTA solution
- Harvest cells with 4 mL of fresh medium and collect everything in a 50 mL tube (FALCON)
- Count of the cells and centrifuge (200xg, 5 min.)
- Remove the supernatant
- Add 300µl of PBS.
- Separate in two aliquots: 20 µL ($6x10^4$ cells) and 10µL ($3x10^4$ cells)
- Analyse the first aliquot with comet assay and the second with FDA-EtBr viability assay (count 400 cells of each treatment)

Preparation of the slides

- Cover the slides with 150 µL of 0.5% normal melting point agarose (NMA) dissolved in Ultrapure H_2O
- Dry (65°C, 10 min.)
- Resuspend the 20 µL aliquot in 75 µL of 0.5% low melting point agarose (LMA) and add carefully onto the first agarose layer and immediately cover with a coverslip
- Allow the agarose solidify (4°C, 10 min.)
- Gently slide off the coverslip and add 75 µL of LMA
- Replace coverslip and allow the agarose solidify (4°C, 15 min.)

Lysing

- Remove the coverslip
- Immerse slides in cold fresh lysing solution (4 °C, 1 h, dark)

Electrophoresis

- Place slides on a horizontal gel electrophoresis tank and fill with cold electrophoresis buffer to allow DNA unwinding at 4 °C for 40 min.
- Electrophore (25 V, 300 mA) the slides in the same buffer (4 °C, 20 min.)

Neutralization

- Remove the slides from the horizontal gel electrophoresis tank
- Rinse twice with 0.4 M Tris (pH=7.5) for 5 min. at room temperature

Fixing

- Drain slides and fix with absolute ethanol for 3 min.

Staining

- Stain slides with 50 µL of EtBr in Ultrapure H_2O (1:6) just before analysis

Analysis

- View images through Komet Image Analysis system fitted with Olympus 3x50 fluorescein microscope equipped with a wide band excitation filter of 480-550 nm and barrier filter of 590 nm. 100 randomly selected cells (25 per run) are analysed and DNA % in tail is considered as the endpoint of the experiment

---

3.5.2. Micronucleus test

Balb/3T3 ($3x10^5$ in 4 mL complete culture medium) were seeded for 24 h in each well of a 6 well plate. They were treated for 24 h with 4 mL of testing material solution. Positive control was 0.5 µM Mitomycin C (MMC).

After treatment, cells were incubated for 24h with fresh medium containing cytochalasin B (4.5 µg/mL), they were washed twice with 4 mL of PBS and harvested in a 15 mL tube, centrifuged (200xg, 5 min.), suspended in pre-fixing solution (5:3 acetic acid/methanol) and centrifuged (200xg, 5 min.) supernatant was removed and cells were suspended in 5 mL of methanol and frosted at -20ºC 4h or overnight. After incubation in methanol, samples were centrifuged (200xg, 5 min) and fixed using fixing solution (1:5 acetic acid/methanol); this procedure was repeated twice. Samples were spotted on glass slides and stained with Giemsa solution (2:100 in H_2O) for 30 min.

Results were analysed calculating the binucleated micronucleated cells (BNMN) frequency as number of binucleated cells containing one or more micronuclei per 1000 binucleated. Moreover, 500 cells were scored to evaluate the percentage of mononucleated (MN), binucleated (BN), trinucleated and tetranucleated (polinucleated, PN) cells. The cytokinesis block proliferation index (CBPI) was calculated using the following formula: CBPI = (1xMN)+(2xBN)+(3xPN). CBPI was between 1 and 2 (Fenech, 2000).

For each treatment the increase in the frequency of binucleated cells with micronuclei (BNMN) was evaluated and considered statistically significant by using the F-Fisher's exact Test ($p<0.05$) (Agresti, 2002).

Table 13. Micronucleus test (MN)

Reagents	Source
▪ Balb/3T3 complete cell culture medium	Table 8
▪ Phosphate Buffer Solution (1X) without calcium, magnesium and sodium bicarbonate (PBS)	GIBCO
▪ Ultrapure water	
▪ Trypsin / EDTA (1X)	GIBCO
▪ Cytochalasin B	SIGMA
▪ 6 well/plate	FALCON
▪ Glass slides	FORLAB, Carlo-Erba
▪ Hypotonic solution: 0,075 M KCl solution in Ultrapure water	SIGMA (freshly prepared)
▪ Staining solution: Giemsa solution (4 % v/v) in Ultrapure water	SIGMA (freshly prepared)
▪ Prefixing solution: methanol : acid acetic = 3:5	SIGMA; Fluka, (freshly prepared)
▪ Fixing solution: methanol : acid acetic = 7:1	SIGMA; Fluka, (freshly prepared)

Protocol

Sample preparation

❑ 1st day

Seed 3x10^5 cells in every well of a 6-well tissue culture plate (Corning Costar) with 4 mL complete cell culture medium

❑ 2nd day

▪ Remove the cell culture medium and treat cells for 24 h with 4 mL of solution

Treatment: testing materials

Negative control: culture medium

Positive control: known mutagenic agent, MMC 0.5μM

❑ 3rd day

▪ Remove testing solution and add 10μL of cytocalasin B (4.5 μg/ mL) for 24 h

❑ 4th day

Hypotonic solution

▪ Warm ipotonic solution at 37 °C
▪ Remove testing material solution
▪ Wash twice with 4 mL of PBS

- Replace the PBS solution with 0.5 mL of trypsin/EDTA solution
- Harvest cells with 4 mL of fresh medium
- Centrifuge (200xg, 5 min)
- Remove the supernatant and wash pellet with 10 mL PBS
- Centrifuge (200xg, 5 min)
- Remove PBS leaving 500 µL PBS
- Mix pellet gently using glass Pasteur pipette
- Add slowly 1 mL hypotonic solution

Prefixing solution

- Add 80 µL prefixing solution and mix slowly using Pasteur pipette
- Centrifuge (200xg, 5 min)
- Remove the supernatant leaving 500 µL solution
- Mix pellet gently using glass Pasteur pipette
- Add 1 mL methanol
- Leave samples and slides at -20 °C for 4 h or overnight

Fixing solution (repeat twice the procedure described)

- Centrifuge (200xg, 5 min)
- Remove the supernatant leaving 500 µL solution
- Mix cells using vortex
- Add 1 mL fixing solution and mix

Slide preparation

- Centrifuge (200xg, 5 min)
- Remove the supernatant leaving 500 µL solution
- Put drops on cold slides (previously incubated at -20 °C) using Pasteur pipette (2 slides each sample)
- Dry samples at room temperature

Staining solution

- Leave slides in 5% Giemsa solution for 10 min.
- Dry samples at room temperature

Analysis

- Analyse cells using optic microscope (objective 20X)

3.6. Biokinetics studies with Caco-2 cells: short- and long-term toxicity

Biokinetics studies (kinetics of transfers, uptake and intracellular distribution) were carried out in the Caco-2 cell line exposed from 0 to 33 days to $Na_2{}^{51}CrO_4$ and from 0 to 17 days to $Na^{73}AsO_2$, Gentamicin Sulfate [^{3}H] and Ochratoxin A [^{3}H(G)] using a 6-well insert system (Table 14, Figure 1).

Cells were examined daily under an inverted optic microscope (Olympus, Italy) to control their level of confluence, morphology and any singhs of microbiological contamination. Trans-Epithelial Electrical Resistance (TEER), expressed using the formula below, measured the epithelial integrity by the Millicell®-ERS system (MILLIPORE, Italy) before and during the experiment to control the influence of the treatment on the epithelium.

$TEER = (R_{total} - R_{blank}) \cdot A\ (\Omega cm^2)$

R_{total} = resistance measured

R_{blank} = resistance of control filters without cells

A = surface of the filter ($4.2cm^2$)

6 well plates insert system $4.2cm^2$ membranes (FALCON plastic) were treated in the apical compartment (fresh medium in the basolateral, apical to basolatoral exposure) and in the basolateral compartment (basolateral to apical exposure).

For the short-term exposure, after 14 days of culture, cells were exposed to 2.5 mL of radiolabelled chromium solutions at 1, 30 and 50 µM from apical to basolatoral and from basolateral to apical exposures.

For the long-term exposure, cells were exposed to 2.5 mL of chromium radiolabeled solutions at 1 µM for 0-33 days from apical to basolatoral compartment. Continuous exposure were done by replacing the chromium solutions at days 1, 3, 6, 10, 13, 18, 21, 26 and 29; discontinuous exposure by adding the chromium solutions at days 1, 6, 13, 21 and 29 and replacing fresh medium at days 3, 10, 18 and 26.

Aliquots of 100 µL of Cr solution were taken out at time 0, 1, 2, 5, 7 and 24 h during the short-term exposure and at days 1, 3, 6, 10, 13, 18, 21, 26, 29 and 33 during long-term exposure from the apical and the basolateral compartments and counted by γ-counter.

The same approach was used to study the adsorption of $Na^{73}AsO_2$, Gentamicin Sulfate [^{3}H] and Ochratoxin A [^{3}H (G)]. Cells were exposed discontinuously by replacing the toxic solutions at 1, 7, 14 days and replacing fresh medium at days 3, 10 and 17.

Aliquots of 100µL of As, Gentamicin and Ochratoxin A solutions were taken out at time 0, 1, 2, 4, 24 h and days 1, 2, 3, 7, 10, 14 and 17 during long-term exposure from the apical and the basolateral compartments and counted by β-counter (1:3 sample/scintillation liquid).

The determination of the fluxes of Cr, As, Gentamicin and Ochratoxin between the two compartments in absence of cells (blank) were carried out in order to assess potential losses due to possible interaction with the walls and membrane of the insert. For short-term exposure, 3 different concentrations of Cr (0.022, 1 and 50 µM) were considered. While, for long-term exposure, we followed 0.1 µM $Na^{73}AsO_2$, 0.7 µM Gentamicin Sulfate [^{3}H] and 1 µM Ochratoxin A [^{3}H(G)] for 0-17 days. Aliquots of 100µL medium from apical and basolateral compartments were collected and counted by γ- and β-counter (1:3 sample/scintillation liquid), respectively.

We expressed results of the transport graphically as concentrations (ng/ mL) of Cr, As, Gentamicin and Ochratoxin in function of time considering the apical and basolateral exposures.

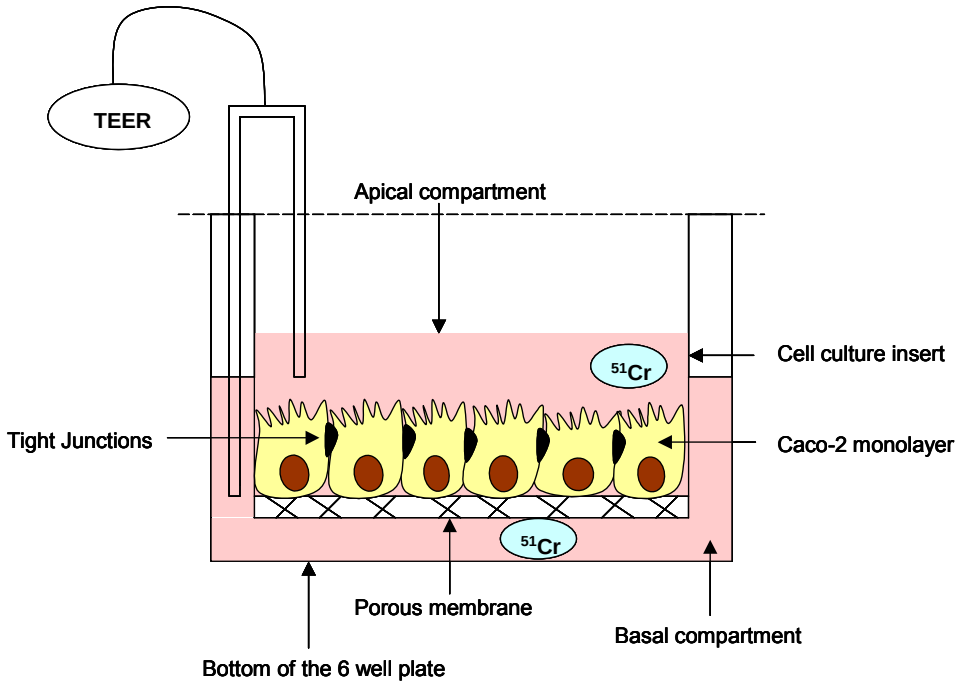

Figure 1. Schematic insert system used for the study of the effect of Cr (VI) on the epithelial intestinal barrier, its transfer among the insert compartments and the uptake by Caco-2 cells

Table 14. Kinetics of transfers, uptake and intracellular distribution

Reagents	Source
▪ Caco-2 Culture Medium	(Table 9)
▪ 6 well plates	FALCON
▪ Insert membrane (pore diameter 0.4 µm, surface 4.2 cm^2)	FALCON

Protocol

❑ 1st day

- Seed 750.000 cells/insert/2.5 mL fresh complete medium (3 wells per treatment, apical compartment)
- Add 2.5 mL of complete culture medium in the basolateral compartment
- Change medium twice/week

❑ 14th day

- Replace the medium with 2.5 mL of testing solution in the apical compartment or basolateral compartment and treat (exposure times from 24 h to 33 days)

Kinetics of transfers

- Take out 100 µL of medium in both the apical and the basolateral compartments
- Count the aliquots by γ-counter (Cr and As) or β-counter (Gentamicin and Ochratoxin)

Uptake

- Harvest both dead (cell in suspension) and alive cells using a scrubber
- Count cells by a "Bürker" chamber 0.0025 mm^2 (Blau-Brand, Germany)
- Wash pellet three times using PBS
- Count the amount of Cr, As, Gentamicin and Ochratoxin in the samples by γ-counter or β-counter

Intracellular distribution (Edel & Sabbioni, 1993)

- Homogenate the sample (1 mL of 10 mM cacodilate buffer (pH=7.4))
- Prepare subcellular fractionation (by differential ultracentrifugation, Uptima-max ultracentrifuge, 130000 rpm, Beckman, USA):

Nuclear fraction	700xg, 10 min
Mitochondria fraction	9000xg, 15 min
Lysosomes fraction	30000xg, 25 min
Cytosol and microsomal fraction	105000xg, 90 min

3.7. Cell morphology

3.7.1. Confocal microscopy

Confocal microscopy was used to study Balb/3T3 morphology after 24 h of exposure to $CoCl_2$ (1, 30, 100 μM) and Co-nano (1, 7, 100 μM). 10^4 cells were seeded on glass slides in 100 μL complete cell culture medium. Cells were incubated under standard cell culture conditions for 24 h. After incubation with testing solutions, cells were washed once with PBS and fixed with 4 % v/v paraformaldehyde (Sigma) in PBS (10 min, room temperature). Following permeabylisation with 0.2 % v/v Triton X-100 (Sigma) in PBS (1 min, room temperature), non-specific binding sites were blocked by incubating cells with 3 % BSA/10 % goat serum/PBS (30min, room temperature). Fixed cells were stained with Alexa Fluor 488 (green)-conjugated phalloidin (Invitrogen, Italy) (1 h, room temperature) in order to visualise actin according to the manufacturer's protocol. To view nuclei, cells were fixed and permeabilised as described above, incubated with propidium iodide (Invitrogen, Italy) (20 $\mu g \cdot mL^{-1}$ in PBS) for 10 min in the dark and washed twice with PBS. Samples were analyzed using confocal microscopy (Biorad Radiance 2000, Italy).

3.7.2. Scanning electron microscopy

$2x10^3$ cells/ 2 mL complete culture medium were seeded on sterile 0.25 cm^2 silicon supports in 35x10 mm dishes (Costar). Cells were incubated in standard cell culture conditions for 24h. Samples were exposed to Co-nano suspensions at concentrations ranging from 1 to 100 μM for 24 h. After exposure cells were washed twice with PBS and fixed using Karnosky solution (over night incubation) and dehydrated using increasing concentrations of ethanol solution (from 10 % v/v to 100 % v/v). Fixed samples were treated using Critical Point Dryer technique (K850, Emitech Ltd, Ashford, Kent, UK). Samples were analysed by SEM-EDX technique (LEO 435P SEM-EDX).

3.8. Statistical treatment of the data

3.8.1. CFE and MTT

Means and standard deviations (SD) were determined for each experiment in which the metal-induced cytotoxicity was investigated by Excel functions. The results were expressed as the mean of percentage inhibition of CFE and viability (by MTT) relative to the control and RSD (%). Experiments were independently performed at least three times (6 replicates/run).

3.8.2. Cell Transformation Assay and Micro Nucleus

The determination of the significances of foci type III scored in relation to the number of cells survived and of the number of micronuclei in the control in 1000 BNMN cells in respect to the treatment in 1000 BNMN cells were carried out by F-fisher's exact test analysis (Agresti, 2002) for each treatment. In this context, data were processed by the web-site (http://www.matforsk.no/ola/fisher.htm) as reported in Figure 2.

3.8.3. Comet assay

According to the recent publication of Duez (Duez et al., 2003) we adapted our experimental design to be able to use the 1-way ANOVA (Graph Pad Prism 4,San Diego, USA) to estimate the significance of DNA damage.

Four runs per treatment and analysed 25 cells per run were carried out. The median was extracted for each run. The 4 median treatments were then tested with 1-way ANOVA test. Given an overall ANOVA p-value<0.05, a post-hoc Dunnett's-test was applied to compare the treatments against the negative control.

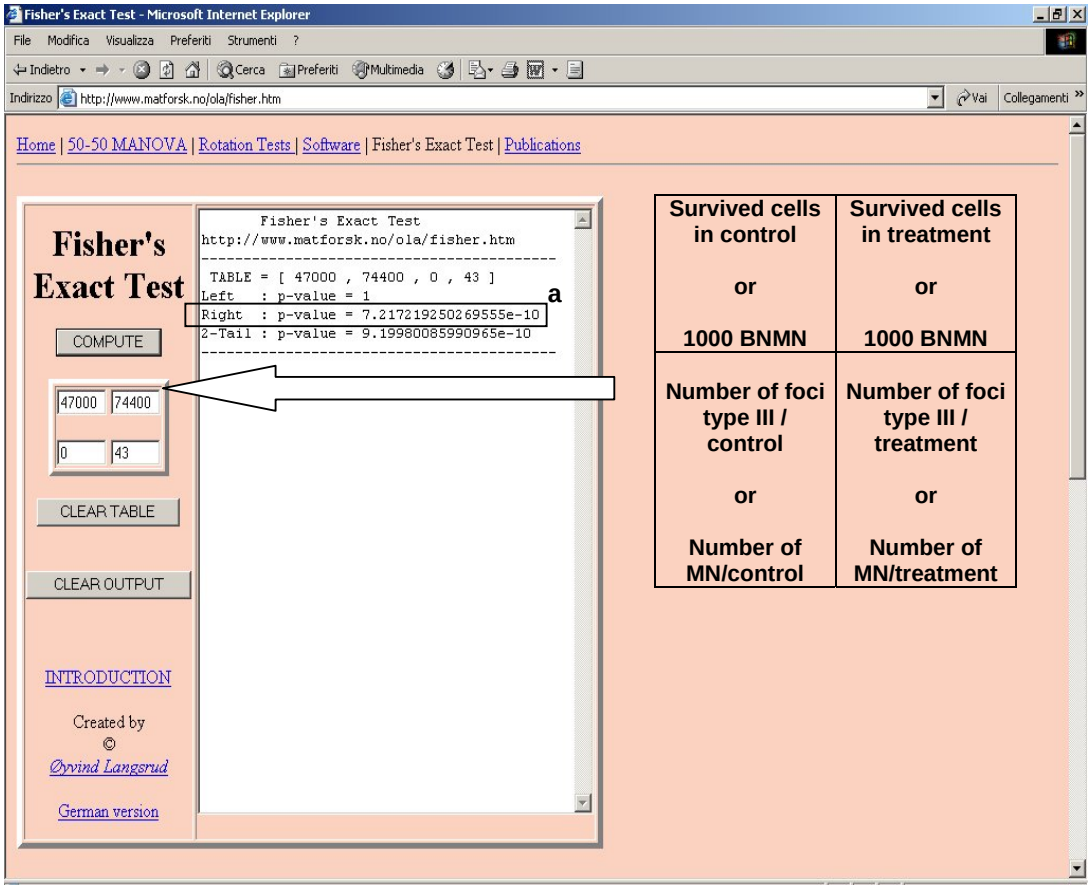

Figure 2. Web site page of Fisher analysis

a: "p-value right" was considered. $p<0.05$/number of treatment means statistically significant results (according to Bonferroni approach)

4. RESULTS

4.1. Screening

In order to determine the cytotoxicity, the carcinogenic potential and the genotoxicity induced by the selected chemicals in Balb/3T3 cell line, we performed a screening of these compounds tested with the Cell Transformation Assay, the Comet and the Micronucleus tests. This allowed us to divide the chemicals into 3 groups of cytotoxicity based on their capability to inhibit the growth of Balb/3T3 cells measured by Colony Forming Efficiency (CFE). In particular, group 1 represents low cytotoxicity (CFE>80%), group 2 medium cytotoxicity (50%<CFE<79%) and group 3 high cytotoxicity (CFE<49%).
The concentrations of chemicals tested in the Cell Transformation Assay (CTA, carcinogenic potential), Comet assay and Micronucleus (MN, genotoxicity) were selected by dose-effect relationships. In general, inhibitory concentrations (IC) corresponding to $IC_{20,}$ IC_{50} and IC_{90} were tested in the CTA as well as MN and IC_{10}, IC_{20} in the Comet Assay.
In addition, since a key aspect in the study of carcinogenicity and genotoxicity of chemicals is their purity, at the beginning of our study we carried out a chemical characterisation considering both their solubility in water and culture medium as well as their purity (see below).

4.1.1. Solubility of $CdMoO_4$, CH_3HgCl, $PtCl_2$ and cisPt

Since it is known that $CdMoO_4$, CH_3HgCl, $PtCl_2$ and cisPt are not easily soluble, their solubility under our experimental conditions was checked by ultracentrifugation (100 µM of each compound in DMEM) and analysis of Cd, Hg and Pt in apical, central and basal aliquots of the supernatant were analysed by ICP-MS (see Material and Methods, section Source and Solubility of metal compounds). The results (not reported here) show that the concentrations of salts in culture medium are close to those expected (100 µM).

4.1.2. Elemental analysis of metal compounds

A key aspect in the study of the carcinogenic potential of metal compounds concerns their chemical purity. If impurities of chemically similar elements are present in the metal compound under study and they are much more toxic than the metal species to be tested, they could create, false positive results. For this reason we carried out the determination of more than 30 elemental impurities in the metal compounds tested in carcinogenicity/genotoxicity studies by ICP-MS. Table 15 presents typical results regarding $Na_2CrO_4 \cdot 4H_2O$ and $NaAsO_2$ as examples.

In the Cr salt elemental impurities ranged from 0.0009 µg g^{-1} to 10 µg g^{-1} for Lu and Fe respectively, while the corresponding values for $NaAsO_2$ were 0.0008 µg g^{-1} and 20 µg g^{-1} for Cs and Fe. In any case, under the experimental conditions used, the estimated concentration of the elements as contaminants in culture medium did not exceed 0.01 µM. In conclusion, we can reasonably exclude, under our experimental conditions, artefacts due to impurities (Mazzotti et all., 2002).

Table 15. Elemental impurities in Na_2CrO_4 and $NaAsO_2$ salts used for carcinogenicity/genotoxicity studies

Element	Concentration			
	Cr (VI)		As (III)	
	µg g^{-1}	µM[a]	µg g^{-1}	µM[a]
Ag	0.07	0.0015	0.002	0.002
Al	0.1	0.01	3	20
As	0.08	0.0025	-	-
Au	0.0006	0.000005	0.02	0.007
Bi	0.2	0.0025	0.05	0.03
Cd	0.005	0.0001	0.1	0.2
Ce	0.004	0.00005	-	-
Co	0.004	0.00015	0.05	0.1
Cr	-	-	0.7	20
Cs	0.002	0.000035	0.0008	0.0008
Cu	-	-	0.1	0.3
Fe	10	0.41	20	50
Hg	-	-	0.8	0.05
Ir	0.0008	0.00001	0.002	0.6
La	0.005	0.0001	-	-
Lu	0.0009	0.00001	-	-
Mn	1.5	0.065	0.3	60
Mo	1	0.025	0.09	0.1
Ni	1.7	0.065	-	-
Pb	0.007	0.0001	0.09	0.06
Pd	0.0005	0.00001	0.002	0.002
Pt	0.002	0.000025	10	0.6
Ru	0.001	0.000025	-	-
Rh	0.004	0.0001	0.002	0.002
Sb	0.14	0.0025	0.2	0.2
Sc	0.003	0.00015	0.03	0.01
Se	1	0.03	0.4	0.7
Sn	0.1	0.002	0.03	0.03
Sr	0.02	0.0005	0.01	0.02
Ta	0.07	0.001	0.01	0.007
Th	0.001	0.00001	0.002	0.001
Tl	0.001	0.00001	-	-
U	0.001	0.00001	0.002	0.0008
V	2	0.09	40	100
W	0.1	0.0015	0.06	0.4
Zn	6	0.21	-	-

a: concentration of 100 µM of each compounds in culture medium under our experimental conditions

4.1.3. Cell Transformation Assay in Balb/3T3 cells

In this section we report results obtained from the study of carcinogenic potential evaluated by the counting of the type III foci (end-point for carcinogenicity in Balb/3T3 cells) formed by Balb/3T3 cells exposed for 72h to selected chemicals, in relation to the number of survived cells (experimental procedures, section Colony Forming Efficiency and Morphological Transformation assay). The cytotoxicity was measured counting the number of colonies formed after 72h of exposure and expressed as Colony Forming Efficiency (CFE, % of the control).

Table 16 shows results of cytotoxicity and morphological neoplastic transformation in Balb/3T3 cell line induced by chemicals divided into the 3 groups of cytotoxicity. The statistical significance of the difference to the control was evaluated by F-fisher exact test analysis and in Table 16 we indicate them as significant (S) or not significant (NS).

In particular, the following results were found:

- the compounds show a CFE ranging from 100% to 1% of the control for $KBrO_3$ (10 μM) and $MnSO_4$ (70 μM), respectively
- morphological neoplastic transformation was statistically significant ($p<0.05$/number of treatment) for $(C_6H_5)_4AsCl{\cdot}H_2O$ (7 μM), Na_2HAsO_4 (20-30 μM), $NaAsO_2$ (5-6 μM), $AuCl_3$ (70 μM), $CdMoO_4$ (5 μM), $CdCl_2$ (1-3-5-6 μM), $Na_2CrO_4{\cdot}4H_2O$ (30-50-60 μM), CH_3HgCl (0.3-0.5 μM), $(NH_4)_2IrCl_6$ (100 μM), $PtCl_2$ (0.1-0.3-0.5-0.7 μM), $PtCl_4$ (10 μM), cisPt (0.5-0.7 μM), carboPt (1-3 μM), $(NH_4)_2PtCl_6$ (7 μM), $Na_2TeO_3{\cdot}H_2O$ (5 μM) and $NaVO_3$ (3-6-10 μM)
- morphological neoplastic transformation was not statistically significant for $La(NO_3)_3{\cdot}6H_2O$ (300 μM), $BeCl_2$ (100 μM), $(C_6H_5)_4AsCl{\cdot}H_2O$ (3-5 μM), $NaAsO_2$ (3 μM), $Bi(NO_3)_3{\cdot}5H_2O$ (25-40 μM), $CdMoO_4$ (5 μM), $Ga(NO_3)_3{\cdot}6H_2O$ (50 μM), CH_3HgCl (0.1 μM), $(NH_4)_2IrCl_6$ (70 μM), $(NH_4)_3IrCl_6{\cdot}H_2O$ (50-70 μM), $PtCl_4$ (7 μM), Oxali Pt (0.5-1-3 μM), $Na_2TeO_3{\cdot}H_2O$ (10-50 μM) and $NaVO_3$ (1 μM)
- no morphological neoplastic transformation was found for $Al(NO_3)_3{\cdot}9H_2O$ (50-100 μM), $BeCl_2$ (50 μM), $KBrO_3$ (10-50-100 μM), $NiSO_4{\cdot}7H_2O$ (50-100 μM), $SnCl_2{\cdot}2H_2O$ (50-100 μM), $UO_2(NO_3)_2{\cdot}6H_2O$ (50-100 μM), $Na_2WO_4{\cdot}2H_2O$ (50-100 μM), $AgNO_3$ (5 μM), MMA (III) (from 0.03 to 0.05 μM), DMA (III) (from 1 to 50 μM), $AuCl_3$ (80 μM), $(C_6H_5)_2BNa$ (30 μM), $Bi(NO_3)_3{\cdot}5H_2O$ (10-25 μM), $CdMoO_4$ (3 μM), $CuSO_4{\cdot}5H_2O$ (30-50 μM), $Ga(NO_3)_3{\cdot}6H_2O$ (30-70 μM), $HgCl_2$ (10-30 μM), $Pb(NO_3)_2{\cdot}6H_2O$ (50-100 μM), $MnSO_4{\cdot}5H_2O$ (30-70 μM), $PtCl_4$ (1 μM), carbo-Pt (0.7 μM), $(NH_4)_2Pt(SCN)_6$ (30-50 μM), $(C_5H_5)_2VCl_2$ (3-5-7 μM) and $(NH_4)_2WS_4$ (3-5 μM).

Table 16. Cell Transformation Assay in Balb/3T3 cell line: screening of 39 chemicals

Compound	[µM]	CFE[a] (%)	Plating efficiency (%)	N° type III foci	Survived cell	Tf ($x10^{-4}$)[b]	F-fisher[c]
Group 1							
Control	-	100					
$BeCl_2$	50	84	20.5	0	34440	-	-
$BeCl_2$	100	81	20.5	1	33210	0.3	0.45 (NS)
Group 2							
$NiSO_4 \cdot 7H_2O$	50	79	18.5	0	29230	-	-
$NiSO_4 \cdot 7H_2O$	100	65	18.5	0	24050	-	-
Group 3							
$AgNO_3$	5	89	72.2	0	128516	-	-
$(C_6H_5)_4AsCl \cdot H_2O$	3	75	72.2	1	108300	0.09	0.43 (NS)
$(C_6H_5)_4AsCl \cdot H_2O$	5	62	72.2	2	89528	0.22	0.15 (NS)
$(C_6H_5)_4AsCl \cdot H_2O$	7	13	72.2	11	18772	5.8	$4.7x10^{-11}$ (S)
$Na_2HAsO_4 \cdot 7H_2O$	20	28	61.7	9	34560	3	$4.4x10^{-5}$ (S)
$Na_2HAsO_4 \cdot 7H_2O$	30	11	52.2	9	11520	8	$4.4x10^{-7}$ (S)
$NaAsO_2$	3	53	31.4	2	33300	0.6	0.17 (NS)
$NaAsO_2$	5	12	90	5	21600	2	$3.1x10^{-3}$ (S)
$NaAsO_2$	6	5	31.4	9	3140	28	$1.3x10^{-12}$ (S)
MMA (III)	0.03	90	29.4	0	53000	-	-
MMA (III)	0.05	67	29.4	0	40000	-	-
MMA (III)	0.1	53	29.4	0	21600	-	-
MMA (III)	0.3	12	29.4	0	5000	-	-
MMA (III)	0.5	9	29.4	0	6400	-	-
DMA (III)	1	91	46.5	0	83720	-	-
DMA (III)	5	87	46.5	0	80040	-	-
DMA (III)	10	85	46.5	0	78200	-	-
DMA (III)	50	5	46.5	0	4600	-	-
$CdCl_2 \cdot H_2O$	1	86	87.2	6	150000	0.4	$9x10^{-3}$ (S)
$CdCl_2 \cdot H_2O$	3	42	89.3	12	75000	1.6	$5.6x10^{-7}$ (S)
$CdCl_2 \cdot H_2O$	5	27	68.5	12	37000	3.2	$9.2x10^{-9}$ (S)
$CdCl_2 \cdot H_2O$	6	16	60.6	7	19400	3.6	$1x10^{-6}$ (S)
$Na_2CrO_4 \cdot 4H_2O$	30	67	52.5	19	70400	0.3	$3.2x10^{-8}$ (S)
$Na_2CrO_4 \cdot 4H_2O$	50	38	52.5	21	39600	0.5	$1.8x10^{-12}$ (S)
$Na_2CrO_4 \cdot 4H_2O$	60	16	69	31	22000	1	$1.9x10^{-27}$ (S)
$HgCl_2$	10	83	25	0	41500	-	-
$HgCl_2$	30	29.4	45.5	0	26754	-	-
CH_3HgCl	0.1	25	25	1	50000	0.2	0.5 (NS)
CH_3HgCl	0.3	4.4	45.5	22	4004	55	$5.9x10^{-31}$ (S)
CH_3HgCl	0.5	3.5	45.5	5	3185	16	$4.4x10^{-8}$ (S)
$PtCl_2$	0.1	79	44.9	6	70942	0.8	$7x10^{-3}$ (S)
$PtCl_2$	0.3	87	44.9	16	78126	2	$5x10^{-6}$ (S)
$PtCl_2$	0.5	73	44.9	8	6554	12	$4.6x10^{-10}$ (S)
$PtCl_2$	0.7	60	44.9	6	53880	1.1	$3x10^{-3}$ (S)
$PtCl_4$	1	48	48	0	46080	-	-
$PtCl_4$	7	27.4	48	2	26304	0.7	0.04 (S)
$PtCl_4$	10	6.7	48	2	6432	3.1	$4x10^{-3}$ (S)
CisPt	0.5	42	50.5	7	21210	3.3	$2x10^{-4}$ (S)
CisPt	0.7	19	23	2	8740	2.3	0.02 (S)
CarboPt	0.7	73	16.7	0	24382	-	-
CarboPt	1	56	16.7	7	18704	3.7	$8x10^{-4}$ (S)
CarboPt	3	22	16.7	30	7348	40.8	$5x10^{-23}$ (S)
OxaliPt	0.5	97	25	4	46172	0.9	0.05 (NS)

Compound	[µM]	CFE[a] (%)	Plating efficiency (%)	N° type III foci	Survived cell	Tf ($x10^{-4}$)[b]	F-fisher[c]
OxaliPt	1	101	25	2	50096	0.4	0.2 (NS)
OxaliPt	3	48	25	2	11232	1.8	0.03 (S)
$(NH_4)_2PtCl_6$	7	65	20.5	6	26650	2.2	$4x10^{-3}$ (S)
$NaVO_3$	1	84	40.6	2	68208	0.29	0.2 (NS)
$NaVO_3$	3	64	26	9	33300	2.7	$2x10^{-3}$ (S)
$NaVO_3$	6	27	40.6	11	21960	5	$4.6x10^{-8}$ (S)
$NaVO_3$	10	11	40.6	9	8932	10	$1x10^{-9}$ (S)

a: percentage of the control, average of 3 experiments,6 replicates each; RSD<20%
b: Tf= Transformation Frequency
c: p<0.05/ number of treatment: S= Statistically Significance; NS= No Statistically Significance

Photo 2-6 illustrate examples of the wild-type confluent Balb/3T3 cells after 5 weeks of culture and the typical type III focus (endpoint for carcinogenicity) induced after 72h of exposure to $(C_6H_5)_4AsCl{\cdot}H_2O$, $NaAsO_2$, cisPt, carboPt, $PtCl_2$ and $PtCl_4$.

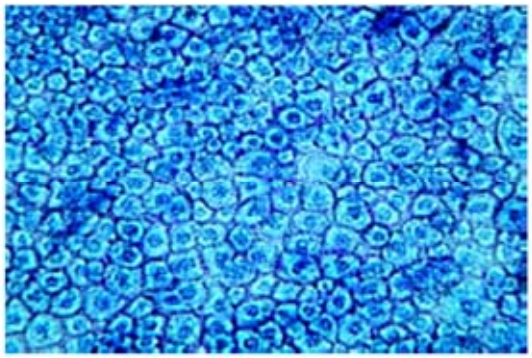

Photo 2. Balb/3T3 cells in monolayer after 5 weeks of culture (control)

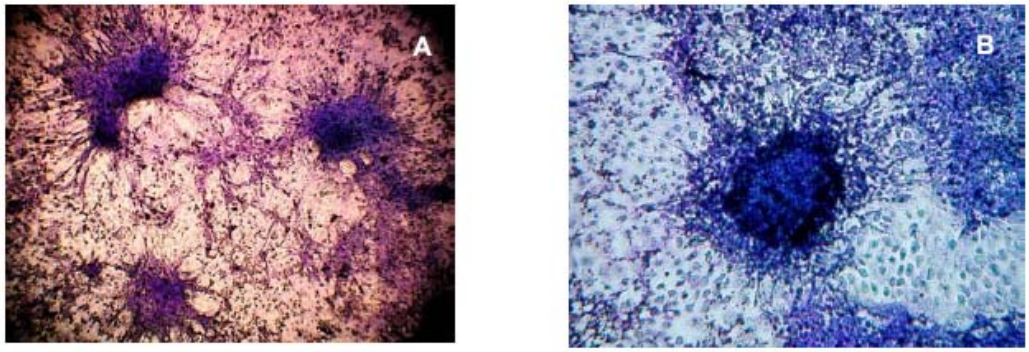

Photo 3. Type III foci induced in Balb/3T3 by exposure to $(C_6H_5)_4AsCl$ 3 µM (A) and $NaAsO_2$ 10 µM(B) for 72h

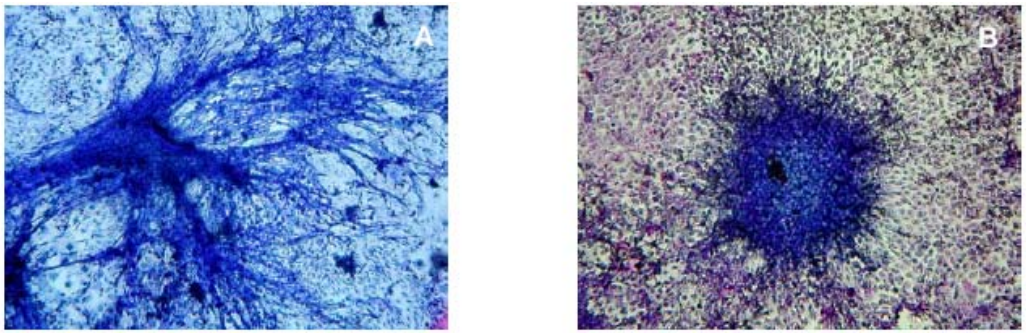

Photo 4. Type III foci induced in Balb/3T3 by exposure to cisPt 1 µM (A) and carboPt 1 µM (B) for 72h

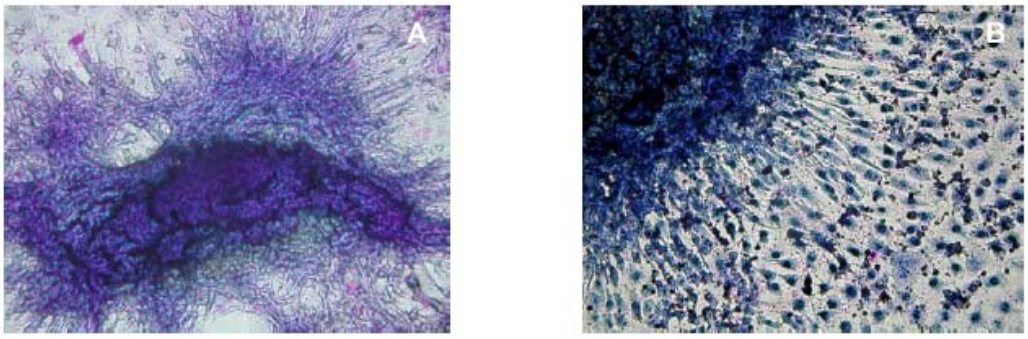

Photo 5. Type III foci induced in Balb/3T3 by exposure to CarboPt 3 µM (A) and CarboPt 1 µM (B) for 72h

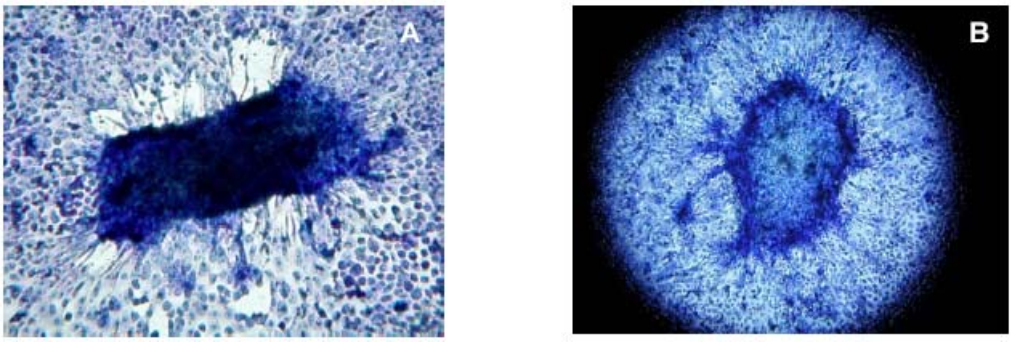

Photo 6. Type III foci induced in Balb/3T3 by exposure to $PtCl_2$ 7 µM (A) and $PtCl_4$ 10 µM (B) for 72h

4.2. Genotoxicity studies

In order to understand the mechanism of action of the selected compounds, in particular if they are genotoxic or not, we performed the Comet assay and the Micronucleus test (MN). The concentrations of the metal compounds were selected by previous screening of dose-effect relationships and they corresponded to inhibitory concentrations (IC) roughly of IC_{20}, IC_{50} and IC_{90} for MN and IC_{10}, IC_{20} for Comet Assay.

Tables 17 and 18 show DNA damage (single and double strand breaks) expressed as percentage tail of DNA (Table 17) and chromosomal aberration expressed as frequency of binucleated micronucleated cells (BNMN) (micronucleus formation) induced by selected chemicals respectively (Table 4).

The statistical significance difference in respect to the control was evaluated by Dunnett's-test ($p<0.05$) for Comet assay and F-fisher exact test analysis for MN. In Tables 17 and 18 we indicated it as significant (S) or not significant (NS).

Figures 4-7 show graphically results obtained from Comet assay of As, Hg, Pt speciation and $AgNO_3$, $BeCl_2$, $NiSO_4$, $CdCl_2$, $Na_2CrO_4.4H_2O$, $NaVO_3$.

The following results were obtained:

4.2.1. Comet assay

- statistically significant DNA damage was observed for: $NiSO_4$ (200 μM), $AgNO_3$ (7-10 μM), Na_2HAsO_4 (10-30-50 μM), $NaAsO_2$ (1-5-7 μM), CH_3AsO (0.05-0.1 μM), $(C_6H_5)_4AsCl\cdot H_2O$ (10 μM), $CdCl_2$ (0.03-0.05-0.1 μM), $Na_2CrO_4\cdot 4H_2O$ (5-7 μM), CH_3HgCl (0.1-0.3-0.5 μM), $HgCl_2$ (5-10-20 μM), OxaliPt (1-3 μM), $PtCl_2$ (1-3-5 μM), $PtCl_4$ (5-10-30 μM), $(NH_4)PtCl_6$ (1-5-10 μM), $NaVO_3$ (3-5-10 μM)
- no statistically significant DNA damage was observed for: $KAsF_6$ (100-200 μM), $NaAsF_6$ (100-200 μM), MMA(V) (100-200 μM), Asβ (100-200 μM), $(C_6H_5)_4AsCl\cdot H_2O$ (1-50 μM), $BeCl_2$ (100 μM), $Na_2CrO_4\cdot 4H_2O$ (1 μM), $NiSO_4$ (100 μM), CisPt (0.1-5-3 μM), CarboPt (0.1-5-3 μM)

4.2.2. Micronucleus test

- a statistically significant increase in the BNMN (micronucleus formation) is observed for: $NiSO_4$ (100 μM), $AgNO_3$ (1 μM), $Na_2CrO_4\cdot 4H_2O$ (10 μM), OxaliPt (1 μM), $PtCl_2$ (0.1-0.3 μM), $PtCl_4$ (10 μM), $(NH_4)_2PtCl_6$ (1-5-10 μM), CisPt (0.5-0.7 μM), CarboPt (5-7 μM).
- no statistically significant increase in the BNMN (micronucleus formation) is observed for: $KAsF_6$ (100 μM), $NaAsF_6$ (100 μM), MMA(V) (100 μM), Na_2HAsO_4 (10-30 μM), $NaAsO_2$ (0.1-1-5 μM), CH_3AsO (0.01-0.3 μM), $(C_6H_5)_4AsCl\cdot H_2O$ (1 μM), Asβ (100 μM), $BeCl_2$ (100 μM), CH_3HgCl (0.5-0.7 μM), $PtCl_4$ (1-5 μM), CisPt (0.1 μM), CarboPt (1 μM), $NaVO_3$ (1-5-10 μM).

The majority of the tested compounds positive by the Comet assay are also positive by the MN with some exceptions such as cis-Pt and carbo-Pt. In particular, they are negative in the Comet assay but positive in MN suggesting an induced genotoxicity due to chromosomal aberration and not to single strand breaks or double strand breaks. In fact, in accordance with the literature, these compounds interact with the DNA (Saris et al., 1996).

Another interesting example is the CH_3HgCl compound that results genotoxic by Comet assay but no by MN probably due to its ability to produce free radicals that can cause DNA damage (Silva-Pereira et al., 2005).

Table 17. Comet assay in Balb/3T3 cells exposed to different compounds for 2h at concentrations ranging from 0.05 to 200 µM

Compound	[µM]	CFE (%)[a]	DNA in tail (%)[b]	ANOVA (p<0.05)[c]	Dunnett's-test (p<0.05)[d]
H_2O_2	300	85	26-70[e]		
control	-	100	3-10[f]		
Group 1					
$KAsF_6$	100	92	20	<0.01	>0.05 (NS)
$KAsF_6$	200	88	12		>0.05 (NS)
MMA(V)	100	97	15	<0.01	>0.05 (NS)
MMA(V)	200	82	16		>0.05 (NS)
Asβ	100	94	5	<0.01	>0.05 (NS)
Asβ	200	88	7		>0.05 (NS)
$NaAsF_6$	100	87	5	<0.01	>0.05 (NS)
$NaAsF_6$	200	81	4		>0.05 (NS)
$BeCl_2$	50	99	10	<0.01	>0.05 (NS)
$BeCl_2$	100	92	16		>0.05 (NS)
Group 2					
$NiSO_4$	100	85	8	<0.01	>0.05 (NS)
$NiSO_4$	200	66	22		<0.01 (S)
Group 3					
$AgNO_3$	7	81	37	<0.01	<0.01 (S)
$AgNO_3$	10	10	30		<0.01 (S)
Na_2HAsO_4	10	96	30	<0.01	<0.01 (S)
Na_2HAsO_4	30	91	41		<0.01 (S)
Na_2HAsO_4	50	80	46		<0.01 (S)
$NaAsO_2$	1	91	40	<0.01	<0.01 (S)
$NaAsO_2$	5	84	41		<0.01 (S)
$NaAsO_2$	7	80	39		<0.01 (S)
MMA (III)	0.05	72	45	<0.01	<0.01 (S)
MMA (III)	0.1	63	40		<0.01 (S)
$(C_6H_5)_4AsCl \cdot H_2O$	1	98	32	<0.01	>0.05 (NS)
$(C_6H_5)_4AsCl \cdot H_2O$	10	96	33		<0.05 (S)
$(C_6H_5)_4AsCl \cdot H_2O$	50	56	33		>0.05 (NS)
$CdCl_2$	0.03	98	30	<0.01	<0.01 (S)
$CdCl_2$	0.05	93	37		<0.01 (S)
$CdCl_2$	0.1	90	35		<0.01 (S)
$Na_2CrO_4 \cdot 4H_2O$	1	92	17	<0.05	>0.05 (NS)
$Na_2CrO_4 \cdot 4H_2O$	5	87	41		<0.05 (S)
$Na_2CrO_4 \cdot 4H_2O$	7	80	56		<0.01 (S)

Compound	[µM]	CFE (%)[a]	DNA in tail (%)[b]	ANOVA (p<0.05)[c]	Dunnett's-test (p<0.05)[d]
$HgCl_2$	5	95	32	<0.01	<0.01 (S)
$HgCl_2$	10	91	36		<0.01 (S)
$HgCl_2$	20	86	40		<0.01 (S)
CH_3HgCl	0.1	84	20	<0.01	<0.01 (S)
CH_3HgCl	0.3	70	19		<0.01 (S)
CH_3HgCl	0.5	53	21		<0.01 (S)
OxaliPt	1	97	40	<0.01	<0.01 (S)
OxaliPt	3	82	43		<0.01 (S)
$PtCl_2$	1	89	39	<0.01	<0.01 (S)
$PtCl_2$	3	81	41		<0.01 (S)
$PtCl_2$	5	68	40		<0.01 (S)
$PtCl_4$	5	87	33	<0.01	<0.01 (S)
$PtCl_4$	10	73	36		<0.01 (S)
$PtCl_4$	30	32	38		<0.01 (S)
$(NH_4)PtCl_6$	1	94	21	<0.01	<0.01 (S)
$(NH_4)PtCl_6$	5	79	25		<0.01 (S)
$(NH_4)PtCl_6$	10	68	26		<0.01 (S)
CisPt	0.5	98	9	<0.01	>0.01 (NS)
CisPt	1	87	10		>0.05 (NS)
CisPt	3	48	7		>0.05 (S)
CarboPt	0.5	92	10	<0.05	>0.05 (S)
CarboPt	1	87	8		>0.05 (S)
CarboPt	3	84	12		>0.05 (S)
$NaVO_3$	3	99	40	<0.01	<0.01 (NS)
$NaVO_3$	5	90	41		<0.01 (S)
$NaVO_3$	10	84	39		<0.01 (S)

a: RSD<15%
b: median of 4 runs; 50 replictates/run
c: statistically significance of the experiment (p<0.05)
d: statistically significance of the result (p<0.05)
e-f: median of DNA (%) in tail minimum and maximum values for complete data set

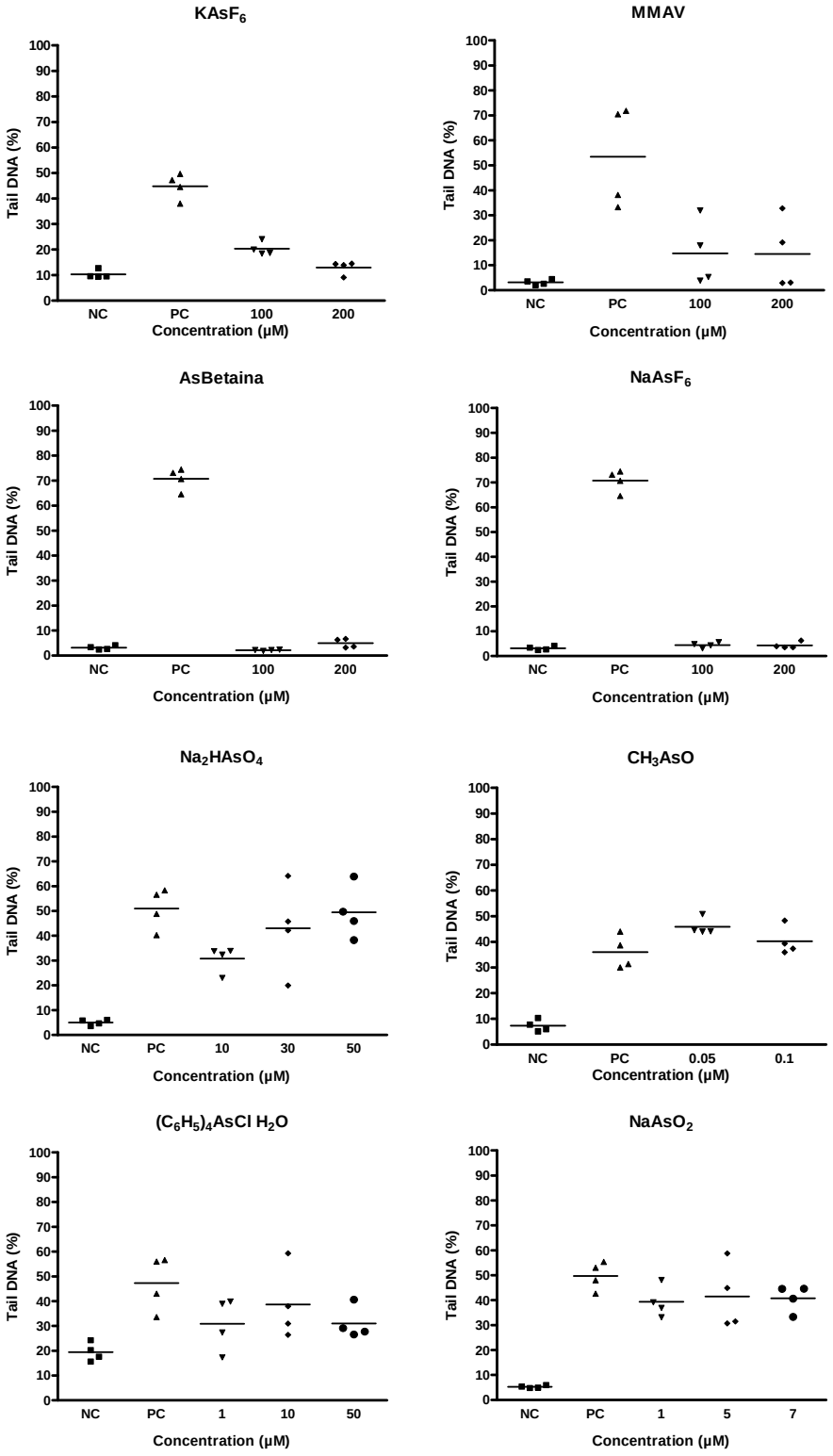

Figure 3. DNA damage expressed as tail DNA percentage (median of 4 runs) in Balb/3T3 exposed for 2h to subtoxic concentrations of As compounds (statistical significance, $p<0.05$, is reported in Table 16). PC=positive control (H_2O_2, 300 µM), NC=negative control (culture medium)

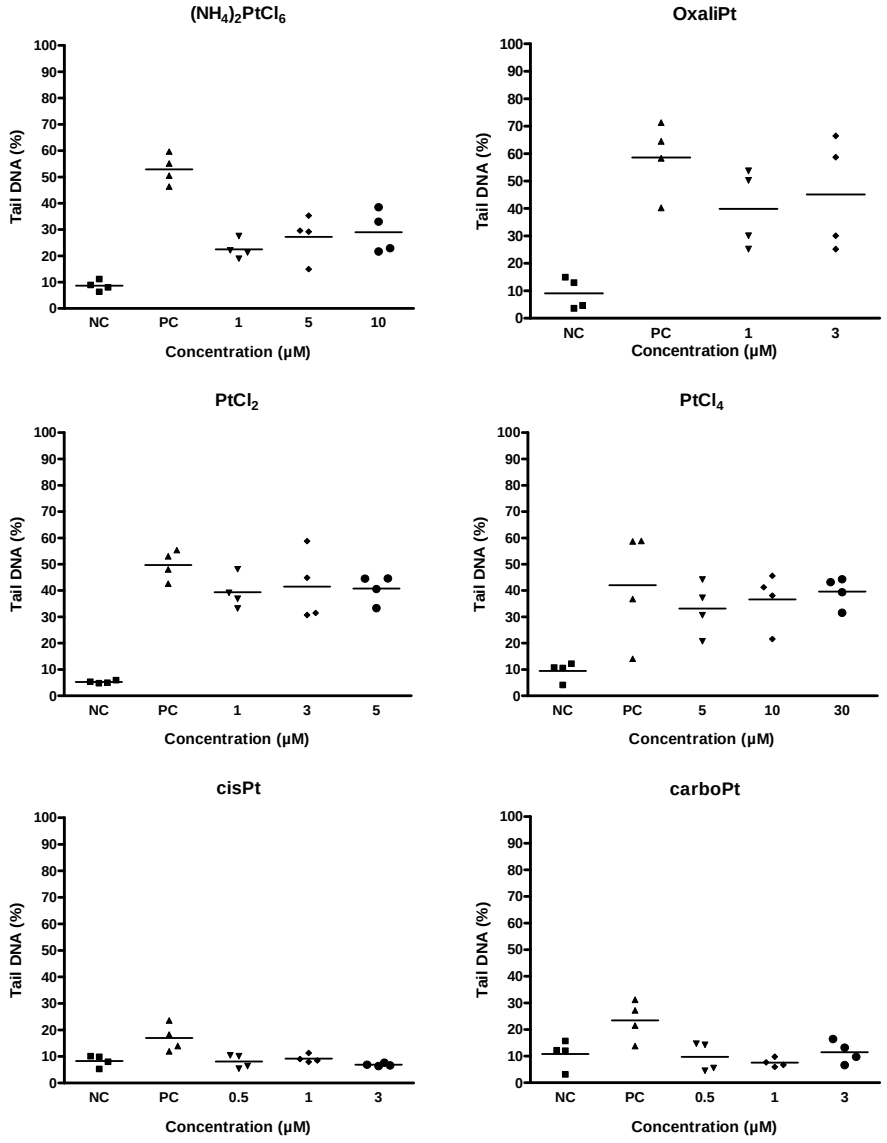

Figure 4. DNA damage expressed as tail DNA percentage (median of 4 runs) in Balb/3T3 exposed for 2h to subtoxic concentrations of Pt compounds (statistical significance, $p<0.05$, is reported in Table 16). PC=positive control (H_2O_2, 300 µM), NC=negative control (culture medium)

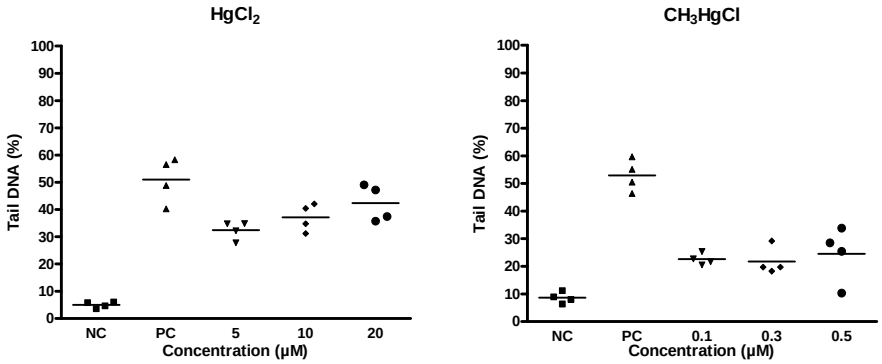

Figure 5. DNA damage expressed as tail DNA percentage (median of 4 runs) in Balb/3T3 exposed for 2h to subtoxic concentrations of Hg compounds (statistical significance, $p<0.05$, is reported in Table 16). PC=positive control (H_2O_2, 300 µM), NC=negative control (culture medium)

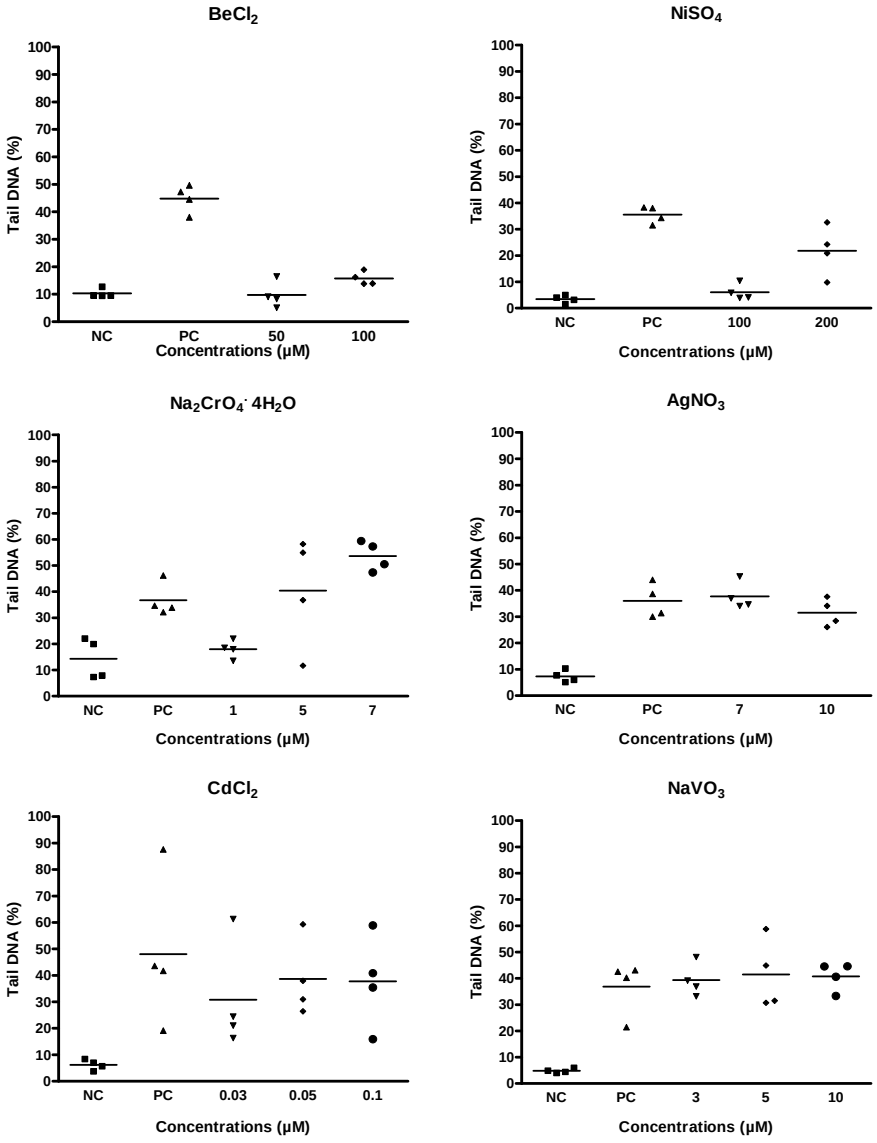

Figure 6. DNA damage expressed as tail DNA percentage (median of 4 runs) in Balb/3T3 exposed for 2h to subtoxic concentrations of Be, Ni, Cr, Ag, Cd, V compounds (statistical significance, $p<0.05$, is reported in Table 16). PC=positive control (H_2O_2, 300 µM), NC=negative control (culture medium)

Table 18. Micro Nucleus tests in Balb/3T3 cells exposed to different compounds for 24h at concentrations ranging from 0.01 to 100 µM

Compound	Conc (µM)	CFE (%)[a]	BNMN[b]	F-Fisher (p<0.05)[c]
control			10	
Mitomycin C (MMC)	0.5	65	86	<0.001
Group 1				
control		100	23	
$KAsF_6$	100	92	29	0.2
$NaAsF_6$	100	89	33	0.1
MMA(V)	100	88	35	0.07
control		100	21	
Asβ	100	93	23	0.4
control		100	21	
$BeCl_2$	100	91	26	0.28
Group 2				
control		100	10	
$NiSO_4$	100	79	29	<0.001
Group 3				
control		100	21	
$AgNO_3$	1	92	36	<0.05
control		100	8	
Na_2HAsO_4	10	83	8	0.7
Na_2HAsO_4	30	68	7	0.8
control		100	19	
$NaAsO_2$	0.1	85	20	0.5
$NaAsO_2$	1	79	18	0.6
$NaAsO_2$	5	77	17	0.7
control		100	15	
MMA (III)	0.01	67	16	0.4
MMA (III)	0.3	21	24	0.07
control		100	16	
$(C_6H_5)_4AsCl \cdot H_2O$	1	80	11	0.8
control		100	5	
$Na_2CrO_4 \cdot 4H_2O$	10	28	102	<0.001
control		100	15	
CH_3HgCl	0.5	35	16	0.5
CH_3HgCl	0.7	24	16	0.4
control		100	21	
OxaliPt	1	91	40	<0.05
control		100	16	
$PtCl_2$	0.1	95	30	<0.05
$PtCl_2$	0.3	85	52	<0.001
control		100	16	
$PtCl_4$	1	86	20	0.2
$PtCl_4$	5	45	23	0.1
$PtCl_4$	10	25	73	<0.001
control		100	12	
$(NH_4)_2PtCl_6$	1	92	24	<0.05
$(NH_4)_2PtCl_6$	5	80	25	<0.05
$(NH_4)_2PtCl_6$	10	65	30	<0.01

Compound	Conc (µM)	CFE (%)[a]	BNMN[b]	F-Fisher (p<0.05)[c]
control		100	19	
CisPt	0.1	87	20	0.5
CisPt	0.5	26	32	<0.05
CisPt	0.7	5	75	<0.001
CarboPt	1	90	23	0.3
CarboPt	5	25	37	<0.05
CarboPt	7	9	51	<0.001
control		100	16	
$NaVO_3$	1	95	9	0.9
$NaVO_3$	5	88	7	0.9
$NaVO_3$	10	58	16	0.5

a: average of 3 experiments, 6 replicates each concentration; RSD<15%
b: binucleated micronucleated cells frequency
c: statistically significance (p<0.05)
1<CBPI<2

4.3. Biokinetics studies

To investigate the effect of ingested chemicals using an *in vitro* cell model, we decided to use the Caco-2 cell line because it allows to study both the epithelial barrier integrity, as an endpoint of cytotoxicity, and the transport through the epithelium. In particular, we studied the *in vitro* effect of apical and basolateral exposure to radiolabelled Cr (VI), As (III), Ochratoxin A and Gentamicin on the barrier function of intestinal epithelium. We report results concerning biokinetics studies (kinetics of transfer, uptake and intracellular distribution) carried out in Caco-2 cell line exposed from 0 to 33 days to $Na_2{}^{51}CrO_4$ and from 0 to 17 days to $Na^{73}AsO_2$, Gentamicin Sulfate [^{3}H] and Ochratoxin A [^{3}H(G)].

Before starting any kind of treatment, the Caco-2 cells were cultured for 14 days on inserts with semi-permeable membrane in order to differentiate cells into intestinal epithelium. The latter was treated from the apical or the basolateral side continuously or discontinuously.

4.3.1. Cytotoxicity and epithelial integrity

Before investigating the adsorption of these four chemicals through the epithelium, we studied their basal cytotoxicity by MTT assay and their effect on the epithelium integrity by the measure of the Trans Epithelial Electrical Resistance (TEER); in order to avoid possible epithelial damage, we selected sub-toxic concentrations not affecting TEER for the four different chemicals tested.

Figure 8 shows cytotoxicity, assessed by MTT, in Caco-2 cells by Na_2CrO_4 and $NaAsO_2$, Gentamicin Sulfate, Ochratoxin A after 24 h and 72 h, respectively.

IC_{50} were 2 µM for Ochratoxin, 80 µM for As, 100 µM for Cr and IC_{50}>100 µM for Gentamicin.

Under our experimental conditions, TEER values (Ω cm^2) in differentiated epithelium suggested a satisfactory integrity of cell monolayer within the exposure times at the selected sub-toxic concentrations tested. This result shows that the transport we observe is really through an undamaged epithelium similar to the *in vivo* conditions.

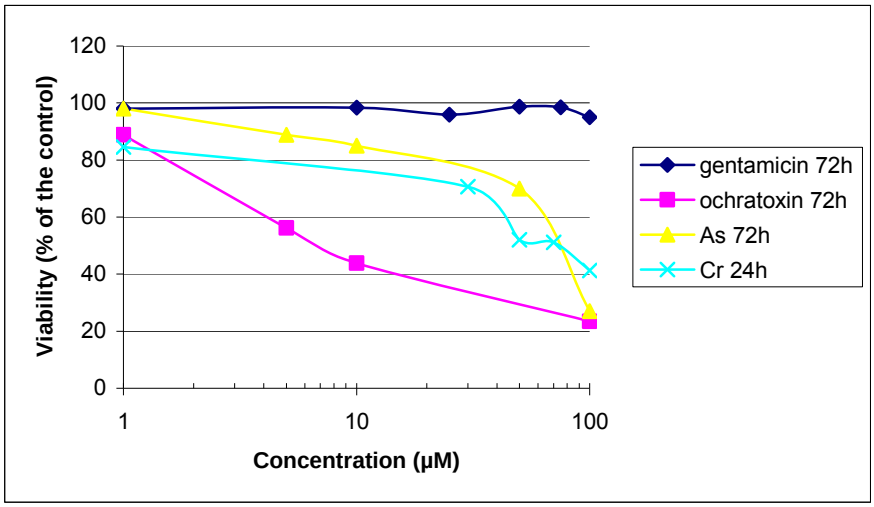

Figure 7. Cytotoxicity induced in Caco-2 cells by Na_2CrO_4 and $NaAsO_2$, Gentamicin Sulfate, Ochratoxin A after 24 h and 72 h respectively

4.3.2. Kinetics of transfer

Hereafter, we report results concerning the kinetics of transfer between the two compartments through the Caco-2 intestinal epithelial barrier. The intestinal epithelium (differentiated after 14 days of culture on inserts) was treated with the four selected chemicals form the apical or the basolateral side continuously or discontinuously. In order to avoid any artefacts due to the possible physicochemical interaction of the chemicals with the plastic membrane of the insert we studied the blank (data shown in Annex 2).

Blank. The fluxes of radiolabelled Cr, As, Gentamicin and Ochratoxin A between the two compartments in absence of cells (blank) were studied for short-term exposure, 3 different concentrations of Cr (0.022, 1 and 50 µM) and for long-term exposure, 0.1 µM $Na^{73}AsO_2$, 7 µM Gentamicin Sulfate [^{3}H] and 1 µM Ochratoxin A [^{3}H(G)] for 0-17 days. Aliquots of 100 µL medium from apical and basolateral compartments were collected and counted by γ- and β-counter (1:3 sample/scintillation liquid), respectively.

From the results we conclude that after 2h of incubation equilibrium was reached for each Cr concentrations. For As we see equilibrium after 1 day of incubation (4.56 ng/mL apical to 4.72 ng/mL basolateral; 4.72 ng/mL basolateral to 5.24 ng/mL apical). For Gentamicin and Ochratoxin A equilibrium is reached after 4 h and 1 day of incubation, respectively (Gentamicin: 2 µg/mL

apical to 1.8 µg/mL basolateral; 2 µg/mL basolateral to 1.96 µg/mL apical; Ochratoxin A: 0.16 µg/mL apical to 0.14 µg/mL basolateral; 0.18 µg/mL basolateral to 1.8 ng/mL apical).

Transfer. Figures 9-11 show graphically the transport of Cr, As, Gentamicin and Ochratoxin A between the two insert compartments in presence of Caco-2 cells exposed to 1, 30 and 50 µM of $Na_2{}^{51}CrO_4$ for 24 h and 1 µM of $Na_2{}^{51}CrO_4$ for 0-33 days (continuous and discontinuous exposure); to 0.1 µM of As, 7 µM of Gentamicin and 1 µM Ochratoxin A for 0-17 days (continuous and discontinuous exposure).

4.3.3. Cr biokinetics

We decided to study Cr because it is a water contaminant and we focused on its eventual transport through the intestinal barrier in our *in vitro* model. Based on our results, we can summarise as follow:

- there was a transport of Cr from apical to basolateral sides and viceversa over time. In the apical to basolateral experiments (Figures 8 a, b, c, apical to basolateral) at 24 h of exposure the concentration of Cr in the two insert compartments were 8 and 7 ng Cr/mL at 1 µM; 400 and 200 ng Cr/mL (30 µM) as well as 1140 and 400 ng Cr/mL (50 µM)
- in the basolateral to apical experiments (Figures 8 a, b, c, apical to basolateral), basolateral to apical) at 24 h of exposure the concentration of Cr into the two insert compartments were 12 and 5 ng Cr/mL at 1 µM; 400 and 290 ng Cr/mL (30 µM) as well as 500 and 360 ng Cr/mL (50 µM)
- in the continuous exposure to 1 µM of Cr there is a constant transport from the apical to the basolateral compartment (Figure 8 d) reaching values of 27 ng Cr/mL in the apical compartment and 18 ng Cr/mL in the basolateral compartment after 33 days of exposure
- the uptake concentrations of Cr (fgCr/cell) in alive Caco-2 cells at the end of the exposure to 1, 30 and 50 µM ranged from of 2 to 3.1% of the doses (Annex 3, Table 5), being more than double compared to the corresponding values in dead cells in both absorptive and exsorptive directions; the uptake at 10, 18 and 33 days of continuous exposure was 1.5, 2 times more than the uptake of the discontinuous exposure (Annex 3, Table 7)
- more than 60% of the Cr accumulated into the alive cells was present in the cytosol for the three concentrations after 24 h of exposure (Annex 3, Table 6) and for 1 µM after 10, 18 and 33 days of continuous and discontinuous exposure (Annex 3, Table 8). Among the other fraction, the highest Cr concentration was in the nuclei for both short- and long- term exposure (Annex 3, Table 6 and 8).

In conclusion, our results show that Cr fluxes in Caco-2 cells occur in both absorptive and secretory directions, with a concomitant similar accumulation of Cr by cells. Interestingly, at the end of the experiment (24h post exposure) the concentration of Cr was of the same order of magnitude in dead and alive cells (Annex 3, Table 7) as well as in the subcellular fractions (Annex 3, Table 8).

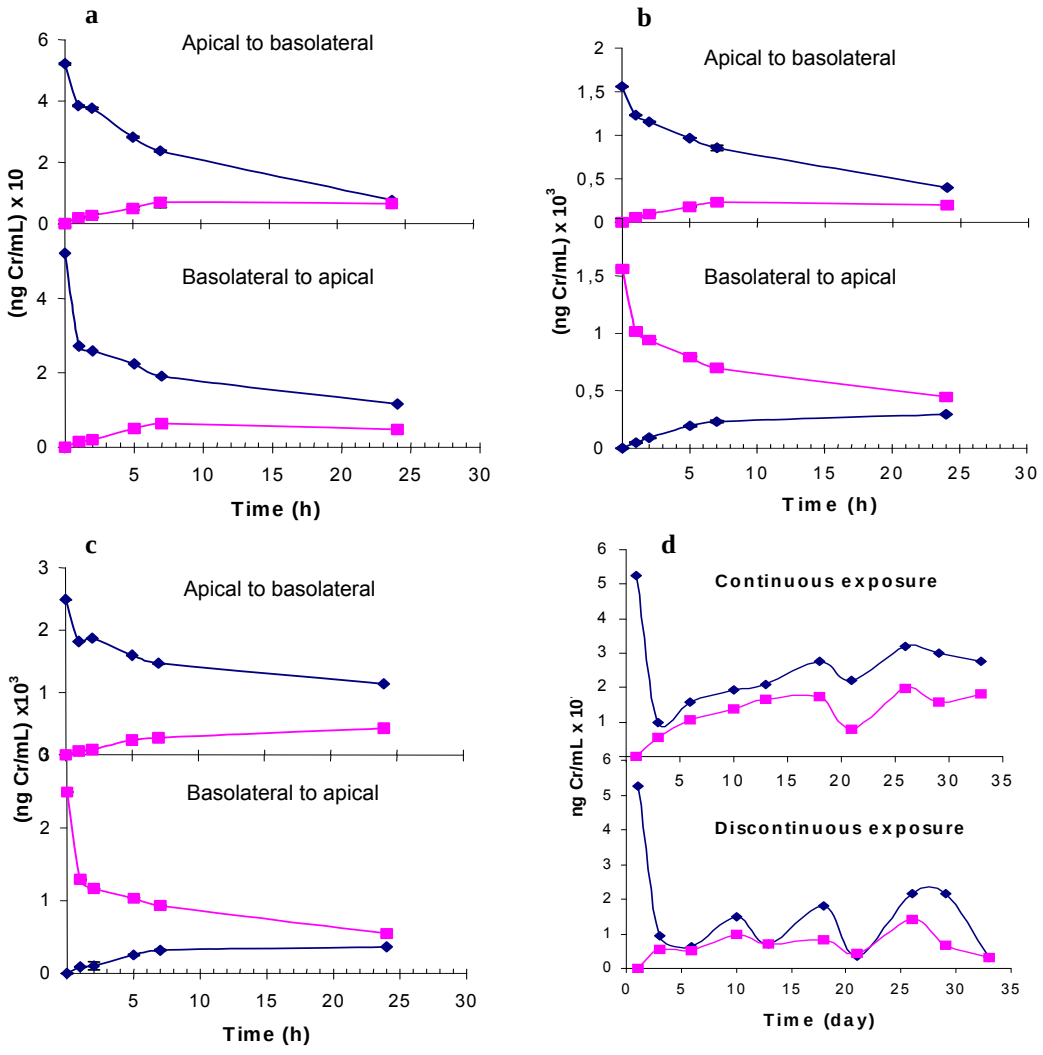

Figure 8. Kinetic of Cr transfer between the two insert compartments (apical; basolateral) in presence of Caco-2 cells exposed to (a) 1, (b) 30 and (c) 50 µM of $Na_2{}^{51}CrO_4$ for 24 h and (d) 1 µM of $Na_2{}^{51}CrO_4$ continuous and discontinuous exposure for 33 days

4.3.4. As biokinetics

The As biokinetics were studied in order to verify, using our cell model, its transport through the intestinal barrier. The importance of the As is due to its presence as food contaminant.
In particular, we obtained the following results:

- there was no transport of As from apical to basolateral sides and viceversa, in the apical to basolateral experiments (Figure 9)
- the uptake of As in alive Caco-2 cells after 17 days of exposure in the apical compartment was 0.87 fg As/cell, while from exposure in the basolateral compartment it was 0.016 fg As/cell (Annex 3, Table 9)
- 69 % and 37 % of the As accumulated into the alive cells was present in the cytosol after 17 days of discontinuous exposure in the apical and in the basolateral compartment, respectively. The distribution of As in the cellular organelles showed a content of 25.2 % in the nuclei for the exposure in the apical compartment; 33.4 % and 22.2 % in the nuclei and mitochondria fractions for the exposure in the basolateral compartment (Annex 3, Table 9).

To sum up, in our experimental design we wanted to avoid interference due to cytotoxicity and damage of epithelial integrity; under these circumstances, we did not observe As transport through the epithelium. Based on the results obtained we can assume that only when the epithelium is damaged, it is permeable to As (III). In addition, we used a discontinuous treatment approach that could permit the cell to eventually repair As toxic effects and allow its uptake (Annex 3, Table 9). So, cells are able to internalise it and probably metabolise it by some kinds of detoxification mechanisms.

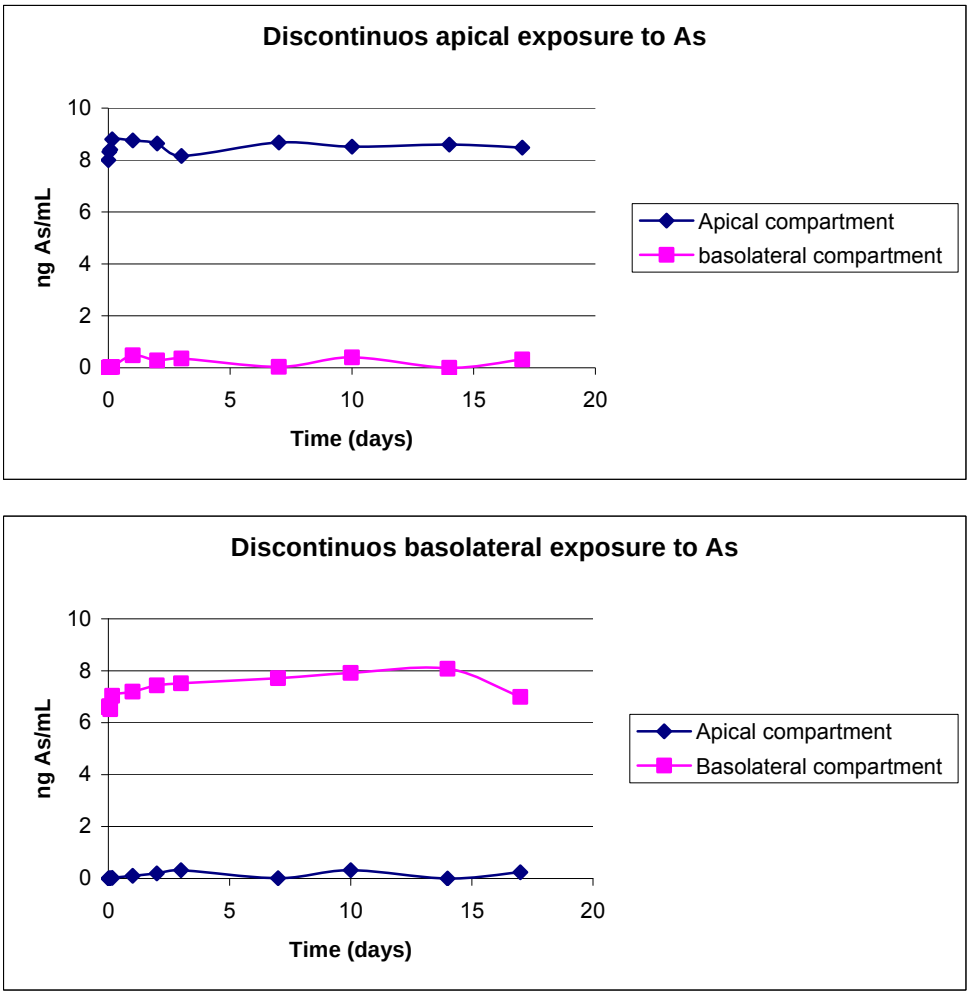

Figure 9. Kinetic transfer of As between the two insert compartments in presence of Caco-2 cells exposed 0.1 µM of $Na^{73}AsO_2$ for 17 days (discontinuous exposure)

4.3.5. Gentamicin biokinetics

We studied this organic compound for its relevance as drug and as prototypic substance in order to investigate an eventual transport through the gastrointestinal barrier.

In particular, we can observe the following results:

- there was no transport of Gentamicin from apical to basolateral sides and viceversa, in the apical to basolateral experiments (Figure 10)
- the uptake of Gentamicin in alive Caco-2 cells after 17 days of exposure in the apical compartment was 76 fg Gentamicin/cell, while from exposure in the basolateral compartment it was 35 fg Gentamicin/cell (Annex 3, Table 10)
- 11.6 % and 11 % of the Gentamicin accumulated into alive cells was present in the cytosol after 17 days of discontinuous exposure in the apical and in the basolateral compartment, respectively. The distribution of Gentamicin in the cellular organelles showed a content of 52.3 % and 29 % in the nuclei and mitochondria fractions for the exposure in the apical compartment; 72 % and 22.2 % in the nuclei and mitochondria fractions for the exposure in the basolateral compartment (Annex 3, Table 10).

Based on our results, we can assert that gentamicin is not transported trough the intestinal epithelium for both directions.

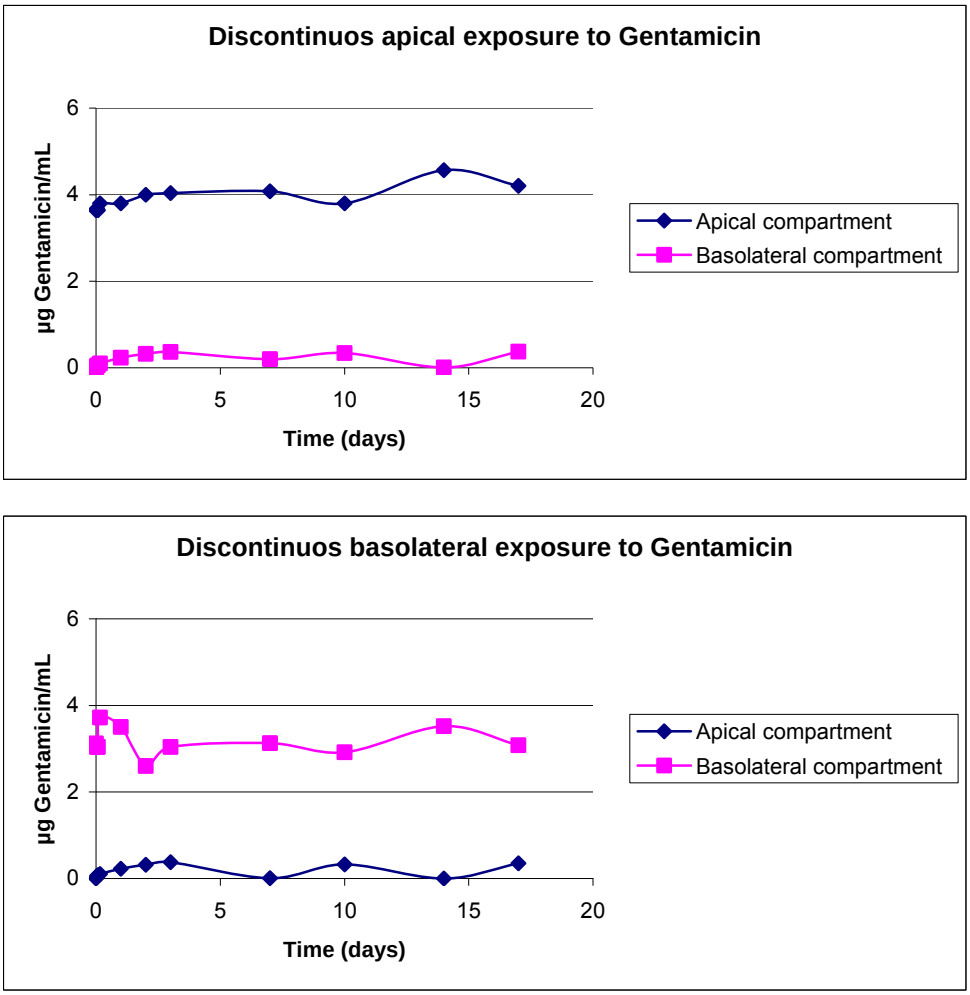

Figure 10. Kinetic transfer of gentamicin between the two insert compartments in presence of Caco-2 cells exposed 7 µM of gentamicin for 17 days (discontinuous exposure)

4.3.6. Ochratoxin biokinetics

We investigate this organic compound for its relevance as food contaminant and as reference compound of an biological toxin.

Based on our results, we can observe that:

- there was no transport of Ochratoxin from apical to basolateral sides and viceversa. In the apical to basolateral experiments (Figure 12)
- the uptake of Ochratoxin in alive Caco-2 cells after 17 days of exposure in the apical compartment was 0.35 fg Ochratoxin /cell, while from exposure in the basolateral compartment it was 0.12 fg Ochratoxin /cell (Annex 3, Table 11)

- 18 % and 40 % of the Ochratoxin accumulated into the alive cells was present in the cytosol after 17 days of discontinuous exposure in the apical and in the basolateral compartment, respectively. The distribution of Ochratoxin in the cellular organelles showed a content of 54 % and 22 % in the nuclei and mithocondria fractions for the exposure in the apical compartment; 40 % and 12 % in the nuclei and mitochondria fractions for the exposure in the basolateral compartment (Annex 3, Table 11).

We can conclude that long term exposure, to low cytotoxic doses, does not allow trans-epithelium transport for Ochratoxin A.

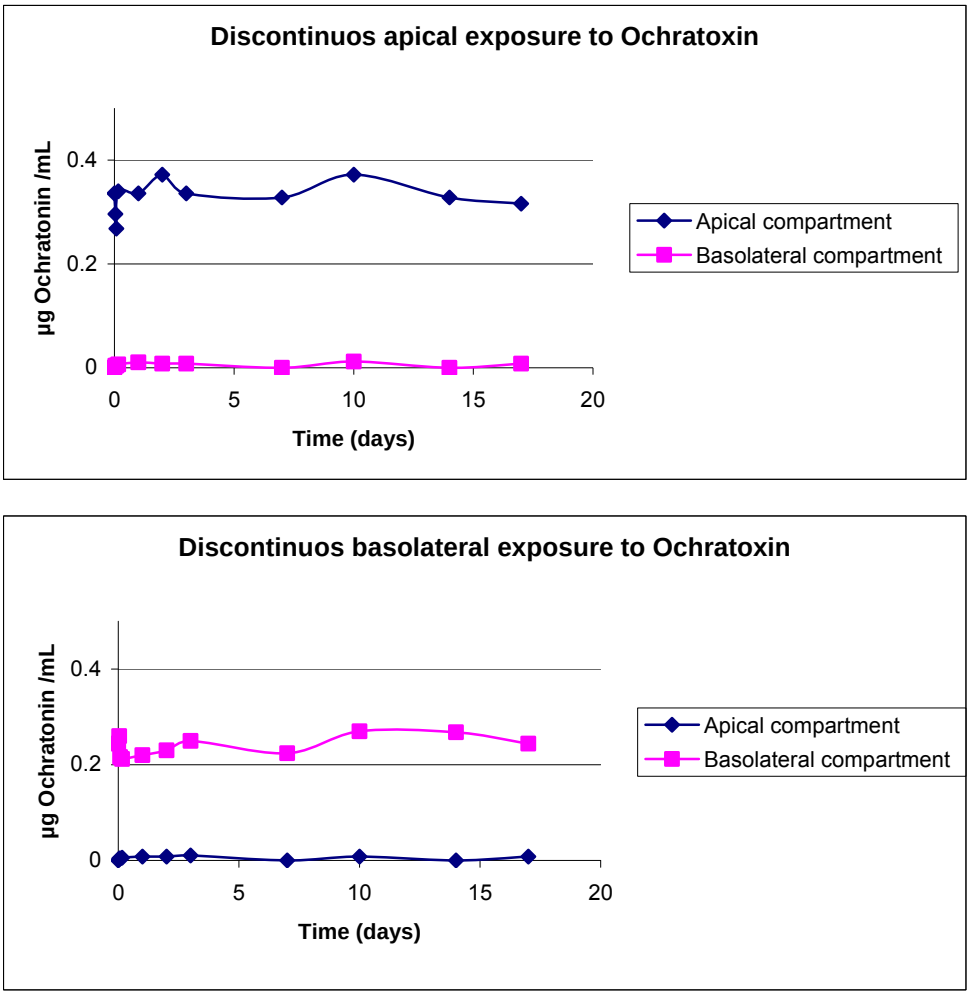

Figure 11. Kinetic transfer of Ochratoxin between the two insert compartments in presence of Caco-2 cells exposed 1 µM of gentamicin for 17 days (discontinuous exposure)

4.4. Nanotoxicology studies

Nanotechnology is a field that involves the development, manufacturing and measurement of materials from sub-micrometers down to few nanometers (nm). However, there is still a lack of information about the impact on environment and on human health of manufactured nanoparticles (mNPs) as well as reliable data on risk assessment. In this context, the research on mNPs toxicology is a fast emerging field.

In order to establish an i*n vitro* basic research strategy to study nanoparticles toxicology, we decided to evaluate the biological effects of this "new" material in *in vitro* systems using a specific approach that includes its physiochemical characterization and cell interaction.

In particular, this study includes the investigation of basal cytotoxicity, genotoxicity and carcinogenicity of Cobalt nanoparticles (Co-nano) in comparison to its corresponding released ions (Co2+). Hereafter we report results concerning: (i) screening study (72h of exposure at 100 µM) of basal cytotoxicity, by Colony Forming Efficiency (CFE) in Balb/3T3 cells, of manufactured nano- and micro-particles and (ii) specific *in vitro* studies on cobalt nanoparticles (Co-nano) in Balb/3T3 including physicochemical characterization, cytotoxicity, carcinogenic potential, genotoxicity, morphological and metabolic studies.

4.4.1. Physicochemical characterization

The first aspect evaluated is the physicochemical characterization of mNPs. This analysis is fundamental to correlate the biological endpoints with the real concentration, size and "soluble part" of the mNPs suspension. In fact, concerning the real concentration tested, since we are working with solid compounds, we must verify that when we prepare stock solutions and subsequent dilutions, we obtain the theoretical estimated concentrations. We must also check the purity of the suspension in terms of elemental impurities that could generate false positive results and the leakage of metal ions corresponding to the metallic particles.

In this section, we show the results concerning determination of Co concentration in Co-nano suspensions, the analysis of elemental impurities, and the Co release in complete culture medium from Co-nano after 2, 24, 48 and 72 h. The morphology and size distribution of Co-nano are also considered.

Determination of Co concentration in freshly prepared Co-nano suspensions. Since the Co-nanoparticles are solid compounds, the probability to dilute them getting a number that does not correspond to the expected one is high. So, when we dilute the stock suspension adding aliquots to culture media, we must check that the real concentrations are similar to the expected ones.

To do this, we prepared different dilutions from 10 to 300µM and we measured the Co concentration by Inductively Coupled Plasma Mass Spectrometry, ICP-MS.

Table 19 shows results of the analysis of the Co in culture medium containing Co-nano. The concentrations of Co in suspensions were consistent with those theoretically expected.

Table 19. Concentration of Co in diluted suspensions in Balb/3T3 culture medium

Theoretical [Co] (µM)[a]	Co Concentration determined (µM)[b]
10	9
30	26
50	45
70	51
100	125
300	286

a: based on stock suspension of Co-nano
b: mean of 3 experiments, RSD<10%

Analysis of elemental impurities. In order to be sure that no elemental impurity could influence the biological results, first of all we decided to investigate the elemental impurity of Co-nano suspension, in particular for known toxic compounds such as arsenic.

52 elemental impurities were analyzed by Inductively Coupled Plasma Mass Spectrometry (ICP-MS). The concentrations of minimum and maximum elementary impurities measured in Co-nano stock solution (100 µM) are respectively 1.7 ng g-1 di Rh and $2.3 \cdot 10^5$ ng g-1 As.

Based on previous studies on basal cytotoxicity induced by different metal compounds (Mazzoti et al., 2002), this result shows a degree of purity excluding any possible artifacts due to As.

Co leakage in complete cell culture medium. Another important point of nanoparticles toxicology is the possibility that, especially from metallic particles, we observe a leakage of the corresponding ions in cell culture media. These ions could induce toxic effects (Mazzotti et al., 2001, 2002).

In this work we decided to study this aspect after incubation of Co-nano in a time dependent way (2-72h). Table 20 reports Co ions (Co^{2+}) leaked in complete culture medium from Co-nano after 2, 4, 24, 48 and 72 h. Results show time-dependent Co ions released from Co-nano suspension 100 µM ranging from 7% to 44%.

These data confirm the effective leakage that must be taken into consideration in the evaluation of the toxicological data as described in next sections (4.4.3. Carcinogenicity and genotoxicity induced by Co-nano and $CoCl_2$.).

Table 20. Co^{2+} leaked from 100 µM Co-nano in complete culture medium expressed as percentage Co^{2+} (%)

Time (h)	(% Co^{2+})
2	7
4	10
24	23
48	34
72	44

a: mean of 3 experiments, RSD<10%

Morphology and size distribution of Co-nano. An important issue related to the characterization of nanoparticles for the study of their biological effects is the investigation of their size distribution. Figure 13 A and B shows Scanning Electron Microscopy (SEM) images of 10 mM Co-nano aggregates suspension in water (Figure 13 A) and complete culture medium (Figure 13 B). Figure 13 C reports size distribution of the aggregates, ranging from 120 to 1000 nm, in water with a mean size of 500 nm determined by Dynamic Light Scattering technique (DLS). This characterization shows that, when nanoparticles of about 80nm, as declared by the supplier, are suspended in water, they form a big aggregate of about 500 nm (Figure 13 A and C). When the same suspension is diluted in culture medium, the aggregates start "dissolving" showing different morphology in respect to the stock suspension (Figure 13 B).

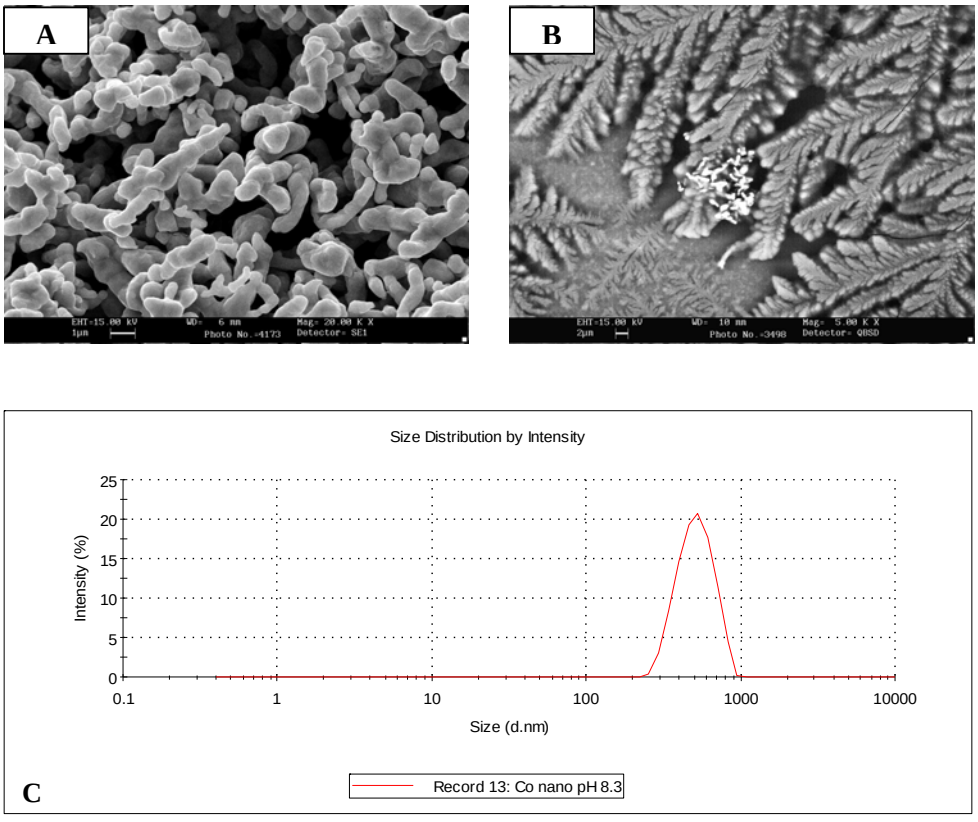

Figure 12. Co-nano aggregates in H_2O (A) and in culture medium (B) by SEM. Size distribution by DLS (C)

4.4.2. Carcinogenicity and genotoxicity induced by Co-nano and $CoCl_2$

Hereafter, we report results concerning carcinogenic potential and genotoxicity induced by Co-nano and $CoCl_2$ in Balb/3T3 cells. As previously described (section results, carcinogenic potential and genotoxicity of metal compounds in Balb/3T3 cell line) the concentrations tested in Cell Transformation Assay (CTA), Comet assay and Micro Nucleus (MN) were selected by dose-effect relationships. In general, inhibitory concentrations corresponding mainly to $IC_{20,}$ IC_{50} and IC_{90} were tested in the CTA and MN and IC_{10}, IC_{20} in Comet Assay.

Basal cytotoxicity. *In vitro* basal cytotoxicity induced by Co-nano was evaluated by Colony Forming Efficiency. This test is typically used to study the dose-effect relationships before the CTA, Micronucleus and Comet assays. This test permits to draw dose-effect curves from which it is possible to extrapolate the correct doses to be used.

In fact, in this work, we performed CFE after different exposure times, 2, 24 and 72h, corresponding to the standardized exposure for Comet assay, Micronucleus and CTA respectively. Figure 14 shows the dose-dependent response obtained for Co-nano and Co^{2+} after 2, 24 and 72 h of exposure. The graphical representation shows the mean values which were obtained from 3 independent experiments, with 6 replicates for each concentration, with a relative standard deviation less than 20% (RSD<20%). An evident cytotoxic dose-dependent and time dependent effect of Co-nano is observable analyzing a wide range of doses at 2, 24 and 72 h. Also in the case of Co^{2+} both a dose and a time-dependent cytotoxic effect is observable, but less pronounced compared with Co-nano (Figure 14) except at 72 h where the two curves are almost overlapping.

In order to compare the effect of Co^{2+} coming from Co-nano, we measured the amount of it in complete culture medium, in the same incubation times used for the 3 tests (Table 20).

Based on the cytotoxicity results obtained we can speculate that, in these experimental conditions, the concentration of Co^{2+}, extrapolated by the percentage of Co^{2+} released in Table 20, is not enough to justify the observed Co-nano toxicity (Figure 14). In fact, for example, considering an exposure time of 2 h at the concentration of Co-nano 100 µM that corresponds to a 7% Co^{2+} release (7 µM), we observed no cell viability for Co-nano, whereas 80% cell viability for Co^{2+}. Consequently the cytotoxic effect seems likely to be induced by nanoparticles and not by Co^{2+} although a complementary and/or a synergic effect cannot be excluded.

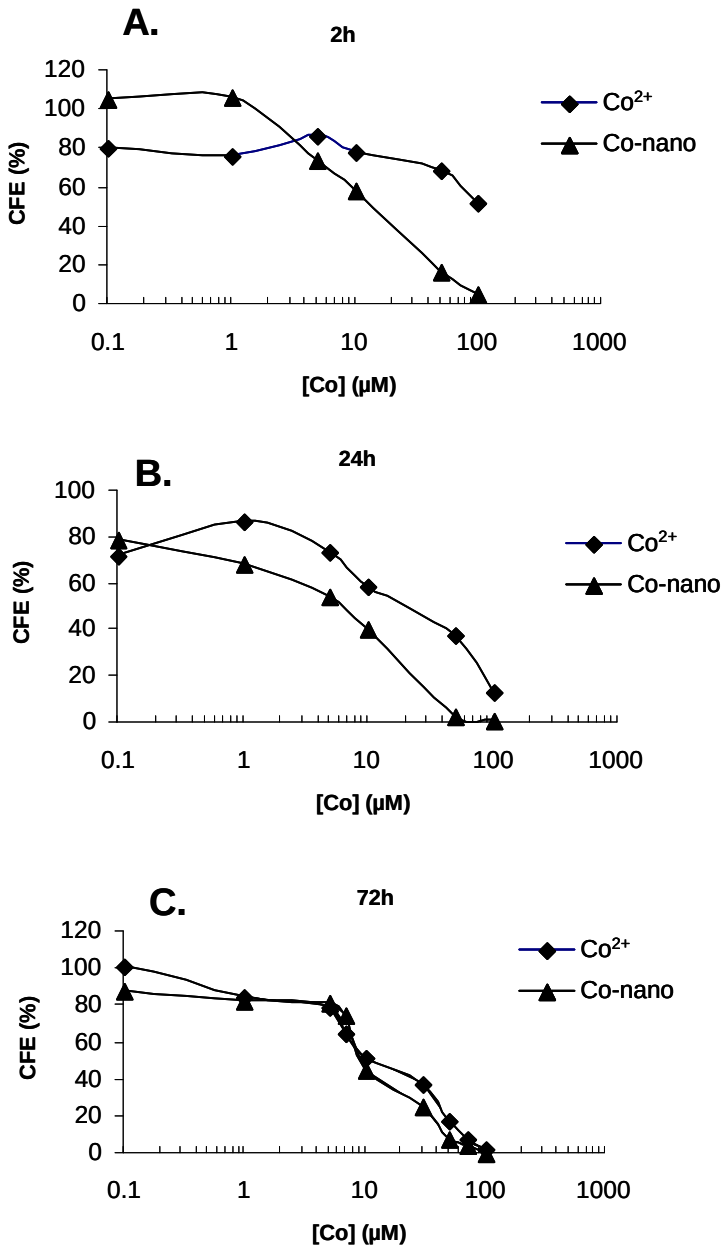

Figure 13. Cytotoxicity, expressed as CFE (% of the control), induced in Balb/3T3 cell lines by Co^{2+}, and Co-nano, after 2, 24,72 h of exposure (A, B and C, respectively). Curves are obtained as average of 3 experiments, 6 replicates each treatment, RSD< 20%.

Carcinogenicity. The *in vitro* Cell Transformation Assay (CTA) is a test that assesses the carcinogenic potential of chemicals in parallel with the evaluation of their basal cytotoxicity by Colony Forming Efficiency test (CFE).

Table 21 summaries results of the CTA carried out in Balb/3T3 cells exposed for 72 h to Co-nano and $CoCl_2$ at concentrations ranging from 1 to 79 µM.

The following results were found:

- the compounds show a CFE ranging from 98% to 15% of the control for Co-nano (1 µM) and $CoCl_2$ (70 µM) respectively
- morphological neoplastic transformation was statistically significant ($p<0.05$ / number of treatments) for Co-nano (7-10-30 µM) (Photo 7)
- induction of type III foci was not statistically significant for $CoCl_2$ (1-7-30 µM)
- no type III foci were found for $CoCl_2$·(70 µM)

Our results showed that Co-nano are cytotoxic and we observed an increase of morphological transformation, expressed as transformation frequency (Tf), for all the concentrations tested (except for Co-nano at 1 µM), while Co^{2+} resulted to be cytotoxic but no statistically significant morphological transformation was observed

Table 21. Concurrent cytotoxicity and morphological transformation induced by Co^{2+}, Co-nano in Balb/3T3 after 72 h of exposure

Compound	[µM]	CFE[a] (%)	Plating efficiency (%)	N° type III foci	Survived cell	Tf ($x10^{-4}$)[b]	F-fisher[c]
Control	-	100	24.7	49400	1	0.20	
Na_2CrO_4 x4H_2O	50	38	52.5	39600	21	0.5	$5.2x10^{-7}$ (S)
Co-nano	1	98	24.7	48412	2	0.41	0.480 (NS)
Co-nano	7	75	46	51750	10	1.93	0.0014 (S)
Co-nano	10	52	24.7	25688	4	1.56	0.008 (S)
Co-nano	30	24	46	16560	11	6.64	$1.4x10^{-7}$ (S)
$CoCl_2$	1	86	46	59340	2	0.33	0.443 (NS)
$CoCl_2$	7	76	46	52440	4	0.76	0.114 (NS)
$CoCl_2$	30	47	24.5	23030	1	0.43	0.53 (NS)
$CoCl_2$	70	15	24.5	7350	0	0	-

a: average of 3 experiments, 6 replicates each concentration; RSD<20%
b: Tf = Transformation Frequency
c: $p<0.05$/ number of treatment: S=Statistically Significant; NS=No Statistical Significance

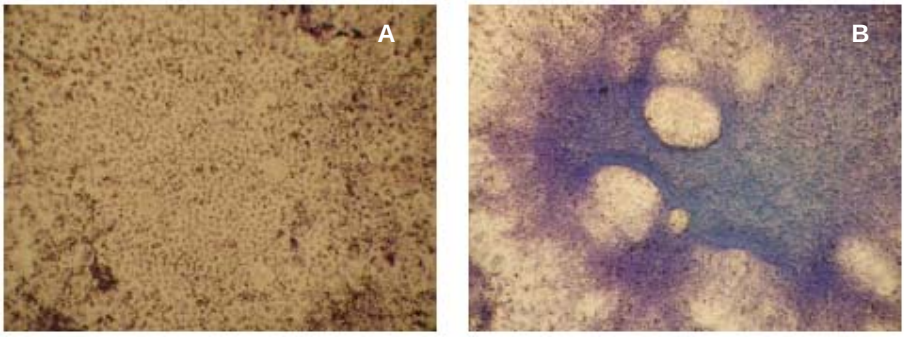

Photo 7. Balb/3T3 cells in monolayer after 5 weeks of culture (control) (A) and type III focus induced in Balb/3T3 by exposure to Co-nano 7 µM for 72 h (B)

Genotoxicity. To evaluate the genotoxic potential of Co-nano and $CoCl_2$, we decided to perform the Comet assay and the MN test because they are complementary. In fact one detects single strand breaks and double strand breaks and the other the chromosomal aberrations. Figure 14 and Table 20 show results obtained by the Comet assay and MN carried out in Balb/3T3 cells exposed for 2 and 24h to Co-nano and $CoCl_2$ at concentrations ranging from 1 to 10 µM.

For the Comet assay we observe: (i) Statistically significant DNA damage is observed for Co-nano (1-3-5 µM) and $CoCl_2$ (1-3-5 µM); (ii) a dose-effect relationship is clearly shown for $CoCl_2$

For the Micronucleus test we observe: (i) Statistically significant micronucleus formation is observed for Co-nano (1-5-10 µM); (ii) no statistically significant micronucleus formation is observed for $CoCl_2$ (1-5-10 µM)

Regarding the genotoxicity assessed by the Comet assay, our data show that the increase of DNA damage for Co-nano is not dose-dependent (Figure 15), whereas for Co^{2+}, although exerting a comparable genotoxic response, a dose-dependent behaviour is observed. The MN test shows for Co-nano a statistical significant induction ($P<0.001$) of chromosomal aberrations at all the concentrations tested, but not dose-dependent; whereas for Co^{2+}, at the same experimental conditions, no genotoxic effect was observed.

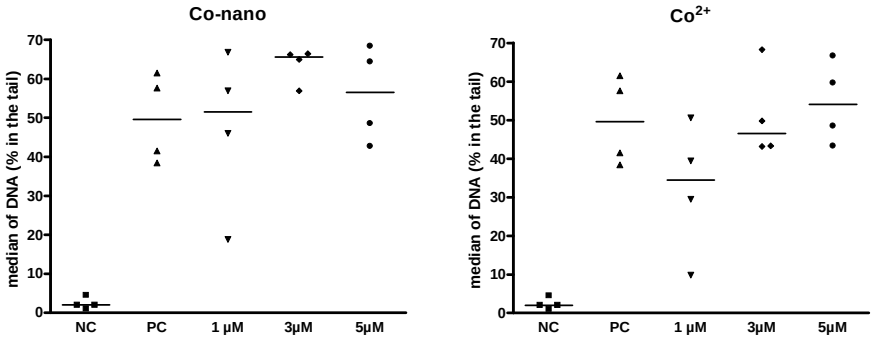

Figure 14. DNA damage expressed as percentage tail DNA (median of 4 experiments) in Balb/3T3 exposed for 2 h to subtoxic concentrations (1-3-5 µM) of Co-nano and $CoCl_2$ (statistical significance, $p<0.01$ for each treatment). PC=positive control (H_2O_2, 300 µM), NC=negative control (culture medium)

Table 22. Chromosomal aberration by MN assay induced by Co-nano and $CoCl_2$ in Balb/3T3 after 24 h of exposure

Compound	[μM]	CFE (%)[a]	BNMN[b]	F-Fisher ($p<0.05$)[c]
control	-	100	24	
MMC	0.5	65	203	$1.2x10^{-33}$ (S)
Co-nano	1	62	106	$4.29x10^{-13}$ (S)
Co-nano	5	50	53	$7.86x10^{-4}$ (S)
Co-nano	10	46	44	0.001 (S)
$CoCl_2$	1	98	28	0.342 (NS)
$CoCl_2$	5	60	28	0.342 (NS)
$CoCl_2$	10	55	31	0.214 (NS)

a: average of 3 experiments, 6 replicates each concentration; RSD<15%
b: binucleated micronucleated cells frequency
c: $p<0.05$/ number of treatment: S=Statistically Significant; NS=No Statistically Significance
proliferation index with blocked cytodieresis: 1<CBPI<2

4.4.3. Morphological studies on Balb/3T3 exposed to Co-nano and $CoCl_2$

The last point we investigated was the morphological changes in Balb/3T3. These studies were carried out by Confocal imaging and SEM-EDX.

In particular, we used this last technique to verify the interaction between the Co-nano and the cells.

Confocal imaging. Photo 8 shows cytoskeleton (green) and nucleus (red) of Balb/3T3 cells exposed for 24 h to Co-nano (1, 7, 100 μM) and $CoCl_2$ (1, 30, 100 μM). We can observe dose-dependent cytoskeleton reorganization (green), while no DNA damage (red) is visible for both Co-nano and $CoCl_2$.

SEM imaging. Photo 9 shows SEM of Balb/3T3 cell exposed to Co-nano 100 μM for 24h. From this picture, we can conclude that Co-nano is able to interact with cells. The light degradation suggests penetration into cells.

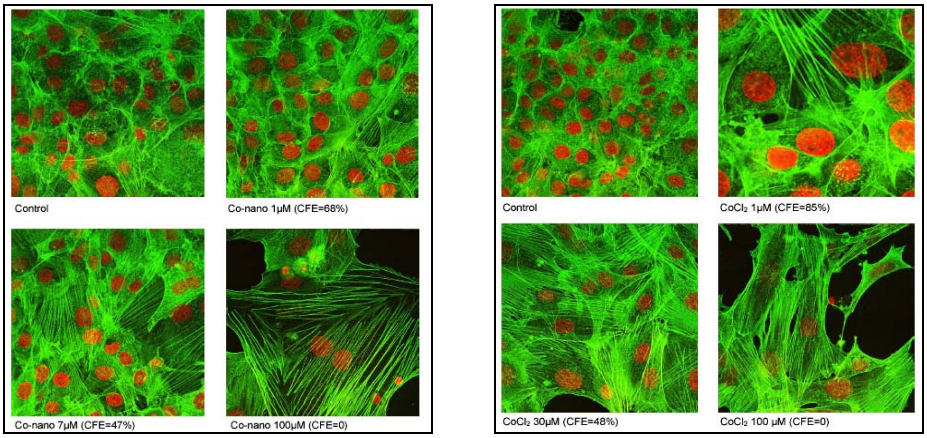

Photo 8. Balb/3T3 morphology after exposure to Co-nano (1-7-100 μM) and $CoCl_2$ (1-30-100 μM) for 24 h, corresponding to the same cytotoxicity, by confocal imaging. Staining: Alexa Fluor 488 (green)-conjugated phalloidin and propidium iodide

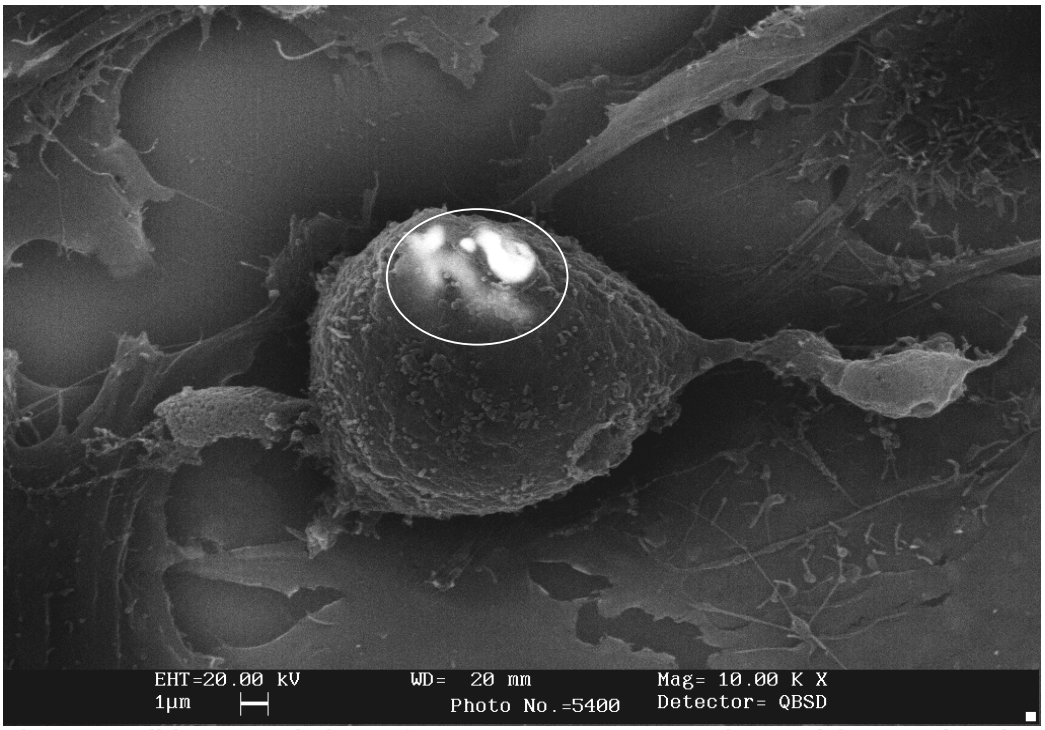

Photo 9. Balb/3T3 morphology after exposure to Co-nano (100 µM) by SEM imaging. White circle indicates a Co-nano aggregate

4.4.4. Metabolic studies on Balb/3T3 exposed to Co-nano and $CoCl_2$

In order to verify that the biological results obtained were due to nanoparticle internalization, we studied the uptake rate of 60Co-nano and 57Co2+ after 2, 24 and 72 h of exposure at the corresponding IC_{50}. In particular, the uptake analysis at the IC_{50} values is performed in order to normalize the results at the same percentage of viable cells.

Thanks to the use of radiotracers, we can quantify the amount of mNPs that interact with cells. In this section, we report results concerning uptake and intracellular distribution of radiolabelled ^{60}Co-nano and $^{57}CoCl_2$ in Balb/3T3 cells.

Uptake. Table 23 summaries results of ^{60}Co-nano and $^{57}CoCl_2$ uptake in Balb/3T3 exposed to concentrations corresponding to IC_{50} for different times (2-24 and 72 h). Co-nano uptake concentration is higher after 2h of exposure (990 fg Co cell^{-1}) than after 24-72 h (250-290 fg Co cell^{-1}. $CoCl_2$ uptake is higher after 2h of exposure (16 fg Co cell^{-1}) while it remains constant after 24 and 72 h of exposure (7 fg Co cell^{-1}).

Results showed an uptake 50-100 fold increase for ^{60}Co-nano in comparison to $^{57}Co^{2+}$ (Table 23). It seems that cells are able to internalize Co-nano.

Table 23. Uptake of ^{60}Co-nano and $^{57}Co^{2+}$ in Balb/3T3 after 2-24 and 72h of exposure to the corresponding IC_{50}

Compound	Exposure time (h)	IC_{50} (µM)	Uptake (fg Co cell^{-1})[a]
$^{57}Co^{2+}$	2	100	16
	24	20	7
	72	10	7
^{60}Co-nano	2	20	990
	24	10	250
	72	10	290

a: mean of 3 experiments, RSD<15%

5. DISCUSSION

5.1. Carcinogenicity/Genotoxicity studies

5.1.1. Importance of purity of metal compounds tested

A key aspect in the study of the carcinogenic potential of metal compounds concerns their chemical purity. If impurities of chemically similar elements are present in the metal compound under study and they are much more toxic than the metal species to be tested, they could create false positive results.

Therefore, the analysis of the elemental impurities of the salts used in the morphological neoplastic transformation and genotoxicity studies was of particular importance (Table 15). Data obtained by ICP-MS showed low concentrations of such impurities that are not able to induce cytotoxic effects in our *in vitro* system (Mazzotti et al., 2002). Moreover, artefacts due to such impurities could be reasonably excluded under our experimental conditions (estimated maximum concentrations were in the range 10^{-13}-10^{-8} M).

5.1.2. Cell transformation assay by Balb/3T3

Studies on Balb/3T3 cells have been carried out at ECVAM in order to establish a database on the carcinogenic potential of metal compounds. The studies were based on a multistage strategy approach which included four steps:

- **systematic screening:** it involves the evaluation of basal cytotoxicity at a fixed dose (100 μM) and time of exposure (72h). The results allowed the ranking in three cytotoxicity groups: group 1 (low cytotoxicity, CFE>80%); group 2 (medium cytotoxicity, 50%<CFE<79%; group 3 (high cytotoxicity, CFE<49%) (Mazzotti et al., 2001)
- **dose effect curves:** groups 2 and 3 metals are tested by CFE assay in a wide range of concentrations (0.01 μM-100 μM) to obtain a dose-effect curves in order to extrapolate IC_{50} values (Mazzotti et al., 2002)
- **morphological transformation:** selected metal compounds are tested for their carcinogenic potential
- **genotoxicity studies:** compounds of particular interest in regarding cytotoxicity and/or carcinogenic potential are tested to detect their genotoxic potential by Comet assay and Micronucleus.

This thesis takes into account the third and fourth phase of the strategy and the aim of this study was to compare the results coming from *in vitro* testing with ones observed from *in vivo.* In particular, metal compounds were tested from systematic screening for their carcinogenic potential (Table 16) and some of them were selected for further tests as to their genotoxic

potential by Comet assay and MN respectively (Table 17 and 18). This latter study was carried out in order to catalogue them as genotoxic or non-genotoxic carcinogens *in vitro.*

These compounds were selected considering their carcinogenic potential as classified by the International Agency for Research on Cancer (IARC) and their relevance for human exposure. Table 24 summaries the comparison of the results obtained using the 3 different tests for 18 metals. Since the test protocols are different especially for the concentrations used and the exposure times, we compared the results based on the same cytotoxicity.

Hereafter, each compound is discussed considering the IARC classification and the *in vitro* results obtained in Balb/3T3 model.

Silver. IARC (IARC, 1987) classifies silver as non-carcinogenic (Table 1), in agreement with our *in vitro* model (Table 16); anyway it shows a strong cytotoxicity and genotoxicity potential (Table 17 and 18).
In our opinion, understanding silver toxicity is important because of its large use as antimicrobial compound in drugs, implants, textiles and recently also in form of nanoparticles (Bosetti et al., 2002). In particular, even if it is reported that silver contained in implants is neither genotoxic nor cytotoxic in specific *in vitro* systems, such as human peripheral blood lymphocytes (Bosetti et al., 2002) and in our *in vitro* model, silver ions are cytotoxic, our conclusion is that the silver ions need to be more investigated to exclude their toxicity.

Arsenic. Inorganic arsenic is known to be a potent human carcinogen. It has long been known that occupational exposure increases the risk for lung cancer (IARC, 1980) (Table 1) and that exposure via drinking water may cause skin cancer, cancer of the urinary bladder and lungs, and possibly also in liver and kidneys (Tseng, 1977; Chapman, 2000).
Our results in Balb/3T3 model show for As (V) and As (III) a carcinogenic potential and a genotoxicity capacity by Comet assay but not by MN test, while for MMA III no carcinogenic potential and no genotoxic effect except for Comet assay. More interesting is the case of the organic form ($(C_6H_5)_4AsCl{\cdot}H_2O$) that shows carcinogenic potential and genotoxicity by Comet but it is negative in MN, while instead it is classified as suspected carcinogen by IARC (Table 16-18 and 24).

Even though a well-known human carcinogen the underlining mechanisms of arsenic carcinogenicity are still not fully understood. For arsenite, proposed mechanisms are the interference with DNA repair processes and an increase in reactive oxygen species production. Even less is known about the genotoxic potentials of its methylated metabolites such as MMA (III) and DMA (III). It is reported that arsenite induces oxidative DNA damage

and that MMA III induces strand breaks in a concentration-dependent manner (Schwerdtle et al., 2003; Colognato et al., 2007), however, a 2-year bioassay did not result in significant increases in the incidence of neoplastic lesions in rats and mice exposed to MMA (III) as reported by the “Agency for toxic substances & disease registry” (ATSDR, tp2-c2).

Interestingly, experimental cancer studies have in general been negative for arsenic. There is also a variation in acute toxicity among mammalian species, and humans seem to be more sensitive than experimental animals. It has been suggested that there is a marked variation in susceptibility among individuals (Chapman, 2000), but there are very few studies designed to address this issue. The variations in susceptibility to arsenic may, at least partly, be related to differences in the biotransformation of arsenic. Possible reasons for such differences include age, nutritional status, concurrent exposures to other agents or environmental factors, and genetic polymorphism**.** Compared with inorganic arsenic, the end-products in the *in vivo* arsenic methylation, MMA and DMA, show a low degree of toxicity, including genotoxicity, in a variety of test systems (Kreppel et al., 1993; Oya-Ohta et al., 1996; Moore et al., 1997; Rasmussen & Menzel, 1997; Lucas, 1998; Sakurai et al., 1998). The methylated metabolites are also less reactive with tissue constituents than the inorganic arsenic, and more readily excreted in the urine (Buchet et al., 1981b; Vahter & Marafante, 1983; Vahter et al., 1984; Marafante et al., 1987; Hughes & Kenyon, 1998; Vahter, 1988). Thus, the data strongly suggest that a lower capacity of arsenic methylation is associated with higher tissue concentrations of arsenic, which is likely to correspond to an increased risk of toxic effects. (Vahter & Marafante, 1985; Vahter et al., 1995; Aposhian et al., 1997 ; Vahter, 2000).

Beryllium. IARC classifies beryllium as human carcinogen (IARC, 1972) (Table 1), but it is not genotoxic and not carcinogenic in *in vitro* Balb/3T3 model (Table 16-18). This result can be explained considering the immune-mediated nature of the beryllium disease. In fact, exposure of people to relatively high concentrations of beryllium causes acute beryllium disease, characterised by chemical pneumonitis and some people inhaling low concentrations of beryllium develop chronic beryllium disease, a granulomatous lung disease characterised by dyspnea, cough, reduced pulmonary function, and a variety of other symptoms, including weight loss (Chang, 1996). The lack of a dose-response relationship between the extent of exposure and development of the disease, long latency periods between exposure and onset, and the low incidence among beryllium-exposed individuals suggests that the disease is immune-mediated. Occupational risk associated with exposure to beryllium-containing alloys has been documented for individuals exposed to beryllium-copper and beryllium-nickel alloys.

Cadmium. There is sufficient evidence in humans and animals to classify cadmium as carcinogenic, independently of the Cd compounds (IARC, 1990; Oldiges et al., 1989) (Table

1). It is genotoxic and carcinogenic in Balb/3T3 *in vitro* model (Table 16-18). Even though the underlying mechanisms are still puzzling, Cd (II) was proven to cause DNA strand breaks and chromosomal aberrations, although these latter were restricted to highly cytotoxic concentration (Hartwig, 1998).

The toxic effects of cadmium compounds have been studied over many years, inconsistent results have been published about their mutagenic, clastogenic and carcinogenic properties. Leonard and Bernard (Leonard & Bernard, 1993) proposed that the response obtained was dependent on the ability of the metal to penetrate the cell and to interact with DNA. Others suggest that the mechanism of metal-induced carcinogenesis is still unknown, but one possible pathway may involve the interaction of metals with DNA, either directly or indirectly (Hartmann and Speit, 1995; Hwua and Yang, 1998). Valverde et al. (Valverde et al., 2001) observed a heterogeneous response to different concentrations of metals (0.01, 0.1, 1 μM) between DNA from cells of the lung, liver and kidney. These results were surprising because we expected the same level of DNA damage among different organs using acellular DNA. These results suggest the possible presence of proteins associated with DNA that could be modulating the metal genotoxic response, as reported by others (Scicchitano and Pegg, 1987). Their results show that this metal did not interact directly with DNA and they suggest two different possible explanations of the genotoxicity observed by inhalation of these metals: (i) the possibility of DNA-associated protein–metal interactions, or (ii) the induction of an indirect mechanism, such as oxidative stress (Valverde et al., 2001). In addition, other indirect mechanisms could be considered, e.g. Dally and Hartwig (Dally and Hartwig, 1997) reported that cadmium at a concentration of 10 μM induced DNA strand breaks but without oxidative DNA base modification.

Chromium. IARC classifies Cr (VI) as carcinogenic in humans and animals (IARC, 1990a) (Table 1). The results obtained in the present work (Table 24) confirm this classification showing genotoxicity (by Comet and MN) (Table 17 and 18) and carcinogenic potential of Cr (VI) in Balb/3T3 *in vitro* model (Table 16).

The carcinogenic potential is well explained by the activation from cells of a detoxification mechanism. In fact, Cr (VI) is a pro-carcinogen that by itself is completely unreactive toward DNA under physiological pH and temperature. In the biological systems, however, Cr (VI) undergoes a series of reduction reactions yielding the thermodynamically stable Cr (III) form.

When this occurs, extra-cellular reduction acts as the detoxification process because of the production of poorly permeable Cr (III) complexes, while, inside the cell, Cr (VI) reduction is the activation event responsible for the generation of genotoxic damage and other forms of toxicity. Unlike the majority of other human pro-carcinogens, Cr (VI) metabolism in mammalian cells does not require any enzymes and relies on the direct electron transfer from ascorbate and nonprotein thiols, such as glutathione and cysteine (Zhitkovich, 2005). Cr (IV)

enters cells through non-specific anion channels and it is reduced to Cr (III). This process leads to stable Cr (III) but also to the formation of binary Cr (III)-DNA adducts as well as various cross-links (Voitkun et al., 1998) that could induce carcinogenic transformation of cells (Aiyar et al., 1991).

Mercury. IARC classifies organic mercury as possible carcinogens (IARC, 1993) (Table 1). In Balb/3T3 *in vitro* model CH_3HgCl results genotoxic (by Comet assay but no by MN, Table 17 and 18) and carcinogenic (Table 16), while $HgCl_2$ is genotoxic but not carcinogenic (Table 16-18).

The organic mercury genotoxicity has been usually attributed to its ability to react with the sulfhydryl groups of tubulin, impairing spindle function and leading to chromosomal aberrations and polyploidy (De Flora et al., 1994). Another important mechanism of mercury genotoxicity is its ability to produce free radicals that can cause DNA damage (Silva-Pereira et al., 2005). *In vivo* studies have demonstrated a clastogenic effect of mercury on people exposed to this element in their work environment or accidentally, through the consumption of contaminated food. Increased numbers of chromosome aberrations and micronuclei have been reported in people who consume contaminated fish (Franchi et al., 1994; Amorim et al., 2000) and in miners and workers of explosive factories (Anwar & Gabal, 1991; Al-Sabti et al., 1992). The effects of CH_3HgCl contamination have been widely studied since the outbreaks in Japan and Iraq. Many of these studies focused on the neurological effects of CH_3HgCl exposure in adult animals (Committee on the Toxicological Effects of Methylmercury, 2000).

Most of the *in vitro* studies with lymphocytes also used high doses of mercury compounds in order to evaluate its clastogenic effects (Betti et al., 1992).

In addition, mercury compounds induce a general collapse of antioxidant mechanisms in the cell by binding to a radical scavenger like the sulfhydryl groups of glutathione. Such a collapse results in cell degeneration, loss of membrane integrity and cell necrosis (Schurz et al., 2000). Necrosis can be indicated by a decrease in mitotic index, as shown by the present results. A decrease in mitotic index followed by an increase in the generation of reactive oxygen species was detected in human blood lymphocytes exposed to CH_3HgCl (Ogura et al., 1996). Another mechanism that may contribute to cell death induced by mercury compounds is apoptosis. Shenker et al. (Shenker et al., 2000) reported that CH_3HgCl caused a significant increase in cytochrome c in the cytosol of T cells. In contrast, $HgCl_2$ did not alter the levels of cytosolic cytochrome c, suggesting that the apoptotic pathway triggered by $HgCl_2$ compounds is independent of cytochrome c release. This effect may justify the higher cytotoxic action of CH_3HgCl, as observed by Silva-Pereira et al. (Silva-Pereira et al., 2005) and in the present study. A higher cytotoxic effect of CH_3HgCl compared to $HgCl_2$ was also found by other authors (Ogura et al., 1996) after exposure of human lymphocytes to these compounds. A number of *in vitro* studies on the genotoxic effects of mercury and its

compounds based on cytogenetic tests have been published. Their results suggest that organic compounds are generally more active, in terms of genotoxicity, than inorganic compounds (De Flora et al., 1994). Thus, free radicals become available to cause DNA damage (Ogura et al., 1996; Harvey et al., 1997; Morgan et al., 1998).

Nickel. IARC classifies nickel as human carcinogens (Table 1) (IARC, 1990b; Kasprzak et al. 2003). In our experimental model, Balb/3T3, we observe genotoxicity by Comet assay and MN (Table 17 and 18) but no carcinogenicity (Table 16).

Nickel (II) is used in modern industry with other metals to form alloys to produce coins, jewelry, and stainless steel as well as for nickel plating and manufacturing Ni-Cd batteries. Among new applications, it is important to note its role as a catalyst for the production of carbon nanoparticles. This new technology increases consumption and contamination with nickel compounds. Workers are exposed at different stages of processing of nickel-containing products. The most important route of human exposure to nickel is inhalation. The exposure to Ni has long been known to cause acute respiratory symptoms and also may cause cardiovascular and kidney diseases, as well as allergic dermatitis (Morgan and Usher 1994). However, nickel carcinogenic activity represents the most serious concern.

As previously discussed for beryllium, nickel (II) exerts its carcinogenic activity most likely through non-genotoxic mechanisms and causes diseases such as bronchitis, pulmonary fibrosis, asthma, and pulmonary edema, through immune-mediated mechanisms (Salnikow K. and Zhitkovich A., 2008).

In various animal models, but not in Balb/3T3, chronic exposure to nickel compounds induces tumors at virtually any site of administration (Biedermann and Landolph 1987; Tveito et al., 1989; Patierno et al., 1993; Rani et al., 1993; Morgan and Usher 1994; Sunderman, 1994; Kasprzak, et al., 2003). Concerning genetic and epigenetic changes, it is reported that although various potentially mutagenic DNA lesions have been shown to occur following nickel exposure, the actual mutagenic activity of nickel compounds, observed in most of the mutational systems examined so far from Salmonella to mammalian cells *in vitro,* has been low (Fletcher et al., 1994; Biggart and Costa, 1986; Arrouijal, et al. 1990; Kargacin et al., 1993). Thus, it is suggested that nickel-induced mutagenic activity is not the primary cause in nickel-induced carcinogenesis. Indeed, the experiments with the SHE system have provided confirmatory evidence that cell immortalization can occur as an indirect consequence of carcinogen exposure following an induced high frequency change in the treated population, rather than through direct targeted mutagenesis (Trott et al., 1995). Epigenetic changes are indicated as primary events in nickel carcinogenesis, which may include changes in the histone acetylation, methylation, or ubiquitylation levels, structural changes, and/or alterations in DNA methylation as well as the activation or suppression of a number of transcription factors (Biedermann and Landolph 1987; Salnikow and Zhitkovich , 2008).

Platinum. The cases of cis- and carboPt (non-genotoxic by Comet assay and genotoxic by MN) compared to $PtCl_2$ and $PtCl_4$, $(NH_4)_2PtCl_6$ and oxaliPt (genotoxic by both Comet assay and MN) are rather interesting.

It is known that the genotoxicity of Pt is determined by oxidation state, conformation and structure (Gebel et al., 1997). Pt compounds with two different oxidation states (II and IV) produce a significant increase in MN frequency and they are able to induce DNA damage via both a direct action and trough the activation of oxidative mechanisms in human lymphocytes (Migliore et al., 2002a).

CarboPt, cisPt and oxaliPt are used as anticancer drugs (Legallicier et al., 1996). CisPt interacts with the DNA and forms cross-link between the guanines of the two strands. This seems to induce the transforming carcinogenic activity (Saris et al., 1996). These observations could explain the negative results obtained by Comet assay (Table 16), which is able only to detect single and double breaks at the DNA.

Vanadium. Vanadate compounds are cytotoxic and mitogenic, and modify several cell functions involved in mitosis. In vitro, V (IV) has been shown to modify DNA synthesis and repair (Sabbioni et al., 1991), Vanadyl sulfate and sodium orthovanadate stimulate the incorporation of thymidine into DNA of cultured quiescent Swiss mouse 3T3 and 3T6 cells in manner similar to colchicine (Smith, 1983). Previous in vitro studies showed a dose-dependent carcinogenic potential of V (V) (but not V (IV)) in Balb/3T3 (Sabbioni et al., 1993b) and dose-time dependent in SHE (Kerckaert et al., 1996). Our study are in agreement with these findings (Table 16-18 and 24).

In addition, the results of the present study on the genotoxic potential of vanadate ions in a dose-dependent way are also in agreement with other literature data. Vanadium acts on DNA in similar but lesser way as chromium, particularly by forming of DNA-protein crosslinks (Nechay et al, 1986). $NaVO_3$, NH_4VO_3, SVO_5 and Na_3VO_4 produce *in vitro* structural aberrations, micronuclei, sister-chromatide exchange or satellite chromosome associations in human lymphocytes (Migliore et al., 1993; Rodríguez-Mercado et al., 2003). No studies are known relating human cancer to vanadium ions exposure. Only V_2O_5 is classified by IARC as possible carcinogen to humans.

5.1.3. Metal speciation

The findings on the morphological transformation induced by the As and Pt compounds tested (Table 16) confirm the great importance of speciation (Ponti, 2001) in metal toxicology. In fact, it is known that the toxicological effects of metal elements depend on their chemical forms (Sabbioni et al., 1985). The carcinogenic response is not only depending on the oxidation state of As and Pt atoms, but it depends also on the ligands and the chemical nature (organic/inorganic) of the As and Pt compounds, factors that probably influence the cellular availability. Table 16 shows that five-folds increase in the concentration of $Na_2HAsO_4 \cdot 7H_2O$ is needed to obtain the same cytotoxic and carcinogenic results as with $NaAsO_2$. This finding is fully confirmed by studies that demonstrate how the inorganic As (III) is more potent than As (V) both in Balb/3T3 (Bertolero et al., 1987) and SHE cells (Lee et al., 1985). In addition, organic forms of As (such as MMA III, DMA III and $(C_6H_5)_4AsCl \cdot H_2O$) show different cytotoxicity (MMAIII > $(C_6H_5)_4AsCl \cdot H_2O$ > DMA III) but no carcinogenic potential in Balb/3T3 (Table 16) confirming the theory of speciation.

Concerning Pt compounds, they show carcinogenic potential (with the exception of oxaliPt and $(NH_4)_2Pt(SCN)_6$) in Balb/3T3 but different cytotoxicity: cisPt > $PtCl_2$ > $PtCl_4$> carboPt > oxaliPt> $(NH_4)_2PtCl_6$ > $(NH_4)_2Pt(SCN)_6$.

Other examples of speciation in terms of cytotoxicity are: $(NH_4)_2WS_4$ > Na_2WO_4 and $CdCl_2$ > $CdMoO_4$. While, for what concerns both cytotoxicity and carcinogenic potential, CH_3HgCl is more toxic than $HgCl_2$ and in addition the organic form (CH_3HgCl) is carcinogenic (Table 16); $NaVO_3$ and $(C_5H_5)_2VCl_2$ induce the same cytotoxicity, but only the first one is carcinogenic (Table 16).

Table 24. Carcinogenic potential and genotoxicity of 18 metal compounds

Compound	*In vitro* (Balb/3T3)			Animal	Human (IARC)
	Comet	MN	CTA		
$AgNO_3$	+	+	-	-	-
$Na_2HAsO_4 \cdot 7H_2O$	+	-	+	?	+
$NaAsO_2$	+	-	+	+[a]	+
MMA (III)	+	-	-	-	?
$(C_6H_5)_4AsCl \cdot H_2O$	+[b]	-	+[b]	?	(+)
$BeCl_2$	-	-	-	+	+
$CdCl_2 \cdot H_2O$	+	ND	+	+	+
$Na_2CrO_4 \cdot 4H_2O$	+	+	+	+	+
CH_3HgCl	+	-	+	+	(+)
$HgCl_2$	+	ND	-	+	(+)
$NiSO_4$	+	+	-	+	+
$PtCl_2$	+	+	+	?	?
$PtCl_4$	+	+	+	?	?
CisPt	-	+	+	+	(+)
CarboPt	-	+	+	?	?
OxaliPt	+	+	-	?	?
$(NH_4)_2PtCl_6$	+	+	+	?	?
$NaVO_3$	+	-	+	?	?

(+): possible human carcinogens
a: only related to inhalation exposure of hamsters (Yamamoto et al., 1987)
b: exposure to 10 µM (Comet)
C: exposure to 7 µM (CTA)
N.D.=not determined

5.2. Biokinetic studies

This study confirms the possibility to use the *in vitro* model for intestinal epithelial adsorption (Caco-2 cells) for the investigation of the effect of ingested chemicals. In fact, in this model we can study both the epithelial barrier integrity (end-point of cytotoxicity) and the transport through the epithelium.

In this work we studied the *in vitro* effect of apical and basolateral exposure to radiolabelled Cr (VI), As(III), Ochratoxin A and Gentamicin on the barrier function of intestinal epithelium. For this purpose a colonic cell line (Caco-2) was apically or basolateral exposed to concentrations of Na_2CrO_4 ranging from 1 to 50 µM for 24 h and apically to 1 µM for 33 days. The administration was performed by continuous and discontinuous exposure. Discontinuous apical and basolateral long-term exposures (17 days) were carried out for 0.1 µM of As(III), 0.7 µM Ochratoxin A and 1 µM Gentamicin. In order to avoid possible cytotoxic effect (Figure 7) and epithelial damage (Annex 1, table 1-3) we used only subtoxic concentrations for the four different chemicals tested (As, Cr, Gentamicin and Ochratoxin).

Chromium. The results obtained in Caco-2 cells exposed to Cr confirm the great potential of radioanalytical methods in *in vitro* investigations of chemical interaction and of mammalian cells metabolism (Sabbioni et al., 1993a).

In particular, the availability of ^{51}Cr with high specific radioactivity and very sensitive detection and measurement of characteristic γ-radiations allowed to assess the absorptive and secretory directions (i.e. from the apical (serosal) and from the basolateral (mucosal) sides) as well as the simultaneous study of the uptake of metal into the cells and its intracellular distribution (Annex 3, table 5 and 6). This fundamental aspect in mechanistically-based *in vitro* toxicology research will allow to develop uptake-effect relationships rather than the traditional external dose-effect relationship (Sabbioni et al., 1999). From this view, the results show that Cr fluxes in Caco-2 cells occur in both absorptive and secretory directions, with a concomitant similar accumulation of Cr by cells (Annex 3, table 5).

Interestingly, at the end of the experiment (24h post exposure) the concentration of Cr was of the same order of magnitude in dead and alive cells (Annex 3, table 5) as well as in the subcellular fractions (Annex 3, table 6). Most of Cr was of cytosolic nature, while, for what concerns the cellular fractions, the highest amount of Cr was contained in the nuclei.

These results are not in contrast with the *in vivo* data reported in literature for Cr (VI) that show its low adsorption (Introduction, section Chromium and gastrointestinal tract). In fact, *in vivo* Cr (VI) undergoes a series of reduction reactions part of the detoxification mechanism, by gastric juice pH, yielding thermodynamically stable Cr (III) whose absorption is very low.

In our experimental design the effect of gastric juice is not considered and a more complicated situation, involving reduction phenomena in cell culture medium in the presence of cells, cannot be excluded.
Anyway it is also reported that exposed animals showed clear signs of toxicity in the liver and other internal organs, indicating the ability of toxic Cr (VI) to avoid detoxification in the gastro-intestinal tract and subsequently entering into the systemic circulation. Sustained elevation of Cr levels in red blood cells of human volunteers following ingestion of Cr (VI)-laced water (Kerger et al., 1997) is also consistent with the absorption of significant amounts of Cr (VI) into the blood (Zhitkovich, 2005).

Arsenic. It has been established that soluble inorganic arsenic is readily absorbed from the gastro-intestinal tract of the human volunteer subjects. For instance, between 80% and 90% of a single dose of arsenite, As (III), or arsenate, As (V), has been found to be absorbed from the gastro-intestinal tracts of humans (Freeman et al., 1979; Tam et al., 1979; Pomroy et al., 1980). The most direct evidence is from measurement of fecal excretion in humans given oral doses of arsenite, wherein 5% was recovered in the feces (Bettley and O'Shea, 1975), indicating that absorption was at least 95%. This is supported by studies in which urinary excretion in humans was found to account for 55–80% of daily oral intakes of arsenate or arsenite (Buchet et al., 1981). In contrast (Mappes, 1977), ingestion of arsenic triselenide (As_2Se_3) did not lead to increase in urinary concentration, indicating that gastro intestinal absorption may be much lower when highly insoluble forms of arsenic are ingested. This is also supported by the observation that, when arsenic-contaminated soil has been used as the matrix (Freeman et al., 1995), the degree of absorption has been found to be 80%.
Both short-term and chronic oral exposures to inorganic arsenicals have been reported to result in irritant effects on gastrointestinal tissues. Numerous studies of acute, high-dose exposure to inorganic arsenicals have reported nausea, vomiting, diarrhea, and abdominal pain, although specific dose levels associated with the onset of these symptoms have not been identified. Chronic oral exposure to 0.01 mg As/kg/day generally results in similar reported symptoms. For both acute and chronic exposures, the gastrointestinal effects generally diminish or resolve with cessation of exposure. Similar gastrointestinal effects have also been reported after occupational exposures to inorganic arsenicals, although it is not known if these effects were due to absorption of arsenic from the respiratory tract or from mucociliary clearance resulting in eventual oral exposure.
On the contrary, our results suggest no transport of As from the apical to the basolateral exposure and viceversa (Figure 9).
Since transport of As was seen reported in the Caco-2 cell model (Laparra et al., 2006) for short time of exposure and high concentrations, our results could be explained considering the fact that in our experimental design we wanted to avoid interference due to cytotoxicity

and damage of epithelial integrity. Under these circumstances we did not observe As transport through the epithelium. Based on the results obtained we can assume that only when the epithelium is damaged, it is permeable to As (III) (Figure 9). In addition we used a discontinuous treatment approach that could permit the cell to eventually repair As toxic effects and allow its uptake (Annex 3, table 9). So cells are able to internalise it and probably metabolise it by some kinds of detoxification mechanisms.

Gentamicin and Ochratoxin. We studied these two organic compounds for they relevance as drug (gentamicin) and food contaminant (ochratoxin A). We exposed Caco-2 cells to low gentamicin concentration for long term and our results are in agreement with the *in vivo* adsorption of undelivered gentamicin (Figure 10). In fact, it was demonstrated that gentamicin can be administrated orally only using organic carriers such as PEG-8 caprylic/capric glycerides (Labrasol) (Hu et al., 2001).

Concerning ochratoxin A, Avantaggiato et al. (Avantaggiato et al., 2007) reported that during the transit of a multitoxin-contaminated feeds through a computer controlled model (TIM system), the mycotoxins were absorbed from the intestinal compartments.

Since, for short time of exposure and high concentrations, transport of Ochratoxin A into the gastro-intestinal tract is reported and its absorption mainly from the upper part of the small intestine (jejunum) and less from the ileum and our results show no transport through Caco-2 epithelium, we can conclude, that long term exposure to low sub-cytotoxic doses does not allow trans-epithelium transport (Figure 11). In addition, Caco-2 cells mimic the colon-rectal part of intestine that probably is not able to absorb ochratoxin A (Figure 11).

5.3. Nanotoxicology studies

The study of manufactured nanoparticles (mNPs) toxicology and their morphological transformation still remain an open question in the scientific community. It was demonstrated in different *in vitro* and *in vivo* studies that the mNPs possess the ability to be internalised into the cells inducing inflammatory responses (Donaldson & Tran, 2002) in relation to their size, shape, and surface areas (Brown et al., 2001).

Moreover, studies of ultrafine particles inhalation suggest that particle size can have a high impact on toxicity more than other physicochemical characteristics, due principally to the large surface area and its reactivity (Tran et al., 2000; Donaldson & Tran, 2002). If surface reactivity is influenced by the size of the particle, the surface properties can be changed by coating the nanoparticles (NPs) with different materials. This interaction of surface area and particle composition in eliciting biological responses adds an extra dimension of complexity in evaluating the potential of adverse events that may result from exposure to these materials (Oberdorster et al., 2005a). There are indications in the literature that manufactured nanoscale materials may distribute in the body in unknown ways and certain NPs have been observed to preferentially accumulate in particular organelles (Wang et al., 2005).

For this work we selected Co-nano to study the possible cytotoxicity, genotoxicity and morphological transformation together with an evaluation of the uptake rate of this NPs type in a selected cell model. Furthermore, we decided to investigate the biological effects of well characterized nanoparticles, taking into account their size distribution and the stability in culture medium in forms of Co^{2+} leakage. In fact a large amount of metallic mNPs (e.g. Co_2FeO_4) produced by industry for different applications (Salata, 2004; Sabbioni et al., 2005) are synthesised without any coating procedure and in many cases, they naturally aggregate and agglomerate, changing therefore their size, and they tend to release in aqueous solvents their corresponding ions, natural effects of a solvatation by solvent due to dissolution. The study of these aspects is fundamental for understanding the *in vitro* biological effects and potentially triggering toxicity (Soto et al., 2007; Raja et al., 2007).

For this reason, we analysed the time-dependent leakage of cobalt ions (Co^{2+}) into culture medium (Table 20). The data show that there is a time-dependent increase in Co^{2+} release for both the concentrations tested, reaching 44% for 100 µM at 72 h. Based on the cytotoxicity results obtained we can speculate that, under these experimental conditions, the concentration of Co^{2+}, extrapolated by the percentage of Co^{2+} released in Table 20, is not enough to justify the observed Co-nano toxicity (Figure 13). In fact, for example, considering an exposure time of 2 h at the concentration of Co-nano 100 µM that corresponds to a 7% Co^{2+} release (7 µM), we observed no cell viability for Co-nano, whereas 80% cell viability for Co^{2+}. Consequently the cytotoxic effect seems likely to be induced by nanoparticles and not by Co^{2+} although a complementary and/or a synergic effect cannot be excluded.

Concerning the morphological transformation of cobalt and its compounds the International Agency for Cancer Research (IARC, 1991) concluded that cobalt and its compounds are possibly carcinogenic to humans (group 2B) (Table 1) since there was sufficient evidence in experimental animal studies but inadequate evidence for carcinogenicity in humans (lung cancer) (Kuo et al., 2006).

In our *in vitro* model, cobalt nanoparticles (Table 21) showed a dose-dependent statistically significant increase in the morphological transformation, expressed as the transformation frequency, ranging from $0.41x10^{-4}$ to $6.64\ x10^{-4}$ for 1-30 µM, respectively. A statistically significant increase in the end-point was also observed if the single dose value data is analyzed versus control (P<0.01), starting from 7 µM (Table 21). For cobalt chloride (Table 21), instead, no statistically significant increase is evident neither for the dose dependency, nor for the single concentration values versus control. This latter evidence is also supported by Lison and co-workers (Lison et al., 2001), which demonstrate that experimental data indicate some evidence of a genotoxic potential for cobalt *in vitro* but there is no evidence available of a morphological transformation (Lison et al., 2001).

Analyzing the genotoxic potential there are data reporting induction of genotoxicity, but almost all are related to cobalt metal or compounds in the soluble forms, whereas for cobalt nanoparticles they are still missing or rare. De Boeck et al. (De Boeck et al., 2003a) explored the *in vitro* genotoxicity of Co metal, and compared it with that of hard metal particles in terms of concentration and time-dependency. Co metal and cobalt chloride produced approximately the same level of DNA damage. Recently, DNA migration (alkaline comet assay) in human lymphocytes after treatment with different combinations of Co metal and metallic carbide particles was assessed by Lison and coworkers (Lison et al., 1995). De Boeck et al. (De Boeck et al., 2003b) assessed the ability of powder mixtures of Cr_3C_2, Mo_2C and NbC with cobalt to induce chromosome/genome mutations (micronucleus test) in human lymphocytes. The exact mechanism by which cobalt compounds induce micronuclei is not clearly identified; it might be the consequence of the direct clastogenic activity, but an aneuploidogenic activity should not be overlooked given the literature data on cobalt (II) (De Boeck. et al., 2003b). Regarding the genotoxicity effects of nanoparticles, the data are rare and have to be well evaluated considering the different type of *in vitro* models. The only data actually available for the genotoxicity of Co-nano are reported by Colognato et al. (Colognato et al., 2008). In this study they used both the alkaline comet assay and the micronucleus test showing that in human peripheral lymphocytes there is, evidently, a dose-dependent increase in the primary DNA damage for Co-nano nanoparticles but not for Co^{2+} whereas analyzing the frequency of micronucleated binucleated cells both the compounds show positive results.

Concerning this specific type of toxicity, our data demonstrate that for both Co-nano and Co^{2+} there is a statistically significant increase (P<0.01) in the induction of single strand and double

strand breaks (Figure 14). While analyzing the genotoxic potential in terms of chromosomal aberrations (Table 22), we observe a statistically significant (P<0.01) increase, not dose-dependent, in the frequency of micronucleated binucleated cells for Co-nano but not for Co^{2+} (Table 22). In addition, for Co-nano we observe low values in the number of micronucleated binucleated cells at the higher concentrations, in comparison with 1 µM, which could be explained by the fact that the cytotoxicity effect (Figure 13) can mask the genotoxic potential. Briefly, an increasing cytotoxicity is counteracted by a decrease in the genotoxicity.
The different behaviour of the two cobalt forms likely suggests that Co-nano is a potential genotoxic carcinogen. In fact, the formation of chromosomal aberrations, in forms of a micronucleus, like in our case for Co-nano, is a process which turns lead to a stable mutation, which with higher probability could trigger a morphological transformation. Instead the production of DNA damage, in forms of single and double strand breaks, like the results obtained for Co^{2+}, is a premutational lesion, easily removed by molecular repairing processes, not necessary reflects the fact that the cells will undergo morphological transformation. Regarding the genotoxicity effects of nanoparticles, the data are rare and have to be well evaluated considering the different types of *in vitro* models. In fact, a study on Co-nano nanoparticles, by Colognato and coworkers (Colognato. et al., 2008), using both the alkaline comet assay and the micronucleus test, show that in human peripheral leukocytess there is, evidently, a dose-dependent increase in the primary DNA damage for Co-nano nanoparticles but not for Co^{2+} whereas analyzing the frequency of micronucleated binucleated cells both the compounds show positive results.

Looking at the relevant biological effects observed by all our assays we decided to investigate the Co-nano interaction with the cell in terms of uptake (Photo 8 and Table 23). Results showed an 50-100 fold increase of uptake for ^{60}Co-nano in comparison to $^{57}Co^{2+}$ (Table 23). This high quantity of Co-nano uptake, in comparison with ions, is possibly due to the chemical nature of Co-nano, since the particles may interact with proteins present in culture medium on their surface, which can lead to easier uptake by the cells (Oberdorster et al., 2005a; Oberdorster et al., 2005b). This type of internalization process due to a nano-protein interaction is also suggested by Limbach and coworkers (Limbach et al., 2007) which indicate that the particles could efficiently enter the cells by a Trojan-horse type mechanism. Other specific studies are ongoing to understand the intracellular trafficking (interaction with cells, uptake and intracellular distribution) of NPs in *in vitro* systems relevant for human exposure.

6. SUMMARY

The experimental work of this study was carried out in order to charcterize the carcinogenicity, genotoxicity, biokinetics of various metals and their nanoparticles by *in vitro* testing alternative to the use of laboratory animals. In particular, we used immortalised mouse fibroblasts (Balb/3T3 cell line) as *in vitro* model for carcinogenicity and genotoxicity testing and human colon rectal cancer cell line (Caco-2) as *in vitro* model of intestinal epithelial barrier for intestinal adsorption.

Carcinogenicity. The detection of carcinogenic chemicals still remains a major challenge, especially in the case of substances acting via non-genotoxic mechanisms. Furthermore, this is an area of high animal consumption per test. No *in vitro* test that detects non-genotoxic chemicals has yet been accepted by regulatory authorities. One of the very promising assays that permits the detection of both genotoxic and non-genotoxic compounds is the *in vitro* cell transformation assay. Extensive research work in this area was done at ECVAM particularly on the immortalised mouse fibroblast Balb/3T3 cell line (Mazzotti, 2001; Ponti 2001) and this test is now under prevalidation at ECVAM. In parallel, other *in vitro* genotoxicity tests such as Comet and Micronucleus assays are being used and evaluated, both at ECVAM and by external partners. In this study we tested 18 metal compounds for the evaluation of their carcinogenic potential and genotoxicity. For the most part, we observed an agreement between our experimental results and the IARC classification or the literature. We believe that the battery of test used in our study could be useful to evaluate the mechanism of action of chemicals on carcinogenicity.

Biokinetics. Information from *in vitro* toxicokinetic studies on the absorption, distribution, metabolism and excretion (ADME) of chemicals and nanoparticles, is fundamental to understand their mechanisms of action and their toxicological profile. These complex studies are possible at JRC by using advanced spectrochemical and radioanalytical and bioanalytical techniques in combination with cell culture methodologies. In this work, biokinetic (adsorption) was studied both in an *in vitro* model of intestinal epithelial barrier for intestinal adsorption (Caco-2 cells) and in single cells (Caco-2 and Balb/3T3) as uptake and intracellular distribution. In particular, we studied the *in vitro* effect of apical and basolateral exposure to radiolabelled Cr (VI), As (III), Ochratoxin A and Gentamicin on the barrier function of intestinal epithelium. We could verify that Cr fluxes in Caco-2 cells in both absorptive and secretory directions, with a concomitant similar accumulation of Cr by cells. Under our experimental conditions, we did not observe As transport through the epithelium probably because only when this is damaged, it is permeable to As. In the case of Gentamicin and Ochratoxin A, we

did not observe transport through the epithelium and this is comparable to the *in vivo* results reported in literature.

***In vitro* nanoparticles toxicology.** In the second half of the 20th century the development of microtechnology has produced a technical revolution opening the dynamic era of nanotechnology. Nanomaterials, typically under 100 nm, have new physicochemical characteristics, novel properties and functions due to their small size. They have been manufactured and used to improve the quality and performances of many consumer products employed daily, medical therapies and tests. Unfortunately, information on nanoparticles toxicology and exposure assessment is severely lacking making impossible health risk assessments of manufactured nanoparticles or nanomaterials.

In this context, *in vitro* systems (cell cultures) that could reduce, refine and replace animal methods are recommended to understand the mechanisms of action of manufactured nanoparticles (e.g., intracellular trafficking, metabolism, toxicological profile and carcinogenic potential). In particular, we studied cytotoxicity, genotoxicity and morphological transformation of cobalt nanoparticles (Co-nano) and cobalt ions (Co^{+2}) in Balb/3T3 cell model. We also evaluated Co-nano dissolution in culture medium and cellular uptake of Co-nano and Co^{+2}. Our results indicate that Co-nano are exerting cytotoxicity (IC_{50}: 20µM after 2h of exposure and 10µM at 24 and 72h). For the Co-nano genotoxicity the results show that indeed the Co-nano is genotoxic (>1 µM) but no evident dose-response relationship was observed. For the morphological transformation, Co-nano show a statistically significant increase in the formation of Type III foci. Moreover, analyzing the internalization of Co-nano we observed a higher uptake if compared with Co^{+2}.

Our results indicate cytotoxicity, morphological transformation and genotoxicity induced by Co-nano, while for Co^{+2} we found cytotoxicity, morphological transformation and genotoxicity, assessed by Comet assay but no by micronucleus test. Taken together, this shows that nanoparticles can have different kinetic and toxicological properties compared to their parent compounds. This might result in the future in new requirements for safety assessments.

7. Zusammenfassung

Der experimentelle Teil dieser Arbeit charakterisiert die Karzinogenität, Genotoxizität und Biokinetik verschiedener Metalle und Metallnanopartikel in *in vitro*-Tests als Alternative zum Tierversuch. Im Speziellen wurden immortalisierte Mausfibroblasten (Balb/3T3-Zelllinie) als *in vitro*-Modell für Karzinogenität und Genotoxizität verwendet sowie eine Zellinie aus einem menschlichem Rektum-Krebs (Caco-2) als *in vitro*-Modell der intestinalen, epithelialen Barriere für intestinale Adsorption.

Karzinogentät. Das Auffinden von karzinogenen Chemikalien ist immer noch eine grosse Herausforderung, insbesondere für Substanzen die über nicht-genotoxische Mechanismen wirken. Kein *in vitro*-Test zum Nachweis von nicht-genotoxischen Chemikalien wurde bisher durch regulatorische Behörden akzeptiert. Einer der sehr vielversprechenden Tests, der sowohl den Nachweis von genotoxischen als auch nicht-genotoxischen Verbindungen erlaubt, ist der *in vitro*-Zelltransformierungs-Test. Umfangreiche Forschungsarbeiten wurden in ECVAM durchgeführt, insbesondere mit der immortalisierten Mausfibroblasten-Zellinie Balb/3T3 (Mazzotti, 2001; Ponti 2001) und dieser Test wird daraufhin zur Zeit durch ECVAM prävalidiert. Parallel dazu werden andere *in vitro*-Genotoxizitätstests wie der Comet- und der Micronucleus-Test verwendet und evaluiert, sowohl in ECVAM als auch durch externe Partner. In der vorliegenden Arbeit haben wir 18 Metallverbindungen auf ihr karzinogenes und genotoxisches Potenzial untersucht. Im Wesentlichen fanden wir eine Übereinstimmung zwischen den experimentellen Resultaten und den IARC-Klassifikationen bzw. der Literatur. Wir glauben deshalb, dass die Testbatterie, die in unserer Arbeit verwendet wurde, nützlich zur Ermittlung des Wirkungsmechanismus von karzinogenen Chemikalien sein könnte.

Biokinetik. Informationen von *in vitro*-Toxikokinetikstudien zur Absorption, Verteilung, Metabolismus und Ausscheidung (ADME) von Chemikalien und Nanopartikeln sind grundlegend, um ihren Wirkmechanismus und toxikologisches Profil zu vestehen. Diese komplexen Studien sind im JRC möglich, da moderne spektrochemische, radioanalytische und bioanalytische Techniken in Kombination mit Zellkulturmethoden zur Verfügung stehen. In der vorliegenden Arbeit wurde die Biokinetik (Adsorption) sowohl in einem in *in vitro*-Modell zur intestinalen, epithelialen Barriere für intestinale Adsorption (Caco-2-Zellen) und in den beiden Zelllinien (Caco-2 and Balb/3T3) bezüglich Aufnahme und intrazellulärer Verteilung untersucht. Im Speziellen, studierten wir den *in vitro*-Effekt von apikaler und basolateraler Exposition zu radiomarkiertem Cr (VI), As (III), Ochratoxin A und Gentamicin auf die Barrierefunktion von intestinalem Epithel. Wir konnten verifizieren, dass Cr in Caco-2-Zellen sowohl in absorptiver als auch in sekretorischer Richtung transportiert wird, wobei gleichzeitig ähnliche Mengen von Cr durch die Zellen akkumuliert werden. Unter unseren experimentellen

Bedingungen konten wir keinen As-Transport durch das Epithel beobachten, da es vermutlich nur nach Schädigung permeabel für As ist. Im Fall von Gentamicin und Ochratoxin A beobachteten wir keinen Transport durch das Epithel und dies entspricht den *in vivo*-Resultaten in der Literatur.

***In vitro*-Nanopartikel-Toxikologie.** In der zweiten Hälfte des 20. Jahrhunderts hat die Entwicklung von Mikrotechnologien eine technische Revolution hervorgebracht, die das hochdynamische Zeitalter der Nanotechnologie eröffnet hat. Nanomaterialien, typischweise unter 100 nm, haben neue physikochemische Eigenschaften, neue Qualitäten und Funktionen aufgrund ihrer kleinen Grösse. Sie werden hergestellt und verwendet, um die Qualität und Verwendbarkeit von vielen alltäglichen Verbrauchsgütern, medizinischen Therapien und Tests zu verbessern. Leider gibt es einen erheblichen Mangel bezüglich der Toxikologie und Expositionsuntersuchung für Nanopartikel, was es unmöglich macht, das Gesundheitsrisiko von hergestellten Nanopartikeln und –materialien zu beurteilen.

In diesem Zusammenhang werden *in vitro*-Systeme (Zellkulturen) empfohlen, die Tierversuche reduzieren, verbessern oder ersetzen könnten, um die Wirkmechanismen von hergestellten Nanopartikeln zu verstehen (z.B. intrazellulärer Transport, Metabolismus, toxikologisches Profil und karzinogenes Potenzial). Im Besonderen studierten wir Zytotoxizität, Genotoxizität und morphologische Transformation von Cobalt-Nanopartikeln (Co-nano) und Cobalt-Ionen (Co^{+2}) im Balb/3T3-Zellmodell. Wir untersuchten ausserdem die Löslichkeit von Co-nano in Kulturmedium sowie die zelluläre Aufnahme von Co-nano und Co^{+2}. Unsere Resultate zeigen, dass Co-nano zytotoxisch sind (IC_{50}: 20µM nach 2h Exposition und 10µM nach 24 und 72h). Für die Genotoxizität von Co-nano fanden wir positive Ergebnisse (>1 µM) aber keine klare Dosis-Wirkungs-Beziehung. Für die morphologische Transformierung zeigte Co-nano einen statistisch signifikanten Anstieg der Bildung von Typ-III-Foci. Darüber hinaus fanden wir beim Studium der Internalisierung von Co-nano eine höhere Aufnahme im Vergleich mit Co^{+2}.

Unsere Resultate weisen somit auf Zytotoxizität, morphologische Transformierung und Genotoxizitet durch Co-nano hin, während für Co^{+2} Zytotoxizität, morphologische Transformierung und Genotoxizität, nachweisbar im Comet- aber nicht im Micronucleustest, beobachtet wurden. Zusammengenommen zeigt dies, dass Nanopartikel unterschiedliche Kinetiken und toxikologische Eigenschaften im Vergleich zu Ausgangsmaterialien haben können. Daraus können sich in Zukunft neue Anforderungen an Sicherheitsprufungen ableiten.

ANNEX 1

The following tables (1 and 2) summarise TEER values, as mean of 3 different measurements, in Caco-2 epithelium cultured for 14 days after exposure to 1, 30 and 50 µM of $Na_2{}^{51}CrO_4$ for 24 h and for 0-33 days to 1 µM (continuous and discontinuous exposure).

Table 3 shows TEER values after exposure to 0.1 µM of As, 7 µM of Gentamicin and 1 µM Ochratoxin A for 0-17 days (continuous and discontinuous exposure).

Table 1. Trans-Epithelial Electrical Resistance (TEER) measured in Caco-2 epithelium cultured for 14 days after exposure to 1, 30 and 50 µM of $Na_2{}^{51}CrO_4$ for 24h

[µM]	TEER[a] (Ω cm^2)					
	0	**1**	**2**	**5**	**7**	**24**
Control	401±15	506±26.7	401±14.2	416±12	422±8.9	470±19
			Apical to basolateral			
1	385±2.4	407±11.1	395±12.6	357±8.4	326±2.4	374±18.3
30	393±12.1	400±12.8	393±10.6	385±6.4	356±17.4	206±7.2*
50	402±6.4	442±6	423±10.6	388±6.4	370±8.4	153±21*
			Basolateral to apical			
1	410±14.7	452±14.7	444±25.3	370±15.1	342±12.1	351±8.7
30	403±7.3	437±7.3	414±8.7	367±18.9	339±12.8	221±20*
50	400±6.4	424±4.2	412±11.1	371±8.7	342±6.4	167±18*

a: mean of three experiments
*: p<0.01, statistically significance by Fisher's exact test

Table 2. Trans-Epithelial Electrical Resistance (TEER) measured in Caco-2 epithelium cultured for 14 days after exposure to 1 µM of Cr for 0-33 days

[µM]	TEER[a] (Ω cm^2)										
	0	**1**	**3**	**6**	**10**	**13**	**18**	**21**	**26**	**29**	**33**
C[b]	395±18	458±14	382±15	483±19	563±31	552±28	637±31	581±23	561±25	470±28	525±25
					Continuous exposure						
1	392±10	377±12	384±15	585±17	735±32	922±28	1063±10	1033±11	1012±14	848±20	571±28
					Discontinuous exposure						
1	394±14	370±15	434±42	529±26	591±25	769±23	769±30	714±20	706±25	567±32	559±32

a: mean of three experiments
b: control

Table 3. Trans Epithelial Electrical Resistance (TEER) measured in Caco-2 epithelium cultured for 14 days after exposure to 0.1 µM of NaAsO2, 7 µM Gentamicin, 1 µM Ochratoxin for 0-17 days

Compound	TEER[a] (Ω cm^2)						
	0	1	3	7	10	14	17
Control	328±5.3	370±5.2	390±8.9	417±3.9	427±9.5	418±2.9	427±7.1
				Apical to basolateral, discontinuous exposure			
$NaAsO_2$	395±7.8	344±5.6	343±6.7	398±2.5	510±9.1	535±5.1	423±3.8
Gentamicin	347±2.9	416±7.0	337±3.2	377±4.7	431±2.9	521±1.7	417±4
Ochratoxin	304±6.0	406±11.0	319±5.2	367±3.5	402±1.5	447±7.6	421±7.8
				Basolateral to apical, discontinuous exposure			
$NaAsO_2$	395±3.0	461±8.7	342±3.2	395±1.7	456±8	553±4.9	403±7
Gentamicin	357±1.7	444±2.9	339±2.1	402±4.7	452±4.2	552±4.8	430±2.1
Ochratoxin	304±4.0	413±7.5	335±3.5	412±4.0	423±4.5	473±2.1	410±9

a: mean of three experiments

ANNEX 2

Table 4. Transfer of Cr from apical to basolateral compartments and viceversa in absence of cells (2h of incubation to different Cr concentrations)

Initial [Cr]		Cr in the compartment[a] (ngCr/mL)			
		Apical to basolateral		Basolateral to apical	
µM	ngCr/g	Apical	Basolateral	Basolateral	Apical
0.022	1.13	0.55	0.58	0.57	0.56
1	52	27.2	24.8	28.0	24.0
50	2600	1324	1276	1333	1267

a: mean of three experiments RSD<7%

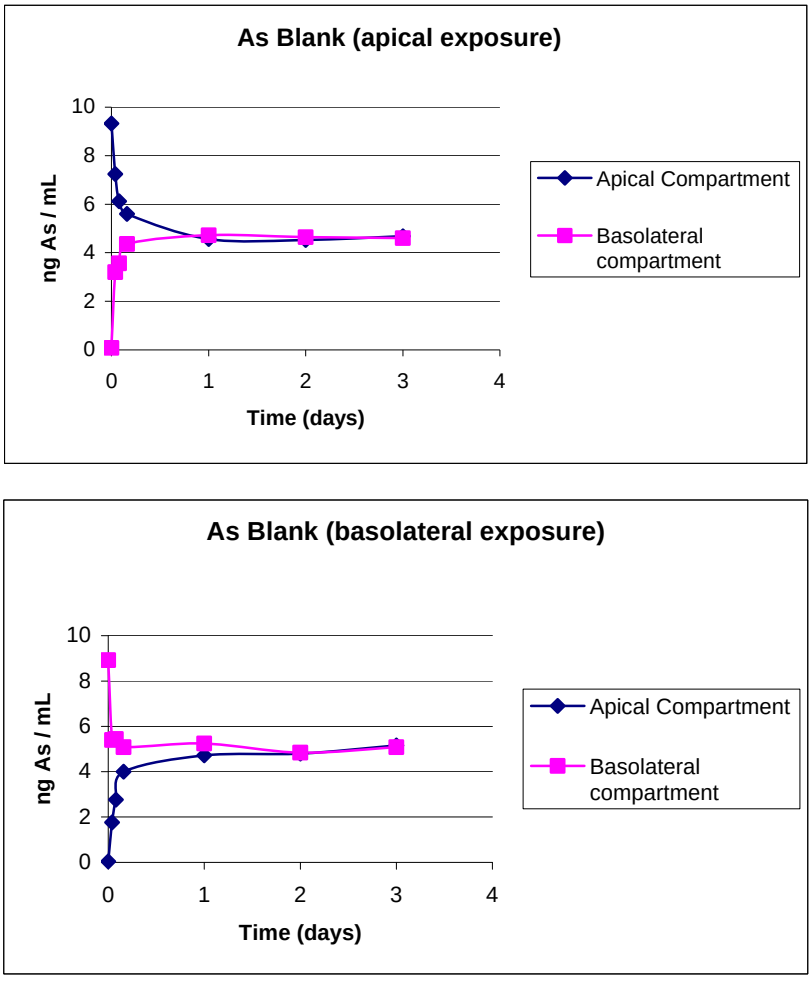

Figure 1. Transfer of As from apical to basolateral compartments and viceversa in absence of cells

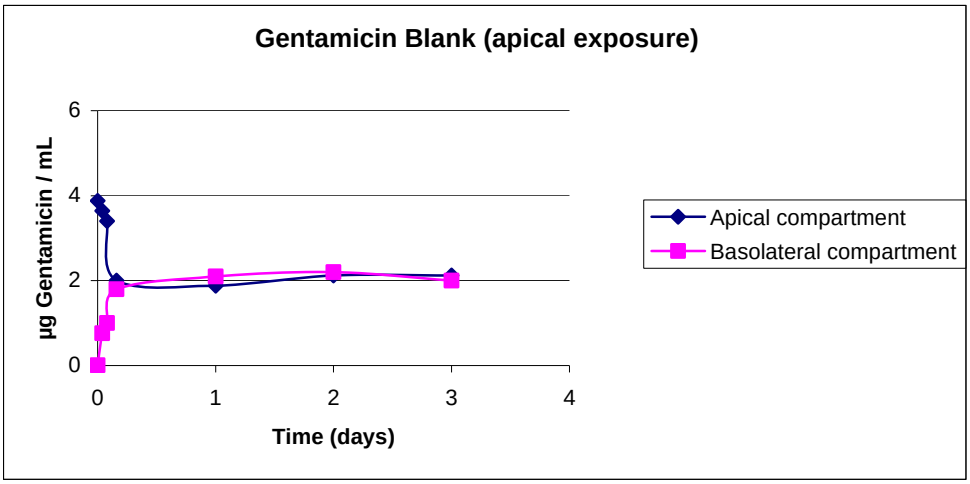

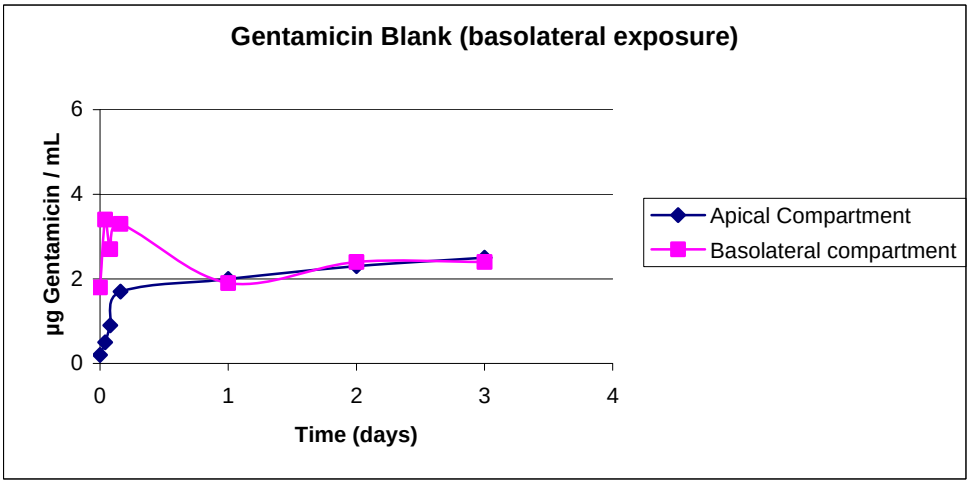

Figure 2. Transfer of gentamicin from apical to basolateral compartments and viceversa in absence of cells

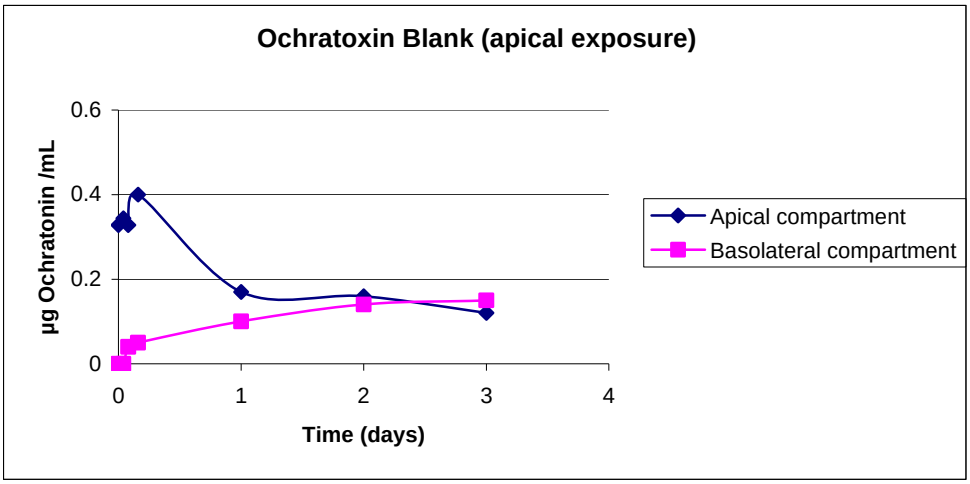

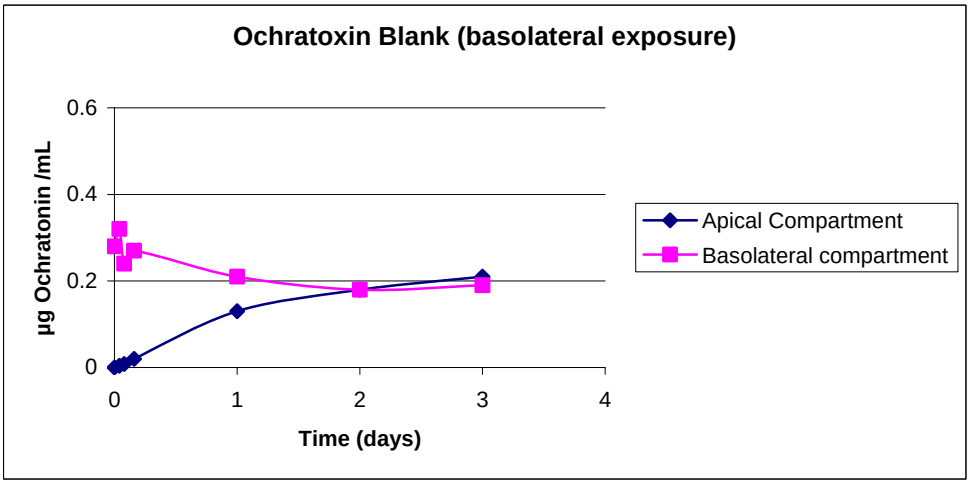

Figure 3. Transfer of ochratoxin from apical to basolateral compartments and viceversa in absence of cells

ANNEX 3

Table 5. Uptake of Cr in Caco-2 dead and alive cells after 24h of exposure (apical to basolateral, basolateral to apical)

[µM]	Uptake*			
	Cell dead		Cell alive	
	fg Cr/cell	%[a]	fg Cr/cell	%[a]
		Apical to basolateral		
1	18	1.1	98	2
30	480	0.9	710	3.1
50	950	0.9	1300	3
		Basolateral to apical		
1	16	0.7	32	3
30	800	1.1	740	3
50	1100	1	1360	2.6

a: percent of the initial Cr concentration.

*: mean of 3 experiments: RSD< 20%

Table 6. Intracellular distribution of Cr in Caco-2 cells after 24h of exposure (apical to basolateral, basolateral to apical) to 1, 30 and 50 µM of Cr

Subcellular fraction	Cr (% of homogenate)*		
	1 µM	30 µM	50 µM
		Apical to basolateral	
homogenate	100	100	100
nuclei	20	10	14
mitochondria	10	8	5
lysosomes	5	5	5
microsomes	5	3	4
cytosol	60	74	72
		Basolateral to apical	
nuclei	22	19	10
mitochondria	9	6	8
lysosomes	4	5	5
microsomes	3	5	2
cytosol	62	65	75

*: mean of 3 experiments :RSD<20%

Table 7. Uptake of Cr in Caco-2 alive cells after 10, 18 and 33 days of exposure (continuous and discontinuous) to 1 µM of Cr

Time (day)	Uptake*	
	Cell alive	
	fg Cr/cell	%[a]
Continuous exposure		
10	90	4
18	200	4.8
33	340	5.6
Discontinuous exposure		
10	100	8
18	80	2.9
33	90	3.9

a: percent of the initial Cr concentration

*: mean of 3 experiments: RSD<20%

Table 8. Intracellular distribution of Cr in Caco-2 cells after 10, 18 and 33 days of exposure (continuous and discontinuous) to 1 µM of Cr

Subcellular fraction	Exposure					
	Continuous			Discontinuous		
	Cr (% of homogenate)*					
	10 days	18 days	33 days	10 days	18 days	33 days
homogenate	100	100	100	100	100	100
nuclei	21.2	17	14.3	14.2	17	22
mitochondria	1.4	2.4	5	3.1	2	6.1
lysosomes	3.8	3.6	2.1	2.5	6.7	3.4
microsomes	4	3.3	2.6	3.9	2.8	3.1
cytosol	69.6	73.7	76	76.3	71.5	65.4

*: mean of 3 experiments: RSD<20%

Table 9. Uptake and intracellular distribution of As in alive Caco-2 cells after 17 days of exposure to $Na^{73}AsO_2$ 0.1 µM

Subcellular fraction	Exposure	
	Apical to basolateral	Basolateral to apical
	Uptake: 0.87 fgAs/cell	Uptake: 0.016 fgAs/cell
	As (% of homogenate)*	
homogenate	100	100
nuclei	25.2	33.4
mitochondria	4	22.2
lysosomes	1	3.7
microsomes	0.8	3.7
cytosol	69	37

*: mean of 3 experiments: RSD<20%

Table 10. Uptake and intracellular distribution of Gentamicin in alive Caco-2 cells after 17 days of exposure to Gentamicin Sulfate [^{3}H] 7 µM

Subcellular fraction	Exposure	
	Apical to basolateral	Basolateral to apical
	Uptake: 76 fg /cell	Uptake: 35 fg /cell
	Gentamicin (% of homogenate)*	
homogenate	100	100
nuclei	52.3	72
mitochondria	29	14
lysosomes	6	1.5
microsomes	1.1	1.5
cytosol	11.6	11

*: mean of 3 experiments: RSD<20%

Table 11. Uptake and intracellular distribution of Ochratoxin in alive Caco-2 cells after 17 days of exposure to Ochratoxin A [^{3}H(G)] 1 µM

Subcellular fraction	Exposure	
	Apical to basolateral	Basolateral to apical
	Uptake: 0.35 fg /cell	Uptake: 0.12 fg /cell
	Ochratoxin (% of homogenate)*	
homogenate	100	100
nuclei	54	40
mitochondria	22	12
lysosomes	4	4
microsomes	2	4
cytosol	18	40

*: mean of 3 experiments; RSD<20%

8. REFERENCES

Aaroson S.A. & Todaro G.J. Development of 3T3-like lines from Balb/c mouse embryo cultures: Transformation susceptibility to SV40. Journal Cellular Physiology. 72: 141-148, 1968.

Agresti A. Categorical data analysis. Second edition. Ed: Wiley Intersciences, Johhn Wiley & Sons, Inc., Hoboken, New Jersey pp. 91, 2002.

Aiyar J., Berkovits H.J., Floyd R.A. & Wetterhahn K.E. Reaction of Chromium (VI) with glutathione or with hydrogen peroxide: identification of reactive intermediates and their role in Chromium (VI)-induced DNA damage. Environmental health Perspectives. 92: 53-62, 1991.

Al-Sabti K., Lloyd D.C., Edwards A.A. & Stenar P. Survey of lymphocyte chromosomal damage in Slovenian workers exposed to occupational clastogens. Mutation Research. 280: 215-223, 1992.

Amorim M.I.M., Mergler D., Bahia M.O., Dubeau H., Miranda D., Lebel J., Burbano R.R. & Lucotte M. Cytogenetic damage related to low levels of methyl mercury contamination in the Brazilian Amazon. Anais da Acadêmia Brasileira de Ciências, 72: 497-507, 2000.

Anwar W.A. & Gabal M.S. Cytogenetic study in workers occupationally exposed to mercury fulminate. Mutagenesis. 6: 189-192, 1991.

Aposhian H.V., Zakharyan R., Wu Y., Healy S. & Aposhian M.M. Enzymatic methylation of arsenic compounds: II-an overview. In: Abernathy C.O., Calderon R.L., Chappell W.R. (Eds.), Arsenic. Exposure and Health Effects. Chapman and Hall, London, pp. 296–321, 1997.

Arrouijal F. Z., Hildebrand H. F., Vophi H. & Marzin D. Genotoxic activity of nickel subsulphide alpha-Ni_3S_2. Mutagenesis. 5, 583–589, 1990.

Avantaggiato G., Havenaar R. & Visconti A. Assessment of the Multi-mycotoxin-Binding Efficacy of a Carbon/Aluminosilicate-Based Product in an in Vitro Gastrointestinal Model. J. Agric. Food Chem. 55: 4810-4819, 2007.

Bagchi D., Bagchi M. & Stohs S.J. Chromium (VI)-induced oxidative stress, apoptotic cell death and modulation of p53 tumour suppressor gene. Biochemistry. 222: 149-158, 2001.

Banu Saleha B., Danadevi K., Jamil K., Ahuja Y.R., Visweswara Rao K. & Ishaq M. *In vivo* genotoxic effect of arsenic trioxide in mice using comet assay. Toxicology. 162; 171-177, 2001.

Bergamaschi E., Bussolati O., Magrini A., Bottini M., Migliore L., Bellucci S., Iavicoli I. & Bergamaschi A. Nanomaterials and lung toxicity: interactions with airways cells and relevance for occupational health risk assessment. Int J Immunopathol Pharmacol. 19: 3-10, 2006.

Bertolero F., Pozzi G., Sabbioni E. & Saffiotti U. Cellular uptake and metabolic reduction of pentavalent to trivalent arsenic as determinants of cytotoxicity and morphological transformation. Carcinogenesis. 8: 803-808, 1987.

Betti C., Davini T. & Barale R. Genotoxic activity of methyl mercury chloride and dimethyl mercury in human lymphocytes. Mutation Research. 281: 255-260, 1992.

Bettley F.R. & O'Shea J.A. The absorption of arsenic and its relation to carcinoma. Br. J. Dermatol. 92: 563-568, 1975.

Biedermann, K. A. and Landolph, J. R. Induction of anchorage independence in human diploid foreskin fibroblasts by carcinogenic metal salts. Cancer Res. 47: 3815-3823, 1987.

Biggart N. W. & Costa M. Assessment of the uptake and mutagenicity of nickel chloride in salmonella tester strains. Mutation Research. 175: 209-215, 1986.

Bosetti M., Massè A., Tobin E. & Cannas M. Silver coated materials for external fixation devices: *in vitro* biocompatibility and genotoxicity. Biomaterials. 23: 887-92, 2002.

Brown D.M., Wilson M.R., MacNee W., Stone V. & Donaldson K. Size-dependent proinflammatory effects of ultrafine polystyrene particles: a role for surface area and oxidative stress in the enhanced activity of ultrafines. Toxicol. Appl. Pharmacol. 175: 191-199, 2001.

Buchet J.P., Lauwerys R. & Roels H. Comparison of the urinary excretion of arsenic metabolites after a single dose of sodium arsenite, monomethylarsonate or dimethylarsinate in man. Int. Arch. Occup. Environ. Health. 48: 71-79, 1981b.

Buchet J.P., Lauwerys R. & Roels H. Urinary excretion of inorganic arsenic and its metabolites after repeated ingestion of sodium meta arsenite by volunteers. Int. Arch. Occup. Environ. Health. 48: 111-118, 1981a.

Chang L.W. (ed.). Toxicology of Metals. Boca Raton, FL: Lewis Publishers, p. 929-30, 1996.

Chantret I., Rodolosse A., Barbat A., Dussaulx E., Brot-Laroche E., Zweibaum A. & Rousset M. Differential expression of sucrose-isomaltase in clones isolated from early and late passages of the cell line CaCo-2: evidence for glucose-dependent negative regulation. Journal of Cell Science. 107: 213-225, 1994.

Chapman P.M. New Strategies for America's Watersheds. National Research Council (1999). National Academy Press, Washington, DC. Marine Pollution Bulletin. 40: 717-718, 2000.

Chiou H.Y., Hsueh Y.M., Hsieh L.L., Hsu L.I., Hsieh F.I., Wei M.L., Chen H.C., Yang H.T., Leu L.C., Chu T.H., Chen-Wu C., Yang M.H., Chen C.J. Arsenic methylation capacity, body retention, and null genotypes of glutathione S-transferase M1 and T1 among current arsenicexposed residents in Taiwan. Mutat. Res. 386: 197-207, 1997.

Colognato R., Bonelli A., Ponti J., Farina M., Bergamaschi E., Sabbioni E. and Migliore L. Comparative genotoxicity of Co nanoparticles and ions in human peripheral leukocytes in vitro. Submitted after revision to Mutagenesis. 2008.

Colognato R., Coppede F., Ponti J., Sabbioni E., Migliore L. Genotoxicity induced by arsenic compounds in peripheral human lymphocytes analysed by cytokinesis-block micronucleus assay. Mutagenesis. 22: 255-261, 2007.

Colvin V. The potential environmental impact of engineered nanomaterials. Nature Biotechnol. 21: 1166-1170, 2003.

Combes R., Balls M., Current R., Fischbach M., Fusenig N., Kirkland D., Lasne C., Landolph J., LaBoeuf R., Marquardt H., McCormick J., Muller L., Rivedal E., Sabbioni E., Tanaka N., Vasseur P. & Yamasaki H. Cell transformation assay as predictors of human carcinogenicity. The report and recommendations of ECVAM, Workshop 39. ATLA. 27: 745-767, 1999.

COM (2204) 338: Communication from the Commission. Towards a European strategy for nanotechnology, 2004.

COM (2005) 243: Communication from the Commission. European Action Plan for Nanosciences and Nanotechnologies

Committee on the Toxicological Effects of Methylmercury, Board on Environmental Studies and Toxicology and National Research Council (2000). Toxicological Effects of Methylmercury. The National Academies Press, Washington, DC, USA, 2000.

Costa M. DNA-Protein complexes induced by Chromate and other carcinogens. Environmental health Perspectives. 92: 45-52, 1991.

Cotelle S. & Ferard J.F. Comet assay in genetic ecotoxicology: a review. Environmental and Molecular Mutagenesis. 34: 246-255, 1999.

Cox C.E. Gentamicin. Med. Clin. North Am. 54, 1970.

Crecelius E.A. Changes in the chemical speciation of arsenic following ingestion by man. Environ. Health Perspect. 19: 147-150, 1977.

Csanaky I., Németi B., Gregus Z. Dose-dependent biotransformation of arsenite in rats--not S-adenosylmethionine depletion impairs arsenic methylation at high dose. Toxicology. 183(1-3):77-91, 2003.

Dally H. & Hartwig A. Induction and repair of oxidative DNA damage by nickel (II) and cadmium (II) in mammalian cells. Carcinogenesis. 18: 1021-1026, 1997.

De Boeck M., Kirsch-Volders M. & Lison D. Cobalt and antimony: genotoxicity and carcinogenicity. Mutat. Res. 533: 135-152, 2003b.

De Boeck M., Lombaert N., De Backer S., Finsy R., Lison D.M. & Kirsch-Volders M. In vitro genotoxic effects of different combinations of cobalt and metallic carbide particles. Mutagenesis. 18: 177-186, 2003a.

De Flora S. & Boido V. Effect of human gastric juice on the mutagenicity of chemicals. Mutation Research. 77: 307-315, 1980.

De Flora S., Benniceli C. & Bagnasco M. Genotoxicity of mercury compounds. A review. Mutation Research. 317: 57-79, 1994.

DHO (Department of Health). Report on health and social subjects, guidelines for the testing of chemicals for mutagenicity. Committee on Mutagenesis of Chemicals in Food, Consumer Products and the Environment. London. UK: HMSO, 2000.

Di Paolo J.A. Quantitative *in vitro* transformation of Syrian golden hamster embryo cells with the use of frozen stored cells. Journal of the National Cancer Institute. 64: 1485-1489, 1980.

Di Paolo J.A., Takano K. & Popescu N.C. Quantitation of chemically induced neoplastic transformation of Balb/3T3 cloned cell lines. Cancer Research. 32: 2686-2695, 1972.

Donaldson R.M. Jr & Barreras R.F. Intestinal absorption of trace quantities of chromium. Journal of Laboratory and Clinical Medicine. 68: 484-493, 1966.

Donaldson,K. & Tran C.L. Inflammation caused by particles and fibers. Inhal. Toxicol. 14: 5-27, 2002.

Duez P., Dehon G., Kumps A. & Dubois J. Statistic of Comet assay: a key to discriminate between geotoxic effects. Mutagenesis. 18: 159-166, 2003.

Edel J. & Sabbioni E. Accumulation, distribution and form of vanadate in the tissues and organells of the mussel *Mytilus edulis* and goldfish *Carrassius auratus.* The Science of the Total Environment. 133: 139-151, 1993.

Elias Z., Poirot O., Baruthio F. & Daniere M.C. Role of solubilized chromium in the induction of morphological transformation of Syrian hamster embryo (SHE) cells by particulate chromium(VI) compounds. Carcinogenesis. 12: 1811-1816, 1991.

Fairbairn D.W., Olive P.L., O'Neill K.L. The comet assay: a comprehensive review. Mutat Res. , 339 (1): 37-59, 1995.

Farina M. Applicazione di tecniche analitiche avanzate in studi *in vitro* di metalli in tracce mediante culture cellulari. Degree thesis, Università degli studi di Pavia, S.P.I.03.165 JRC-Ispra. 2003.

Fenech M., Morley A.A. Cytokinesis-block micronucleus method in human lymphocytes: effect of in vivo ageing and low dose X-irradiation. Mutat Res.,161(2):193-8, 1986.

Fenech M. Cytokinesis-block micronucleus cytome assay. Nature Protocols 2: 1084-1104, 2007.

Fenech M. The in vitro micronucleus technique. Mutat Res., 455(1-2): 81-95. 2000.

Fletcher G. G., Rossetto F. E., Turnbull J. D. & Nieboer E. Toxicity, uptake, and mutagenicity of particulate and soluble nickel compounds. EnViron. Health Perspect. 102: 69-79, 1994.

Franchi E., Loprieno G., Ballardin M., Petrozzi L. & Migliore L. Cytogenetic monitoring of fishermen with environmental mercury exposure. Mutation Research, 320: 23-29, 1994.

Freeman G.B., Schoof R.A., Ruby M.V., Davis A.O., Dill J.A., Liao S.C., Lapin CA, Bergstrom PD. Bioavailability of arsenic in soil and house dust impacted by smelter activities following oral administration in cynomolgus monkeys. Fundam Appl Toxicol., 28(2): 215-22, 1995.

Freeman H.C., Uther J.F., Flemming R.B., Odense P.H. Ackerman R.G., Landry G., Musical C. Clearance of arsenic ingested by man from arsenic-contaminated fish. Bull. Environ. Contam. Toxicol. 22: 224-229, 1979

Fujihara J., Kunito T., Agusa T., Yasuda T., Iida R., Fujii Y. & Takeshita H. Population differences in the human arsenic (+3 oxidation state) methyltransferase (AS3MT) gene polymorphism detected by using genotyping method. Toxicology and Applied Pharmacology. 225: 251–254, 2007.

Fusenig N.E. & Boukamp P. Multiple stages and genetic alterations in immortalisation, malignant transformation, and tumor progression of human skin keratinocytes. Molecular Carcinogenesis. 23: 144-158, 1998.

Gebel T., Lantzsch H., Plessow K., Dunkelberg H. Genotoxicity of platinum and palladium compounds in human and bacterial cells. Mutat Res. 17;389(2-3): 183-90, 1997.

Gibson D.P., Aardema M.J., Kerckaert G.A., Carr G.J., Brauninger R.M. & LeBoeuf R.A. Detection of aneuploidy-inducing carcinogens in the Syrian hamster embryo (SHE) cell transformation assay. Mutation Research. 343:7-24, 1995.

Gottman E., Kramer S., Pfahringer B. & Helma C. Data quality in predictive toxicology: reproducibility of rodent carcinogenicity experiments. Environmental Health Perspectives. 109: 509-514, 2001.

Gres M.C., Julian B., Bourrie M., Meunier V., Roques C., Berger M., Boulnec X., Berger Y. & Fabre G. Correlation between oral drug absorption in humans, and apparent drug permeability in TC7, a human epithelial cell line: comparison with the parenteral CaCo-2 cell line. Pharmaceutical research. 15: 726-733, 1998.

Guillamet Cros E. Estudi de la genotoxicitata d'alguns metals mitjancant la tècnica del Cometa. Master in genetics. Universitat Autonoma de Barcelona (UAB), Facultat de Ciènces, Departement de genètica i de Microbiologia. 2001.

Guillamet E., Creus A., Ponti J., Sabbioni E., Fortaner S., Marcos R. In vitro DNA damage by arsenic compounds in a human lymphoblastoid cell line (TK6) assessed by the alkaline Comet assay.Mutagenesis. 19:129-35, 2004.

Harrap K.R., Jones M., Wilkinson C.R., Clink H.M., Sparrow S., Mitchley B.C.V., Clarke S. & Veasey A. Antitumour, toxic and biochemical properties of cisPt and eight other platinum complexes, in: Cisplatin. Current status and new developments. Prestayko A.W., Crooke S.t. & Carter S.K. eds. New York: Academic Press. 193-212, 1980.

Hartmann A. & Speit G. Genotoxic effects of chemicals in the single cell gel (SCG) test with human blood cells in relation to the induction of sister-chromatid exchanges (SCE). Mutation Research Letters. 346: 49-56, 1995.

Hartung T., Bremer S., Casati S., Coecke S., Corvi R., Fortaner S., Gribaldo L., Halder M., Roi A.J., Prieto P., Sabbioni E., Worth A. & Zueg V. ECVAM's Response to the changing political environment for alternatives: consequence of the European Union Chemical and Cosmetic Policies. ATLA. 31: 473-481, 2003.

Hartung T., Bremer S., Casati S., Coecke S., Corvi R., Fortaner S., Gribaldo L., Halder M., Hoffmann S., Roi A.J., Prieto P., Sabbioni E., Scott L., Worth A. & Zuang V. A modular approach to the ECVAM principles on test validity. ATLA. 32 ; 467-472, 2004.

Hartwig A. Carcinogenicity of metal compounds: possible role of DNA repair inhibition. Toxicology Letters. 102: 235-239, 1998.

Harvey A.N., Costa N.D., Savage J.R. & Thacker J. Chromosomal aberrations induced by defined DNA double-strand breaks: the origin of achromatic lesions. Somatic Cell and Molecular Genetics. 23: 211-219, 1997.

Hayashi Y. Overview of genotoxic carcinogens and non-genotoxic carcinogens. Exp Toxicol Pathol.,44(8): 465-71, 1992.

Honaoka K., Goessler W., Ohno H., Irgolic K.J. & Kaise T. Formation of toxic arsenical in roasted muscles of marine animals. Appl. Organometallic Chemistry. 15: 61-66, 2001.

Hopkins L.L. Jr.. Distribution in the rat of physiological amounts of injected ^{51}Cr (III) with time. American Journal of Physiology. 209: 731-735, 1965.

Hu Z., Tawa R., Konishi T., Shibata N., Takada K. A novel emulsifier, Labrasol, enhances gastrointestinal absorption of gentamicin, Life Sci. 69: 2899-2910, 2001.

Hughes M.F. & Kenyon E.M. Dose-dependent effects on the disposition of monomethylarsonic acid and dimethylarsinic acid in the mouse after intravenous administration. J. Toxicol. Environ. Health. 53: 95-112, 1998.

Hwua Y.S. & Yang J.L. Effect of 3-aminotriazole on anchorage independence and mutagenicity in Cd- and Pb-treated diploid human fibroblasts. Carcinogenesis. 19: 881-888, 1998.

IARC (International Agency for Research on Cancer). IARC monographs on the evaluation of the carcinogenic risk of chemicals to humans: Some metals and metallic compounds. 23, 1980.

IARC Monograph on the evaluation of carcinogenic risk to humans. Chromium, nickel and welding. IARC, International Agency for Research on Cancer, Lyon, 49, 1990a.

IARC Monograph on the evaluation of carcinogenic risk to humans. Nickel, metallic [7440-02-0] and alloys. 49, 1990b.

IARC Monograph on the evaluation of carcinogenic risk to humans. Methylmercury compounds. 58, 1993.

IARC Monographs on the evaluation of Carcinogenic Risks to Humans, Suppl. 6. Genetic and Related Effects: An Updating of selected IARC Monographs from Vol. 1 to 42: 729, 1987.

IARC. Chlorinated drinking-water chlorination by-products some other halogenated compounds cobalt and cobalt compounds. IARC Monogr Eval Carcinog Risks Hum. 52: 1-544, 1991.

IARC. Monographs on the Evaluation of the Carcinogenic Risk of Chemicals to Man. Geneva: World Health Organization, International Agency for Research on Cancer. (Multivolume work), p. 58, 103, 1972-PRESENT.

IARC/NCI/EPA Working-Group, Cellular and molecular mechanisms of cell transformation and standardization of transformation assays of established cell lines for the prediction of carcinogenic chemicals: overview and recommended protocols. Cancer Research. 45: 2395-2399, 1985.

Itoa Y., Tomohiro K., Makoto I., Riichi T., Nobuhito S. & Kanji T. Oral solid gentamicin preparation using emulsifier and adsorbent Journal of Controlled Release. 105: 23-31, 2005.

Kakunaga T. A quantitative system for assay of malignant transformation by chemical carcinogens using a clone derived from Balb/3T3. International Journal of Cancer. 12: 463-473, 1973.

Kaloyandres G.J. & Munoz E.P., Aminoglycoside nephrotoxicity. Kidney Int. 18: 571-582, 1980.

Kargacin B., Klein C. B. & Costa M. Mutagenic responses of nickel oxides and nickel sulfides in Chinese hamster V79 cell lines at the xanthine-guanine phosphoribosyl transferase locus. Mutat. Res. 300: 63-72, 1993.

Kasprzak K. S., Sunderman F. W. and Salnikow K. Nickel carcinogenesis. Mutat. Res. 533: 67-97, 2003.

Katz S. A. & Salem H. The biological and environmental chemistry of chromium. VCH, New York, 1994.

Kerckaert G.A., LeBoeuf R.A. & Isfort R.J. Use of the Syrian hamster embryo cell transformation assay for determining the carcinogenic potential of heavy metal compounds. Fundamenatals of Applied Toxicology. 34: 67-72, 1996.

Kerger B. D., Finley B. L., Corbett G. E., Dodge D. G. & Paustenbach D. J. Ingestion of chromium(VI) in drinking water by human volunteers: Absorption, distribution, and excretion of single and repeated doses. J. Toxicol. EnViron. Health. 50: 67-95, 1997.

Keshava N., Zhou G., Hubbs A.F., Ensell M.-X. & Ong T. Transforming and carcinogenic potential of cadmium chloride in BALB/c-3T3 cells. Mutation research. 448: 23-28, 2000.

Kirsch-Volders M., Vanhauwaert A., Eichenlaub-Ritter U., Decordier I. Indirect mechanisms of genotoxicity. Toxicol Lett. 140: 63-74, 2003

Kitasato I., Yokota M., Inoue S., Garashi M.I. Comparative ototoxicity of ribostamycin, dactimicin, dibekacin, kanamycin, amikacin, tobramycin, gentamicin, sisomicin and netilmicinin the inner ear of guinea pigs, Chemotherapy. 36: 155-168, 1990.

Koning H.P., Kock H. & Hertel R.F. Analytical determination of platinum with regard to the car catalyst issue, in "5th Colloquium Atomspektrometrische Spunrenanalytik", ed. Welz B., 1989.

Kreppel H., Bauman J., Liu J., McKim J.M. Jr & Klaassen C.D. Induction of metallothionein by arsenicals in mice. Fundam. Appl. Toxicol. 20: 184-189, 1993.

Kuo C.Y., Wong R.H., Lin J.Y., Lai J.C. & Lee. Accumulation of chromium and nickel metals in lung tumors from lung cancer patients in Taiwan. J Toxicol Environ Health A. 69: 1337-1344, 2006.

Laparra J.M., Dinoraz V., Reyes B., Granero L., Polache A., Montoro R. & Rosaura F. Cytotoxic effect of As(III) in Caco-2 cells and evaluation of its human intestinal permeability. Toxicology in Vitro. 20: 658–663, 2006.

Laszlo J. Antiemetics and cancer chemotherapy. Williams and Wilkins eds. Baltimore, Md. pp 184, 1983.

Le Ferrec E., Chesne C., Artursson P., Brayden D., Fabre G., Gires P., Guillou F., Rousset M., Rubas W. & Scarino M-L. *In vitro* Models of intestinal barrier. The report and recommendations of ECVAM workshop 46. ATLA. 29: 649-688, 2001.

Lee T.C., Oshimura M. & Barret J.C. Comparison of arsenic induced cell transformation, cytotoxicity, mutation and cytogenetic effects in Syrian hamster embryo cells in culture. Carcinogenesis. 6: 1421-1426, 1985.

Legallicier B., Leclere C., Monteil C., Elkaz V., Morin J.P., Fillastre J.P. The cellular toxicity of two antitumoural agents derived from platinum, cisplatinum versus oxaliplatinum, on cultures of tubular proximal cells. Drugs Exp Clin Res. 22:41-50, 1996.

Léonard A. & Bernard A. Biomonitoring exposure to metal compounds with carcinogenic properties. Environ Health Perspect. 101 Suppl 3:127-33, 1993.

Leonard A. & Gerber G.B. Mutagenicity, carcinogenicity and teratogenicity of vanadium compounds. Mutation research. 317; 81-88, 1994.

Lewin B., chapter 37, in "Genes VI", International Student Edition. 1131-1171, 1997.

Limbach L.K., Wick P., Manser P., Grass R.N., Bruinink A. & Stark W.J. Exposure of engineered nanoparticles to human lung epithelial cells: influence of chemical composition and catalytic activity on oxidative stress. Environ Sci Technol. 41: 3791-3792, 2007.

Lin S., Shi Q., Nix F.B., Styblo M., Beck M.A., Herbin-Davis K.M., Hall L.L., Simeonsson J.B.& Thomas D.J. A novel S-adenosyl-Lmethionine: arsenic (III) methyltransferase from rat liver cytosol. J. Biol. Chem. 277: 10795-10803, 2002.

Lindberg A.L., Kumar R., Goessler W., Thirumaran R., Gurzau E., Koppova K., Rudnai P., Leonardi G., Fletcher T. & Vahter M. Metabolism of low-dose inorganic arsenic in a central European population: influence of sex and genetic polymorphisms. Environ. Health Perspect. 115: 1081-1086, 2007.

Lison D., Carbonnelle P., Mollo L., Lauwerys R. & Fubini B. Physicochemical mechanism of the interaction between cobalt metal and carbide particles to generate toxic activated oxygen species. Chem. Res. Toxicol. 8: 600-606, 1995.

Lison D., De Boeck M., Verougstraete V. & Kirsch-Volders M. Update on the genotoxicity and carcinogenicity of cobalt compounds. Occup. Environ. Med. 58: 619-625, 2001.

Little J.B. Quantitative Studies of Radiation Transformation with the A31 -11 Mouse BALB/3T3 Cell Line1. Cancer Research. 39, 1474-1480, 1979.

Lucas F. Acute and chronic toxicity assessment of MSMA and DSMA. Book of Posters. Third International Conference on Arsenic Exposure and Health Effects, San Diego. 1998

Mantle P.G. Risk assessment and the importance of ochratoxins, International Biodeterioration & Biodegradation. 50: 143-146, 2002.

Mappes R. Experiments on the excretion of arsenic in urine, in German. Int. Arch. Occup. Environ. Health. 40: 267-272, 1977.

Marafante E., Vahter M., Norin H., Envall J., Sandstro M., Christakopoulos A. & Ryhage R. Biotransformation of dimethylarsinic acid in mouse, hamster and man. J. Appl. Toxicol. 7: 111-117, 1987.

Marnell L.L., Garcia-Vargas G.G., Chowdhury U.K., Zakharyan R.A., Walsh B., Avram M.D., Kopplin M.J., Cebrián M.E., Silbergeld E.K. & Aposhian H.V. Polymorphism in the human monomethylarsenic acid (MMAV) reductase/hGSTO1 gene and changes in urinary arsenic profiles. Chem. Res. Toxicol. 16: 1507-1513, 2003

Maronpot R.R. Chemical carcinogenesis, in Handbook of Toxicology Pathology. 91-129, New York, USA, Academic Press, 1991.

Mass M.J., Tennant A., Roop B.C., Cullen W.R., Styblo M., Thomas D.J. & Kligerman A.D. Methylated trivalent arsenic species are genotoxic. Chem. Res. Toxicol. 14: 355-361, 2001.

Matthews E.J., Spalding J.W. & Tennent R.W. Transformation of Balb/c-3T3 cells: V. Transformation responses of 168 chemicals compared with mutagenicity in Salmonella and carcinogenicity in rodent bioassays. Environmental Health Perspective. 101: 347-482, 1993.

Mazzotti F., Sabbioni E., Ghiani M., Cocco B., Ceccatelli R. & Fortaner S. *In vitro* assessment of cytotoxicity and carcinogenic potential of chemicals: evaluation of cytotoxicity induced by 58 metal compounds in Balb/3T3 cell line. ATLA. 29, 601-611, 2001.

Mazzotti F., Sabbioni E., Ponti J., Ghiani M., Fortaner S. & Rossi G.L. In vitro setting of dose–effect relationships of 32 metal compounds in the Balb/3T3 cell line as a basis for predicting their carcinogenic potential. ATLA 30: 209–217, 2002.

Mertz W., Roginski E.E. & Schroerder H.A. Some aspects of glucose metabolism of Chromium-deficient rats raised in a strictly controlled environment. Journal of Nutrition. 86: 107-112, 1965.

Mertz W., Roginski E.E., Feldman R.J. & Thurman D.E. Dependence of Chromium transfer into the rat embryo on the chemical form. Journal of Nutrition. 99: 363-367, 1969.

Migliore L., Bocciardi C., Macri C. & Lo Jacono F. Cytogenetic damage induced in human lymphocytes by four vanadium compounds and micronucleus analysis by fluorescence in situ hybridisation with a centromeric probe. Mutation Research. 319, 205-213, 1993.

Migliore L., Frenzilli G., Nesti C., Fortaner S. & Sabbioni E. Cytogenetic and oxidative damage induced in human lymphocytes by platinum, rhodium and palladium compounds. Mutagenesis. 17/5; 411-417, 2002a.

Migliore L., Naccarati A., Zanello A., Scarpato R., Bramanti L. & Mariano M.. Assessment of sperm DNA integrity in workers exposed to styrene. Human Reproduction. 17: 2912-2918, 2002b.

Moller P., Knudsen L.E., Loft S. & Wallin H. The comet assay as a rapid test in biomonitoring occupational exposure to DNA-damaging agents and effects of confounding factors. Cancer Epidemiol. Biomarkers Prev. 9: 1005-1015, 2000.

Moore M.M., Harrington-Brock K. & Doerr C.L. Relative genotoxic potency of arsenic and its methylated metabolites. Mutat. Res. 386: 279-290, 1997.

Morgan L. G. and Usher V. Health problems associated with nickel refining and use. Ann. Occup. Hyg. 38: 189-198. 1994.

Morgan W.F., Corcoran J., Hartmann A., Kaplan M.I., Limoli C.L. & Ponnaiya B. DNA double-strand breaks, chromosomal rearrangements, and genomic instability. Mutation Research. 404: 125-128, 1998.

Nechay R.B., Nanninga L.B. & Nechay P.S.E. Vanadyl (IV) and vanadate (V) binding to selected endogenous phosphate, carbonyl and amino ligands; calculation of cellular vanadium species distribution. Archives in Biochemistry and Biophysics. 251: 128-138, 1986.

NRC, 1999. Arsenic in Drinking Water. National Academy Press, Washington, DC.

Oberdörster G., Maynard A., Donaldson K., Castranova V., Fitzpatrick J., Ausman K., Carter J., Karn B., Kreyling W., Lai D., Olin S., Monteiro-Riviere N., Warheit D. & Yang Y. A report from the ILSI Research Foundation/Risk Science Institute National Toxicity Screening Working Group. Principles for characterizing the potential human health effects from exposure to nanomaterials: elements of a screening strategy. Part. Fibre Toxicol. 6: 2-8, 2005b.

Oberdorster G., Oberdorster E. & Oberdorster J. Nanotoxicology: An emerging discipline evolving from studies of ultrafine particles. Env Health Persp. 113: 823-839, 2005a.

Ogura H., Takeuchi T. & Morimoto K. A comparison of the 8- hydroxydeoxyguanosine, chromosome aberrations and micronucleus techniques for the assessment of the genotoxicity of mercury compounds in human blood lymphocytes. Mutation Research. 340: 175-182, 1996.

Oldiges H., Hochreiner D. & Glaser U. Long term inhalation study with Wistar rats and four cadmium compounds. Toxicol. Environ. Chem. 19: 217-222., 1989.

Olive P.L. DNA damage and repair in individual cells. Applications of the comet assay in radiobiology. International Journal of Radiation and Biology. 75: 395-405, 1999.

Oya-Ohta Y., Kaise T. &Ochi T. Induction of chromosomal aberrations in cultured human fibroblasts by inorganic and organic arsenic compounds and the different roles of glutathione in such induction. Mutat. Res. 357: 123-129, 1996.

Patierno, S. R., Dirscherl, L. A., and Xu, J. Transformation of rat tracheal epithelial cells to immortal growth variants by particulate and soluble nickel compounds. Mutat. Res. 300, 179-193. 1993.

Petralia M.C. Impatto sanitario di metalli rari impeiegati in tecnologie avanzate. Studi metabolici e tossicologici relativi al problema del rilascio di platino, rodio, e palladio da marmitte catalitiche. Degree thesis. 1994.

Pitot H.C. & Dragan Y.P. Chemical carcinogenesis, in Casarett and Doull's toxicology: the basic science of poison, Doull J., Klaassen C.D., Amdur M.O., eds. 2nd ed. New York, Macmillan. 201-265, 1996.

Pomroy C., Charbonneau S.M., McCullough R.S. & Tam G.K.H. Human retention studies with 74Arsenic. Toxicol. Appl. Pharmacol. 53: 550-556, 1980.

Ponti J. Effetti tossicologici e potenziale cancerogeno: studi in vitro mediante colture cellulari. Degree thesis. Università degli Studi dell'Insubria, Varese, Italy, S.P.I.02.44 JRC-Ispra, 2001.

Ponti J. In vitro metal toxicology research. A study carried out by Balb/3T3, HaCaT and CaCo-2 cell lines. Traball de Magíster UAB, 2004.

Ponti J., Ceriotti L., Munaro B., Farina M., Munari A., Whelan M., Colpo P., Sabbioni E. & Rossi F. Comparison of Impedance-based Sensors for Cell Adhesion Monitoring and In Vitro Methods for Detecting Cytotoxicity Induced by Chemicals. ATLA. 34: 515-525, 2006.

Ponti J., Munaro B., Fischbach M., Hoffmann S. & Sabbioni E. An optimised data analysis for the Balb/c 3T3 transformation assay and its application to metal compounds. International Journal of Immunopathology and Pharmacology. 20: 673-684, 2007.

Poretz D.M. Outpatient use of intravenous antibiotics, Am. J. Med. 97:1-2, 1994.

Raja P.M., Connolley J., Ganesan G.P., Ci L., Ajayan P.M., Nalamasu O. & Thompson D.M. Impact of carbon nanotube exposure, dosage and aggregation on smooth muscle cells. Toxicol Lett. 28: 51-63, 2007.

Rani A. S., Qu D. Q., Sidhu M. K., Panagakos F., Shah V., Klein K. M., Brown N., Pathak S., and Kumar S. Transformation of immortal, non-tumorigenic osteoblast-like human osteosarcoma cells to the tumorigenic phenotype by nickel sulfate. Carcinogenesis 14: 947-953, 1993.

Rasmussen R.E. & Menzel D.B. Variation in arsenic-induced sister chromatid exchange in human lymphocytes and lymphoblastoid cell lines. Mutat. Res. 386: 299–306, 1997.

Recchia J., Lurantos M.H.A., Storey J., Kensil C.R. A semisynthetic quillaja saponin as a drug delivery agent for aminoglycoside antibiotics. Pharm. Res. 12: 1917– 1923, 1995.

Reznikoff C.A., Bertram J.S., Brankow D.W. & Hidelberger C.A. Quantitative and qualitative studies on chemical transformation of cloned C3H mouse embryo cells, sensitive to post-confluence inhibition of cell division. Cancer Research. 33: 3239-3249, 1973.

Rodríguez-Mercado J.J., Roldán-Reyes E. & Altamirano-Lozano M. Genotoxic effects of vanadium(IV) in human peripheral blood cells. Toxicol Lett. 144: 359-369, 2003.

Rojas E., Lopez M.C. & Valverde M. Single cell electrophoresis assay: methodology and applications. Journal of Chromatography B: Biomedical Applications. 722: 225-254, 1999.

Sabbioni E., Edel J. & Goetz L. Trace metal speciation in environmental toxicology research. Nutrition Research. 1: 32-43, 1985.

Sabbioni E., Pietra R., Serra M.A., Fortaner S., Edel J. & Minoia C. Application of nuclear, radiochemical and spectrochemical techniques in metal toxicology. Journal of Trace and Microprobe Techniques. 11: 217, 1993a.

Sabbioni E., Ponti J. & Rossi F. In vitro toxicology research on metallic nanoparticles, FAME, first summer school of WP4-JPR2 and WP6-JPR4, la Grande Motte (France), 02-07 October 2005, Proceeding book, pp. 333-340 (2005).

Sabbioni E., Pozzi G., Devos S., Pintar A., Casella L. & Fischbach M. The intensity of vanadium(V)-induced cytotoxicity and morphological transformation in Balb/3T3 cells is dependent on glutathione-mediated bioreduction to vanadium(IV). Carcinogenesis. 14: 2565-2568, 1993b.

Sabbioni E., Pozzi G., Pintar A., Casella L. & Garattini S. Cellular retention, cytotoxicity and morphological transformation by vanadium (IV) and vanadium (V) in Balb/3T3 cell line. Carcinogenesis. 12; 47-52, 1991

Saffiotti U. & Bertolero F. Neoplastic transformation of Balb/3T3 cells by metals and the quest for induction of a metastatic phenotype. Biological Trace Element Research. 21: 475-482, 1989.

Saffiotti U., Bertolero F., Bignami M., Cortesi F., Ficarella C. & Kaighn M.E. Studies on chemically induced neoplastic transformation and mutation in the Balb/3T3 Cl A31-1-1 cell line in relation to the quantitative evaluation of carcinogens. Toxicology and Pathology. 12: 383-390, 1984.

Sakurai T., Kaise T. & Matsubara C. Inorganic and methylated arsenic compounds induce cell death in murine macrophages via different mechanisms. Chem. Res. Toxicol. 11: 273-283, 1998.

Salata O.V. Applications of nanoparticles in biology and medicine. J Nanobiotechnology. 2: 3, 2004.

Salnikow K. and Zhitkovich A. Genetic and Epigenetic Mechanisms in Metal Carcinogenesis and Cocarcinogenesis: Nickel, Arsenic, and Chromium. Chem. Res. Toxicol. 21: 28–44, 2008.

Sande M.A., Mandel G.L., Rall T.W., Nies A.S. & Taylor P. The Pharmacological Basis of Therapeutics, 8th edition, Pergamon Press, New York, pp. 1098-1116, 1990.

Saran R., Tiwari R.K., Reddy P.P. & Ahuja Y.R. Risk assessment of oral cancer in patients with pre-cancerous states of the oral cavity using micronucleus test and challenge assay. Oral Oncology. 44: 354-360, 2008.

Saris C.P., van de Vaart P.J.M., Reitbroek R.C. & Blommaert F.A. In vitro formation of DNA adducts by cisplatin, loboplatin and oxaliplatin in calf thymus DNA in solution and cultured human cells. Carcinogenesis. 17: 2763-2769, 1996.

Satoh K., Fukuda Y., Torii K. & Katsuno N. Epidemiological study of workers engaged in the manufacture of chromium compounds. Journal of Occupational Medicine. 23: 835-838, 1981.

Schurz F., Sabater-Vilar M. & Fink-Gremmels J. Mutagenicity of mercury chloride and mechanisms of cellular defence: the role of metal-binding proteins. Mutagenesis, 15: 525-530, 2000.

Schwerdtle T., Walter I. & Hartwig A. Arsenite and its biomethylated metabolites interfere with the formation and repair of stable BPDE-induced DNA adducts in human cells and impair XPAzf and Fpg. DNA Repair. 2:1449-1463, 2003.

Scicchitano D.A. & Pegg A. E. Inhibition of O6-alkylguanine-DNA-alkyltransferase by metals. Muat. Res. 192: 207-210, 1987.

Shenker B.J., Guo T.L. & Shapiro I.M. Mercury-induced apoptosis in human lymphoid cells: evidence that the apoptotic pathway is mercurial species dependent. Environmental Research. Section A. 84: 89-99, 2000.

Silva-Pereira L.C., Cardoso P.C.S., Leite D.S., Bahia M.O., Bastos W.R., Smith M.A.C. & Burbano R.R. Cytotoxicity and genotoxicity of low doses of mercury chloride and methylmercury chloride on human lymphocytes in vitro Brazilian Journal of Medical and Biological Research. 38: 901-907, 2005.

Simeonova P.P. & Luster M.I. Mechanisms of arsenic carcinogenicity: genetic or epigenetic mechanisms? J Environ Pathol Toxicol Oncol. 19: 281-286, 2000.

Smith J.B. Vanadium ions stimulate DNA synthesis in Swiss mouse 3T3 and 3t6 cells. Proceeding of National Academy of Sciences. USA. 80: 6162-6166, 1983.

Smith T.J., Crecelius E.A. & Reading J.C. Airborne arsenic exposure and excretion of methylated arsenic compounds. Environ. Health Perspect. 19: 89-93, 1977.

Soto K., Garza K.M., Murr L.E. Cytotoxic effects of aggregated nanomaterials. Acta Biomater. 3: 351-358, 2007.

Steinmaus C., Moore L.E., Shipp M., Kalman D., Rey O.A., Biggs M.L. & Hopenhayn C. Genetic polymorphisms in MTHFR 677 and 1298, GSTM1 and T1, and metabolism of arsenic. J. Toxicol. Environ. Health, Part A 70: 159-170, 2007.

Styblo M., Del Razo L.M., Vega L., Germolec D.R., LeCluyse E.L., Hamilton G.A., Reed W., Wang C., Cullen W.R., Thomas D.J. Comparative toxicity of trivalent and pentavalent inorganic and methylated arsenicals in rat and human cells. Arch. Toxicol. 74: 289-299, 2000.

Sunderman F. W. Jr. Carcinogenicity of nickel compounds in animals. Nickel compounds efficiently transform rodent and human cells in Vitro IARC Sci. Publ. 127-142, 1984.

Tam G.K.H., Charbonneau S.M., Bryce F., Pomroy C. & Sandi E. Metabolism of inorganic arsenic (74As) in human following oral ingestion. Toxicol. Appl. Pharmacol. 50: 319-322, 1979.

Terheggen P.M., Floot B.G., Lempers E.L., van Telligen O., Begg A.C. & den Engelse L. Antibodies against cisplatin modified DNA and cisplatin modified dinucleotides. Cancer Chemiotheraphy and Pharmacology. 8: 185-191, 1991.

Thun M.J., Elinder C.G. & Friberg L. Scientific basis for an occupational standard for cadmium. American Journal of Industrial Medicine. 20: 629-642, 1991.

Tice R.R., Agurell E., Anderson D., Burlinson B., Hartmann A., Kobayashi Y., Rojas E., Ryu J-C & Sasaki Y.F. The single cell gel/comet assay: guidelines for in vitro and in vivo genetic toxicology testing. SCG/Comet Assay Genetic Toxicology Guidelines. 1999.

Tran C.L., Buchanan D., Cullen R.T., Searl A., Jones A.D. & Donaldson K. Inhalation of poorly soluble particles. II. Influence of particle surface area on inflammation and clearance. Inhal Toxicol. 12: 1113-1126, 2000.

Trott D. A., Cuthbert A. P., Overell R. W., Russo I. & Newbold, R. F. Mechanisms involved in the immortalization of mammalian cells by ionizing radiation and chemical carcinogens. Carcinogenesis. 16: 193-204, 1995.

Tryinda L. & Kuduk-Jaworska J. Impact of K_2PtCl_4 on the structure of human serum and its binding ability of heme and bilirubin. Journal of Inorganic Biochemistry. 53: 249-260, 1994.

Tseng W-P. Effects and dose-response relationships of skin cancer and blackfoot disease with arsenic. Environ Health Perspect. 19: 109-119, 1977.

Tveito, G., Hansteen, I. L., Dalen, H., and Haugen, A. Immortalization of normal human kidney epithelial cells by nickel(II). Cancer Res. 49, 1829–1835. 1989.

Vahter M. & Marafante E. Intracellular interaction and metabolic fate of arsenite and arsenate in mice and rabbits. Chem. Biol. Interact. 47: 29-44, 1983.

Vahter M. Genetic polymorphism in the biotransformation of inorganic arsenic and its role in toxicity. Toxicology Letters. 112: 209–217, 2000.

Vahter M., Arsenic. In: Clarkson T.W., Friberg L., Nordberg G.F. & Sager P.R. (Eds.), Biological Monitoring of Toxic Metals. Plenum Press, New York, pp. 303-321, 1988.

Vahter M., Couch R., Nermell B. & Nilsson R. Lack of methylation of inorganic arsenic in the chimpanzee. Toxicol. Appl. Pharmacol. 133: 262–268, 1995.

Vahter M., Marafante E., Dencker L. Tissue distribution and retention of 74As-dimethylarsinic acid in mice and rats. Arch. Environ. Contam. Toxicol. 13: 259-264, 1984.

Vahter, M. & Marafante, E. Reduction and binding of arsenate in marmoset monkeys. Arch. Toxicol. 57: 119-124, 1985.

Valverde M., Trejo C. & Rojas E. Is the capacity of lead acetate and cadmium chloride to induce genotoxic damage due to direct DNA-metal interaction?. Mutagenesis. 16: 265-70, 2001.

Van der Laan J.W. Current status and use of short/medium-term model for assessment of carcinogenicity of human pharmaceuticals: Regulatory perspectives. Toxicol Lett. 112: 567-572, 2000.

Van der Merve K.J., Steyn P.S. & Fourie L. Mycotoxins. Part II. The constitution of ochratoxins A, B and C, metabolities of Aspergillus ochraceus Wilh. Journal of Chemical Society. 7083-7088, 1965.

Voitkun V., Zhitkovich A. & Costa M. Cr(III)-mediated cross-links of glutathione or amino acid to the DNA phosphate backbone are mutagenic in human cells. Nucleic Acid Research. 26: 2024-2030, 1998.

Wang K., Xu J.J. & Chen H.Y. A novel glucose biosensor based on the nanoscaled cobalt phthalocyanine-glucose oxidase biocomposite. Biosensors & Bioelectronics. 20: 1388-1396, 2005.

Wood J.M. Biological cycles for toxic elements in the environment. Science. 183: 1049-1052, 1974.

Yamamoto A., Hisanaga A., Ishinishi N. Tumorigenicity of inorganic arsenic compounds following intratracheal instillations to the lungs of hamsters. Int J Cancer 40(2): 220-3, 1987.

Yang M.H., Jiang J.H., Yang Y.H., Chen X.H., Shen G.L. & Yu R.Q. Carbon nanotube/cobalt hexacyanoferrate nanoparticle-biopolymer system for the fabrication of biosensors. Biosensors & Bioelectronics. 21: 1791-1797, 2006.

Yuspa S.H. & Poireier M.C. Chemical carcinogenesis: from animal models to molecular models in one decade. Advances in cancer Researcher. 50: 25-70, 1988.

Zeiger E. Genetic toxicity test for predicting carcinogenicity, in Genetic Toxicology and Cancer Risk Assessment (ed. W.N. Choy), pp 29-46. New York, NY, USA: Marcel Dekker. 2001.

Zhitkovich A. Importance of chromium-DNA adducts in mutagenicity and toxicity of chromium(VI). Chem. Res. Toxicol. 18: 3–11, 2005.